Electronic Realizations of Chaotic Circuits: From Breadboard to Nanotechnology

Gaurav Gandhi

A dissertation submitted for the degree of
Doctor of Philosophy (Ph.D.)

Scientific advisor:
Tamás Roska, D.Sc.
Ordinary member of the Hungarian Academy of Sciences

Faculty of Information Technology
Péter Pázmány Catholic University

Budapest, 2008

Dedicated to my father who taught me how to dream and to my entire family and friends who stood by all my dreams

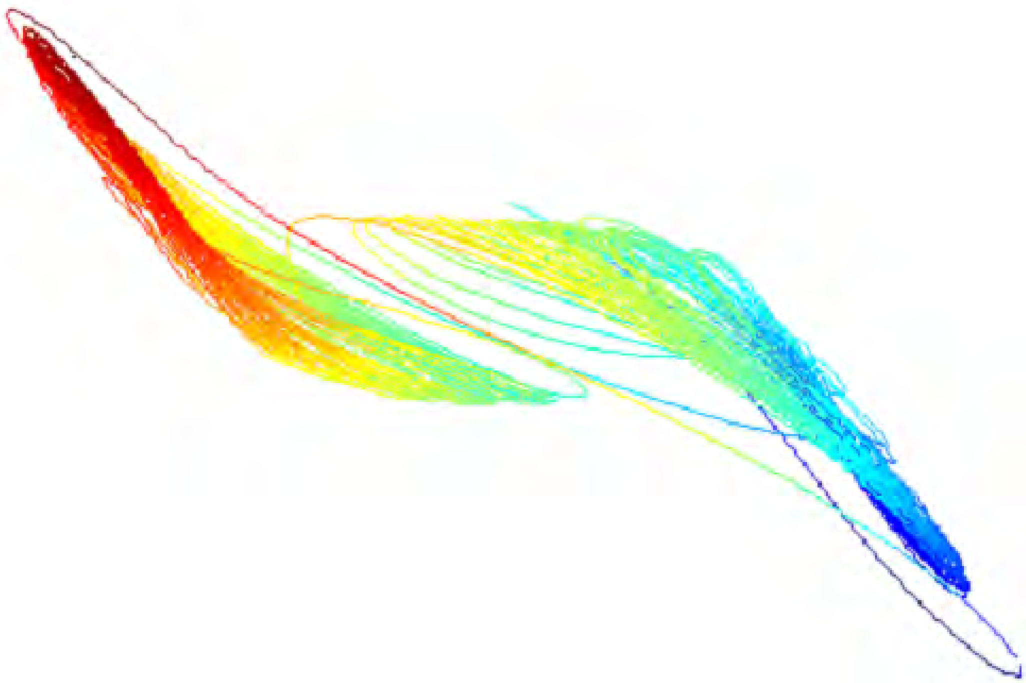

The Double Scroll

Acknowledgements

In the first place, I would like to thank my supervisor, Professor *Tamás Roska*, for his unbroken enthusiasm, consistent support, and also his outstanding personal qualities. He has been a friend, philosopher and guide to me. Under his careful guidance, I was introduced to the wealth of material that ultimately led to this dissertation. It is owing to him that I was able to interact and work with pioneers like *Leon Chua*. Working and spending time with *Prof. Leon Chua* in his lab at UC Berkeley was a dream come true for me which would not have been possible without the help, encouragement and support of *Prof. Roska*. I consider it a great privilege to be part of his highly qualified research.

I am very grateful to *Prof. Leon Chua*, *Prof. Yusuf Leblebici*, *Prof. Zoltan Vidnyánszky* and *Prof. B.E. Shi* for the time I could spend with their research teams. Cooperation with their research teams was a learning experience as I have learnt some lessons of life. I hope I can get another opportunity in the future to co-operate with them.

I am also grateful to *Prof. Árpád Csurgay* who, like Prof. Roska, for several informal discussions on human behaviour in society. His discussions exposed me to nanotechnology and has also taught me the importance of being a nice human.

It is difficult to make a complete list of all those who made the past few years an enriching experince in several respect. I recall *Alexandre Schmidt* from the EPFL and *Bharath* from *Prof. Chua's Lab* at UC

Berkeley.

It is difficult to mention all of them who have helped me one or the other point of time during my doctoral days. Special thanks to *György Cserey* for his unstinted support in all aspects of my stay at Budapest including the pre-review of this dissertation and to *Ákos Zarándy*, *Péter Földesy* and *Péter Szolgay* for a number of helpful discussions; to *Ákos Tar* and *Ádám Rák* for their assistance during my work at Robotic Lab, and to the colleagues *Béla Weiss*, *Viktor Gál*, *Mária Ravasz*, *Dániel Hillier*, *Csaba Benedek*, *Barnabás Hegyi*, *Gábor Vásárhelyi*, *Attila Kiss*, *Zoltán Fodróczi*, visiting researchers *Sung Eom*, *Giovanni Pazienza* and the others who made my stay in Budapest a memorable one.

I am equally indebted to *Katalin Keserű*, *Éva Szitáné Németh*, *Márta Szomolányi*, *Katalin Schulek* for their practical and official aid and making sure that my lack of knowledge of Hungarian language and culture is not a obstacle in my studies.

I would like to thank Indian friends, who other than being a nice company also enhanced my knowledge about my own culture and religion. *Surjit Singh*, *Ramandeep Singh* and *Varun Aggarwal* need specific mention. I also thank *Varun*, my ex-colleague, for his passive contribution to automation of chaotic circuits. Thanks are also due to *Brijesh Gulati*, who enhanced my knowledge about the role of Chaos theory in finance through several informal discussions.

I thank the financial and administrative support of the *Péter Pázmány Catholic University* and the *Computer and Automation Research Institute* where I spent my years as a doctoral student.

I would also like to thank my *family and friends* who have been supportive, when I lost my father during the course of my doctoral studies.

Thanks are due to my *father* whose consistent support, constant teaching and undying encouragement made me complete my thesis which otherwise would not have been possible.

Contents

Chapter 1

Introduction

The world of chaos and fractals is fascinating. The visual scrolls and patterns attract all of us but somehow most of us lack the mindset to understand the same. In fact, it has been argued that the answer to several economic depressions and stock market crashes lies in nonlinear dynamics and chaos theory.

From the days of *Sir Issac Newton* and *Pierre-Simon Laplace* to that of *Albert Einstein* and *Neil's Bohr*, there has always been a hunt for hidden parameter leading to unusual behavior of the physical world. It was not before 1905, that a mathematician named *H. Poincare* discovered the fascinating field of Chaos.

In mathematics, chaos theory describes the behavior of certain dynamical systems i.e. systems whose state evolves with time - that may exhibit dynamics that are ***highly sensitive to initial conditions***. Chaos, along with Quantum Mechanics and the Theory of Relativity, has been hailed as one of the major discoveries of the 20^{th} century. However, despite being such a fascinating field it remained almost dormant until *E. Lorentz* discovered the fact that weather is indeed a chaotic system.

The lack of right mindset is attributed to the slow development of this field. It has been well pointed out by *Prof. Peter Kennedy* that we have a mindset of *linearize, then analyze* which leads to ignoring several interesting dynamical behavior as noise. In fact, the name "Chaos Theory" in itself is a misnomer and is a manifestation of our *inability to understand things beyond our developed mindset.* The established mindset was so strong that during the early development of chaos theory, emphasis was paid on convincing the research community that chaos is actually a phenomenon and not a mathematical fallacy.

This is one of the reasons why *Chua's circuit* (a circuit which celebrates itself as a paradigm of chaos) was rigorously proved to be chaotic both mathematically and experimentally to convince the community. With its presence in almost every field from weather to finance, from economics to hydraulics and now nanotechnology, Chaos theory is now witnessing a lot of increased enthusiasm in interdisciplinary sciences. However, there still lies a need to develop a mindset to understand patterns, fractals and other bizzare phenomenon.

Other than the lack of right mindset, unavailability of a robust chaotic system to validate certain theories concerning chaos can also be one of the reason for slow progress of the field. This can be observed from the fact that since its inception 24 years ago, there are not more than a dozen different implementations of *Chua's circuit* [4, 12, 13]. Historically seen, *Chua's circuit* was the first successful physical implementation of a system designed to exhibit chaos [9]. This circuit is the first system rigorously proved to be chaotic [85]. *Chua's circuit* is also the simplest [11] circuit where chaos can be observed experimentally.

Other than *Chua's circuit*, several other Chaotic circuits are also being explored by the research community. *M.E. Yalcin's* MultiScroll MultiGrid (MSMG) chaotic circuit is based on a simple third order differential equation. This circuit is an extension of Chua type double scroll circuit [17].

The behavior of this system maps to that of *Chua's Circuit* in several aspects. It is simpler than *Chua's Circuit* to comprehend but has neither been proved chaotic nor is able to show as many attractors as *Chua's circuit.* The rich behavior of *Chua's oscillator* is due to the fact that it contains three different bifurcation parameters (i.e. α, β, γ) whereas for MGMS it is only one in the present case (i.e. a).

Yalcin et. al. have modified the third order differential equation given by [17] to generate a whole new class of MSMG Chaotic circuits [15]. They have given a breadboarded implementation of the same as a proof of concept. However, looking at the advantages of such a system, sooner than later a VLSI implementation may be required. In fact, [17] refers to one such implementations of simple Chua type double scroll circuits in 0.5 micron technology. But a VLSI implementation of MSMG Chaotic circuits is still non-existent.

Another important gap that has been identified in the research community is lack of an electronic (controllable) chaotic system in nanotechnology. The presence of chaos at atomic level has been known since long, yet not many efforts have been reported to design chaotic circuits using exotic technologies like single electron transistors.

Thus to summarize, following are four problems in electronic realizations of chaotic systems, which I tried to handle through my work.

- Finding and implementing a robust *Chua's Circuit*.
- Automation of *Chua's Circuit* design using Genetic Algorithms.
- Designing a VLSI integrated circuit architecture implementation for MSMG Chaotic circuits and validating it at 0.5 micron technology using SPICE.
- Developing a Chua type double scroll chaotic circuit using Single Electron Transistors (SETs).

Along with these problems, the thesis also tries to address two more issues as an application of the research conducted.

- Developing a mindset of chaotic systems by designing a PCB based, plug-n-play, robust *Chua's Circuit* kit for high school students.
- Developing a 3D-Cellular NonLinear Network composed of *Chua's Circuit* Plug-n-Play kits.

The dissertation is organized as follows. Chapter 2 and 3 develops Thesis I where electronic realizations of *Chua's circuits* in different form was rigorously studied. Previously published breadboard versions of *Chua's circuits* were extensively studied and the most robust and easily implementable design among them is chosen. Using this design a plug and play kit is developed which is used to teach chaos theory to the high school students via *Chua's circuit*. This kit is explained in the applications section. Chapter 3 moves one step ahead and tries to automate the designing of *Chua's Circuit*. Chapter 4 and 5 (Thesis II and III) explores new forms of simple double scroll systems in different technologies. Whereas Chapter 4 presents a VLSI integrated circuit design architecture of a MSMG double scroll attractor, Chapter 5 focuses on designing similar double scroll circuits for nanoscale using SETs. Build for the first time for nanoscale, SET based chaotic circuit could also open a way to design chaotic systems using nanoelectronics.

A suggested applications of the current dissertation is a real time design of a 3D CNN architecture with *Chua's Circuit* as a cell or the automation of electronic realization of *Chua's Circuit*. However, the most important application of the current dissertation is the development of *Chua's Circuit* kit to teach chaos theory to the high school students in order to develop a mindset for the same at grassroot level. A mindset developed at high school will automatically gets transcended to undergraduate curriculum. Glossary of most commonly used terminologis is provided in a separate section in appendix. However readers are refered to wikipedia and Internet to explore further into these terminologies.

Use of colored figures is partly a style and partly a requirement. For instance, bifurcation diagram, birth and death of double scroll and windows screenshots are more appealing in color compared to grayscale. Hence a color printed version is recommended for reading.

Chapter 2

Chua's Circuit

Thesis I. *Robust electronic realizations of Chua's chaotic circuit including designing Chua's Circuit kit and automation of Chaotic circuits including Chua's Circuit*

2.1 Introduction

With the purpose of designing the simplest autonomous electronic circuit to generate chaotic signals, *Chua's Circuit* was first proposed in 1984 [9]. The presence of chaotic attractor in this 3^{rd} order, extremely simple, autonomous circuit was first presented by *T. Matsumoto* [11] using computer simulations. The dynamics of *Chua's Circuit* is described by the following set of equations

$$\begin{aligned} C_1\frac{dv_1}{dt} &= G(v_2 - v_1) - f(v_1), \\ C_2\frac{dv_2}{dt} &= G(v_1 - v_2) + i_3, \\ L\frac{di_3}{dt} &= -v_2. \end{aligned} \tag{2.1}$$

Where v_1, v_2 *and* i_3 denotes the voltage across capacitor C_1, voltage across C_2 and current across inductor L, respectively and $f(v_R)$ is a nonlinear function defined by

$$i_R = f(v_R) = G_b v_R + 0.5 * (G_a - G_b)\{|v_R + B_P| - |v_R - B_p|\}. \tag{2.2}$$

Here G_a and G_b are the slopes of the segments and B_p denotes the breakpoint as shown in Fig. 2.1.

Figure 2.1: V-I characteristics of Chua's Diode

For specific parameter values, this circuit [11] was shown to behave chaotically. It was later confirmed experimentally [30, 86] as well as mathematically [85] that indeed *Chua's Circuit* is the simplest autonomous circuit, which exhibits chaotic behavior. Since then, almost 1000 research papers [www.chuacircuit.com] have been published on this versatile chaotic circuit, which has established itself not only as a paradigm of chaos but also has created a niche in the emerging field of non-linear circuit design. It is due to *Chua's Circuit* and its experimental confirmation on circuits that proposal of newly developed chaotic systems are always accompanied by an electrical circuit equivalent [78, 80, 47, 74, 79, 80, 82, 83, 89, 57].

It was later shown that adding a simple resistor to the inductor gives rise to a canonical circuit to *Chua's Circuit* also called as *Chua's Oscillator* [56].

Since then the field has bifurcated into several domains. Attempts were made to understand *Chua's Circuit* using several different approaches: mapping different bifurcation phenomenon on canonical realizations of *Chua's Circuit*, finding applications to *Chua's Circuit*, understanding Spatio-temporal phenomenon in arrays of *Chua's Circuits*, searching suitable and better electronic realizations of *Chua's Circuits* , understanding nonlinear dynamical systems using *Chua's Circuit* and it's equations, enhancing the complexity of *Chua's Circuit*, etc.

Attempts have also been made by electronic designers to develop different ways of designing *Chua's Circuit*. However, the versatilities of these designs are not fully exploited by non-electrical engineers to validate their theories concerning *Chua's Circuit*. Most of the non-electrical engineers/researchers rely on software simulations for their theories. Reasons can be the technicality involved and excessive use of jargons in papers concerning electronic implementation. Another important point is that despite being a versatile circuit, *Chua's Circuit* has not been able to mark its presence in undergraduate electrical engineering curriculum.

In the present chapter I would like to outline several methods employed by researchers to achieve improvements to the original *Chua's Circuit / Chua's Oscillator*. Herein improvement means alternative realization of *Chua's Circuit* making it suitable for VLSI implementations. The chapter also discusses the factors affecting the frequency, size and robustness of the system and how the designers can achieve a suitable trade-off between these parameters. The final target is to find the most robust, yet easily implementable *Chua's Circuit* so that a kit can be developed to be used by amateurs to understand Chaos Theory through *Chua's Circuit*.

2.1.1 *Chua's Circuit*: An Introduction

Chua's Circuit consists of four linear elements (two grounded capacitors, one grounded inductor and one linear resistor) and one non-linear resistor and is de-

Figure 2.2: Chua's circuit

scribed by the following set of differential equations as given in equation 2.1

Fig. 2.2 shows the circuit diagram of the *Chua's Circuit*, which is an autonomous dynamical system, i.e. it evolves through its natural dynamics even in the absence of any external input.

By substituting:

$$
\begin{aligned}
&x = \frac{v_1}{B_p}, y = \frac{v_2}{B_p}, z = i_3\left(\frac{R}{B_p}\right),\\
&\alpha = \frac{C_2}{C_1}, \beta = \frac{R^2 C_2}{L}, k = sgn\,(RC_2),\\
&a = RG_a, b = RG_b, \tau = \frac{t}{|R\,C_2|}\\
&G_k = \frac{1}{R_K},
\end{aligned}
\tag{2.3}
$$

the equations in dimensionless form can be written as

$$\begin{aligned}\frac{dx}{d\tau} &= k\alpha(y - x - f(x)),\\ \frac{dy}{d\tau} &= k(x - y + z),\\ \frac{dz}{d\tau} &= -k\beta y\end{aligned}\quad, \tag{2.4}$$

$$f(x) = bx + 0.5(a - b)\{|x + 1| - |x - 1|\}. \tag{2.5}$$

Here *sgn(x)* is a standard sign function. The parameter k, which can take the value 1 or -1, specifies the direction of the *Chua's Circuit* dynamics.

These equations, also called as *Chua's equation*, can be studied either through computer simulations [11] or by physical electronic implementations [10]. By adding a linear resistor in series with the inductor, the circuit can generate many more chaotic behaviors than those observed by *Chua's Circuit*. This unfolded *Chua's Circuit* is known as *Chua's Oscillator* and the associated equations are called *canonical Chua's equation* [56, 35].

The book *Chua's Circuit: A Paradigm of Chaos* [56] along with software ABC++ (available at `www.mathworks.com`) serves as an interesting reference for the electronic engineers who wish to explore non-linear dynamic through *Chua's Circuit*.

2.1.2 Chua's Equation and Lorenz Equation

Another chaotic system that has generated worldwide interest is the *Lorenz system*. Originally designed as an approximate model of weather, *Lorenz system* is described by the following set of equations:

$$\begin{aligned}\dot{x} &= \sigma(y - x),\\ \dot{y} &= rx - y - xz,\\ \dot{z} &= xy - bz.\end{aligned} \tag{2.6}$$

where σ, r and b are control parameters.

In comparison to *Chua's Circuit* and *Chua's Oscillator*, Lorenz system contains two non-linearities where as Chua's system consists of only one non-linear term, minimally required for a system to exhibit chaos [64].

Furthermore, in view of electronic implementations, both in VLSI and using discrete components, Chua's diode is easier to implement, as it doesn't contain multiplication of state variables. Note that the implementation of multipliers require more complex circuits (both in VLSI and using discrete implementation) as compared to linear circuits. Further with the recent proposal of four transistors based cubic Chua's diode [48], it becomes much easier to design Chua's system electronically than Lorenz system [47].

The existence of strange attractors in *Chua's Circuit* was proved just after its inception [85], whereas rigorous mathematical proof of existence of chaos in Lorenz system has been recently reported [72, 54]

It has been shown that any third order odd symmetric chaotic autonomous system with three equilibrium points can be easily mapped on *Chua's Circuit* of *Chua's Oscillator* [56]. *Chua's Oscillator* is shown to exhibit more distinct non-periodic chaotic attractors than any of the other chaotic systems known so far [35].

All these aspects along with ease of building, designing, measuring, modeling, low cost implementation and VLSI friendliness [60, 46] makes *Chua's Circuit* above par any chaotic circuit known up to date and hence a paradigm for chaos [56].

2.2 Electronic realizations of Chua's circuit

One of the most interesting features of *Chua's Circuit* is its easy electronic implementation. Soon after its inception, the circuit was studied experimentally [33] thereby confirming the presence of double scroll in it. Due to the presence of linear passive devices, the task of designing *Chua's Circuit* was reduced to designing Chua's diode. In fact, unlike many other chaotic systems, the presence of grounded capacitors and inductors makes *Chua's Circuit* a VLSI friendly chaotic system.

During early phases of *Chua's Circuit* development, the main constraint was that the final circuit should be faithfully able to reproduce the mathematical analysis. However, as the research progressed, attempts were made to completely exploit this versatile chaos generator.

Electronic realization of *Chua's Circuit* is constrained by the following factors:

1. Frequency of operation: The parasitic associated with Chua's diode plays a crucial role in the frequency of operation of *Chua's Circuit*.

2. Size: Apart from battery, the inductor used in *Chua's Circuit* occupies the maximum area. This becomes a major bottleneck when an array of *Chua's Circuit* is being studied. This is one of the motivations for search of inductor-less versions of *Chua's Circuit*.

3. Robustness: One of the important features of the electronic implementation of *Chua's Circuit* is its sensitivity to components used. A robust implementation is dependent on the way inductor and the Chua's diode has been implemented electronically.

Apart from these constraints, researchers also tried to exploit the designed *Chua's Circuit* for purposes like taping third state variable (i.e. current across inductor) [12], easy array implementation [4], low voltage operation [14], easy VLSI implementation [73] and many others.

2.2.1 Chua's Diode

One of the necessary conditions for a circuit to exhibit Chaos is the presence of at least one non-linear element [64]. In case of *Chua's Circuit*, Chua's diode serves as the non-linear element responsible for the stretching and folding dynamics of the attractor [55]. To make the circuit implementation simple, *Chua's circuit* has been originally designed as a piecewise linear circuit [11, 9]. However, smooth non-linearity has also been exploited to design Chua's diode [31, 104, 101]

2.2.2 Piecewise Linear Implementation

Piecewise Chua's diode follows the current-voltage (I-V) characteristics as given in the Equation 2.2.

There has been several attempts to electronically design Chua's diode. The first electronic realization of Chua's diode consists of two Operational amplifier (explained later) and resistors. It exploits the saturation characteristics of operational-amplifiers [67] to implement breakpoints in the I-V curve while varying the values of associated resistors to change the position of the breakpoint [10].

Chua's diode can also be designed using one operational amplifier and diodes as shown in Fig. 2.3 [85].
Herein diodes are responsible for the breakpoint selection [88]. However, due to the presence of high parasitic capacitance, this circuit is unable to operate at higher frequencies. Note that high frequency in this chapter refers to frequency above 1MHz.

M.P. Kennedy gave the earlier robust implementation of one of the *Chua's diode* using off-the-shelf components [10]. His paper, in a tutorial fashion, presents a systematic procedure of designing *Chua's diode*. Owing to its simplicity and use of off-the-shelf components, it has been the most extensively used *Chua's diode* implementation for validating theories concerning *Chua's Circuit* [56].

Few implementations of Chua's diode using devices operating in current mode have also been presented recently [12, 74, 4, 36]. However, whereas [4] focus more toward VLSI implementation, implementation in [12] uses highly precise

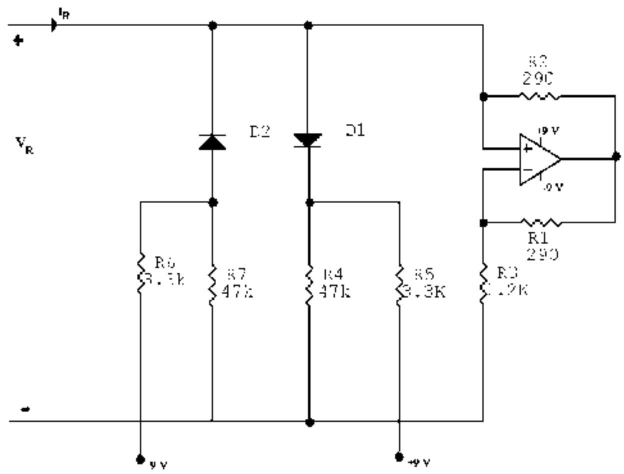

Figure 2.3: One possible implementation of Chua's diode

components and voltages to achieve double scroll. Hence implementation of either of these designs does not attract *Chua's Circuit* designing using standard available off-the-shelf components.

2.2.3 Smooth Non-linearity Implementation

It has been shown recently that all the features of the *Chua's circuit* cannot be represented by piecewise non-linearity. The equation governing the cubic Chua's diode is given by

$$i_R = f(v_R) = av_R + cv_R^3, \tag{2.7}$$

where $a< 0$ and $c>0$ real parts.

Chua's Circuit using smooth nonlinear Chua's diode is presented for the first time in [31]. The implementation uses several high voltage components to realize cubic polynomial V-I characteristic of Chua's diode. A much simpler and better implementation of *Chua's Circuit* with smooth non-linearity has been presented recently in [48]. Owing to its lower parasitic capacitance, the latter implementation operates at frequencies much higher than those reported earlier.

An alternate implementation for Chua's diode can be given by the following equation

$$i_R = f(v_R) = av_R + cv_R\left|v_R\right|, \tag{2.8}$$

where $a < 0$ and $c > 0$.

The circuit implementation using several analog components is presented in [38]A point worth noting is that since the Chua's diode implementation normally requires exploitation of saturation characteristics of active devices used, the values of passive resistors and supply voltages will vary with the type of device used.

The value of capacitance C_1 is limited by the parasitic capacitance associated with Chua's diode which in-turn limits the maximum frequency of operation. In order to compare the performances of different Chua's diodes at different frequencies, different reported implementations of *Chua's diodes* were connected in series with a 1 kΩ resistor and were studied .The results are shown in Fig. 2.4.
These results suggest that maximum frequency of operation can be achieved by the Senani-Gupta implementation of *Chua's diode*.

2.2.4 Inductorless Chua's circuit

One of the major motivations toward search for inductorless version of *Chua's Circuit* is the ease of design as most of the inductors are to be prepared separately in most of the applications and are quite bulky compared to other components

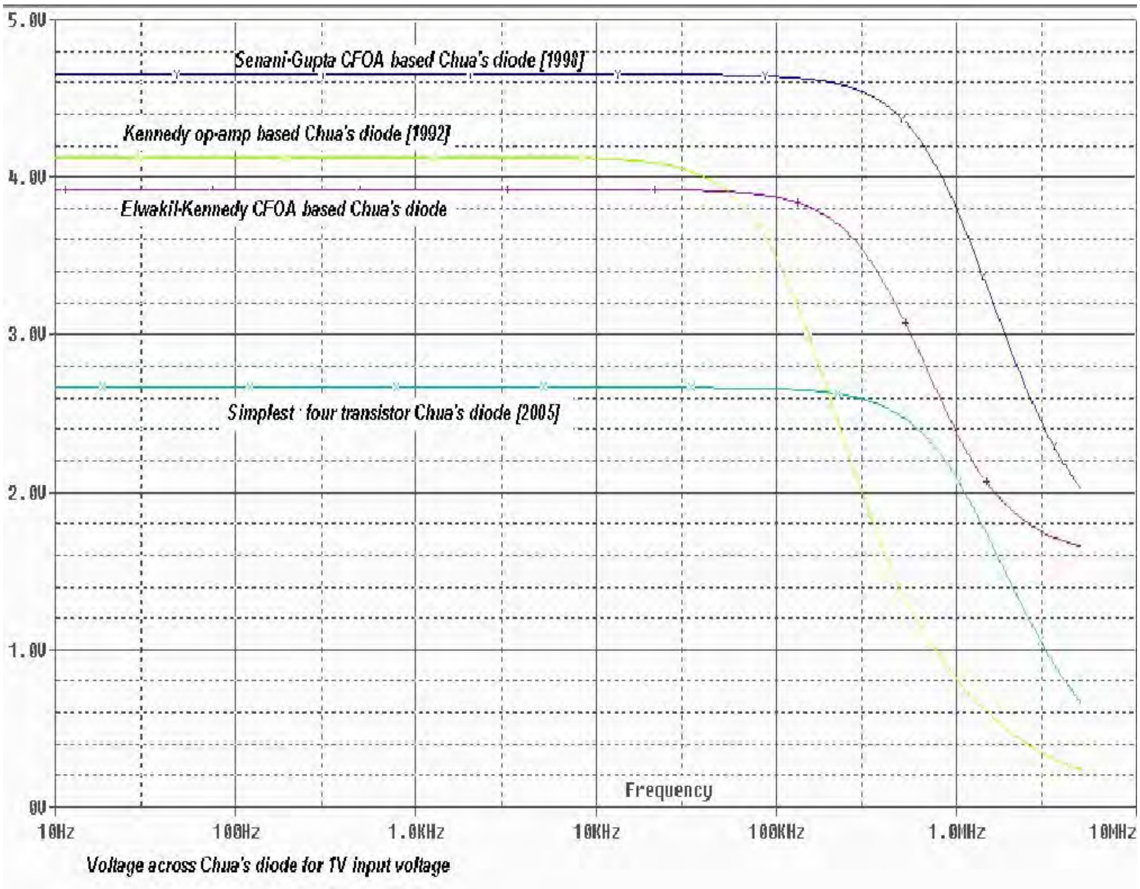

Figure 2.4: SPICE simulation results for Chua's diode. Here X axis represents the frequency of operation while Y axis the voltage (from 0 to 1 V)

[36]. Moreover, inductors are not as ideal as other circuit elements and an inductorless design is also more favorable for VLSI implementation.

There are several ways to design an inductorless version of *Chua's Circuit* . Easiest way is to replace the inductor by a circuit i.e. an R-C (resistor –capacitor) network that imitates its function [84, 43, 12, 4, 37]. Alternatively, the core of *Chua's Circuit* i.e. L-C (inductor-capacitor) tank circuit can also be replaced by a suitable Active-RC sinusoidal oscillator [52, 74]. However, due to the lack of set of necessary and sufficient conditions to exhibit chaos, replacing the tank oscillator by a sinusoidal oscillator serves only as a sufficient condition for *Chua's*

Circuit [74].

First inductorless *Chua's Circuit* implementation was given by Morgul et.al [52]. Herein, the LC tank circuit is replaced by a Wine's bridge oscillator [52, 37, 4]. As shown in [74], replacing the LC tank oscillator with a suitable sinusoidal oscillator yields similar properties as that of *Chua's Circuit* and hence the newly designed circuit can be described as inductorless *Chua's Circuit*.

Replacing the inductor by Active-RC network has been successfully exploited by [12] to design *Chua's Circuit* . For instance, [12] have used a Current Feedback Operational Amplifier (explained later) based inductor realization whereas [37] uses Antonio's GIC (Generalized Impedance Converter) [93] to implement the inductor. Similarly, [4] designed a circuit DOCCII (described later) and then used it to implement the inductor to be used in *Chua's Circuit*.

The advantage of replacing the inductor rather than the tank circuit lies in the fact that bifurcation with respect to β can be studied by varying the inductance (hence only one component). In case of tank circuit replacement, this is achieved by changing several parameters to meet both the condition as well as the frequency of operation.

2.2.5 Frequency of operation

In case of a sinusoidal oscillator, the output power is concentrated in a single-frequency component around the operating frequency of the sinusoidal oscillator *(ω_{osc})*. However, as the system is moved around the chaotic region, the power is spread to more frequency components around ω_{osc}.

The linearized form of *Chua's Circuit* is given by

$$s^3 + a_2 s^2 + a_1 s + a_0 = 0, \tag{2.9}$$

where

$$a_2 = \frac{G}{C_2} + \frac{G + m_i}{C_1}, a_1 = \frac{1}{LC_2} + \frac{G + m_i}{C_1 C_2}, a_0 = \frac{G + m_i}{LC_1 C_2}, \tag{2.10}$$

Here

$$m_i = \begin{cases} m_0, & \text{for inner segments } (= \ -0.8 \text{ normally}) \\ m_1, & \text{for outer segments } (= \ -0.5 \text{ normally}) \end{cases} \tag{2.11}$$

The condition for system to oscillate is given by $(a_1 a_2 = a_0)$

$$G = -\frac{C_1^2 + LC_2 m_i^2}{Lm_i(C_1 + C_2)}, \tag{2.12}$$

and the frequency of oscillation is given by $(\omega_0 = \sqrt{a_1})$:

$$\omega_0 = \frac{1}{\sqrt{LC_2}}\sqrt{1 + \frac{GLm_i}{C_1}}. \tag{2.13}$$

Now whenever a tank oscillator is replaced by Active-RC sinusoidal oscillator, it is done in such a way that the frequency of oscillation of the sinusoidal oscillator is given by

$$\omega_{osc} = \frac{1}{\sqrt{LC_2}}, \tag{2.14}$$

Thus estimated frequency range covered by the spectrum of generated signal is given by

$$\omega_0 = \omega_{osc}\sqrt{1 + \frac{GLm_i}{C_1}} \tag{2.15}$$

Thus, whereas L and C_2 specify the central frequency of operation, L, G, m_i and C_1 are responsible for the range covered by the spectrum. It is clear from simulations in Fig. 2.4 that the highest frequency (above 1 MHz) can be achieved by Senani-Gupta's circuit.

2.2.6 Robustness of Chua's circuit

One of the most important parameters of any system is its robustness. Robustness of *Chua's Circuit* depends on the sensitivity of the system on the components. Adaptive circuits can be used to design a very robust *Chua's Circuit*. However, since this class of *Chua's Circuit* is not currently available, the robustness of several implementations of *Chua's Circuit* with respect to variation in their passive components is studied.

In order to study various implementations of *Chua's Circuit* with respect to variations in their passive components, Monte Carlo simulations on SPICE simulator [44] were done. The parameters of all the *Chua's Circuit* were chosen to make the circuit work in the Double Scroll region and then the values of passive components were varied randomly (following Gaussian distribution) with the specified tolerance values. The results are reported in Table 2.1.

Note that since commercially available inductors have high tolerance value, simulations were performed with high tolerance values for inductance. Even though 50 circuits are not enough to assess the robustness of a given design; they give a fair idea of comparative robustness of the circuits.

A closer look to Table 2.1 yields that the most robust implementation of the design can be achieved through Kilic's Current Feedback Operational Amplifier based Implementation of *Chua's Circuit*. However, *M.P. Kennedy's* implementation is the moderately robust and yet easy to build.

2.3 Electronic Implementations of Chua's circuit

In this section, several proposals of *Chua's Circuit* implementations are presented and explained in context of above sections.

2.3.1 Kennedy's Robust Op-amp realization of Chua's circuit

Obtaining a robust implementation using off-the-shelf components motivated the design of *Chua's Circuit* in this research. It uses two operational amplifiers (op-amps) and 6 resistors to implement the *Chua's diode*, two capacitors, one inductor and a variable resistor.

Figure 2.5: Chua's Circuit in electronic form

The paper presents a systematic procedure to design Chua's diode using op-amp and passive resistors. This implementation of diode has been extensively used to practically confirm the theories concerning *Chua's Circuit* [56]. The practical realization of *Chua's Circuit* using eight-pin dual op-amp IC is shown in Fig. 2.5.

For the values of components reported in appendix A the designed system exhibits Double Scroll behavior. The total cost of producing this design in the laboratory is less than $10.
SPICE simulations were performed to confirm the design and the result is as shown in Fig. 2.6. SPICE simulations were also performed to study the behavior of the circuit at higher frequencies by varying different parameters of the design.

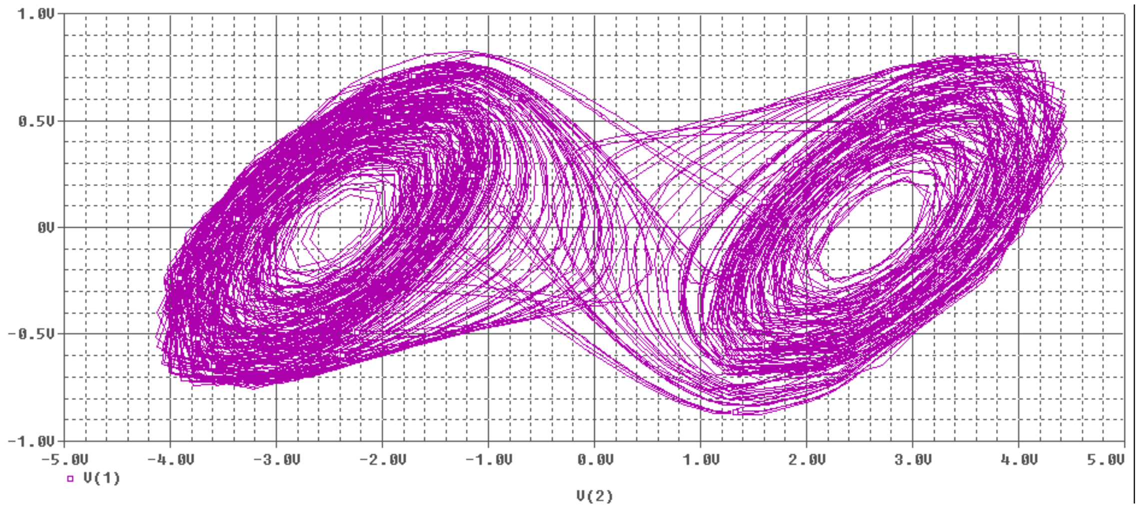

Figure 2.6: Double Scroll observed from Kennedy's implementation

2.3.1.1 *Operational Amplifier*

A simple operational amplifier is a 5 terminal device and acts as a real world approximation to voltage controlled voltage source. Two of its terminals, *V+* and *V-*, are connected to positive and negative power supplies respectively. It has two input terminals designated as inverting (in-) and non-inverting (in+) inputs respectively and an output terminal (out) as shown in Fig. 2.7.

When the voltage difference between the inverting terminals is small in magnitude, the voltage at the output varies nearly linearly with input. This range is called the linear range. In case the input voltage difference is very large and is

Figure 2.7: Operational Amplifier

positive in magnitude, the output attains a value $+E_{sat}$ (positive saturation region), while when it is negative, the output is $-E_{sat}$ (negative saturation region). This characteristic behavior is shown in Fig. 2.8.

Note that Fig. 2.7 assumes that the current through the input terminals is zero and v_{os} represents the input offset voltage in non-ideal op-amp. Thus the characteristic equations of the op-amp can be described by

$$v_{out} = \begin{cases} +E_{sat}, \text{ positive saturation region} \\ Av_d + v_{os}, \text{ linear range. } A \approx 10^5 - 10^9 \\ -E_{sat}, \text{ negative saturation region} \end{cases} \tag{2.16}$$

Figure 2.8: Voltage characteristic of operational amplifier. Here v_d represents difference of the voltage across the input terminals

2.3.2 Torres *et al* Op-amp Realization

One of the disadvantages of the previous design is the use of the inductor as there is a limited range of off-the-shelf commercial inductors. Also, the trade off between the coil size and the maximum allowed inductance leads to very large and inaccurate inductors. Thus the alternative is to replace the inductor with a suitable device that imitates its function.

The inductor of *Chua's Circuit* is replaced by Antoniou's gyrator [94] as shown in Fig. 2.9. The value of inductance is given by

$$L = \frac{C_{L1}R_{L1}R_{L3}R_{L4}}{R_{L2}}. \tag{2.17}$$

Thus, any of these resistors can be used to vary the value of inductance. The complete *Chua's Circuit* designed is as shown in Fig. 2.10.

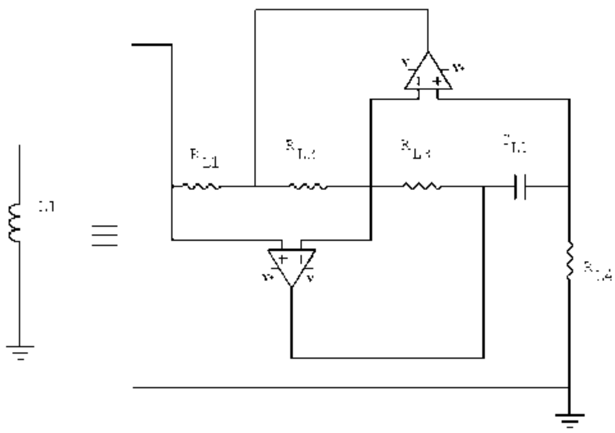

Figure 2.9: Inductor realization using operational amplifier

One of the advantages of the present proposal is its easy and robust implementation using off-the-shelf components. This design also opens the possibilities of controlling and studying *Chua's Circuit* and many of the associated phenomenon through a personal computer [37].

2.3.3 PCChua

In [37] an actuator based *Chua's Circuit* setup called PCChua was designed which has the following features

1. It has a *Chua's Circuit* with three actuators for three state variable of *Chua's Circuit* allowing mono and multi-variable control.
2. These actuators are controlled by the standard analog I/O board.
3. The I/O board is driven by software written for Linux.
4. The inductorless version of *Chua's Circuit* is used thus permitting control over the frequency of operation.

Figure 2.10: Chua's circuit using Inductor realization.

Thus PCChua provides interesting possibilities for studying chaotic phenomenon via *Chua's Circuit* and can serve as an interesting tool for students interested in the field. Note that since the system is driven by hardware-software and mixed signal co-design, it is advisable to use it for lower frequencies as at higher frequencies several non-ideal effects can play the significant role. The original circuit was studied at the resonant frequency of 1.6Hz.

2.3.4 Senani *et al* Current Feedback Operational Amplifier based implementation

Even though this design [37] can be used to monitor the current across the inductor, it cannot be used to extract the same current from the device that can be used later on for the interconnection of two or more *Chua's Circuit* [56]. Also, the parasitic associated with Chua's diode in the design limits its maximum frequency of operation.

Senani *et al* have designed an inductorless version of *Chua's Circuit* using current mode device, called Current Feedback Operational Amplifier.

2.3.4.1 *Current Feedback Operational Amplifier*

Current Feedback Operational Amplifier is a 6 terminal device shown in Fig. 2.11. Apart from *V+* and *V-* terminals which act as power supplies to the device, the characteristic equation of the device is described by

$$\begin{aligned} v_x &= v_y, \\ i_y &= 0, \\ i_z &= i_x, \\ v_w &= v_z, \end{aligned} \tag{2.18}$$

where v and i represents the voltage and current through the terminal in subscript *(x,y,z or w)* respectively.
It can also be represented as a combination of the Current Conveyor (CCII) and a voltage buffer [36]. It is commercially available as AD844 from Analog devices.

In order to achieve high frequency operation, Current Feedback Operational Amplifier based Chua's diode was also designed in Senani's implementation of *Chua's Circuit*. The designed *Chua's Circuit* is shown in Fig. 2.12. For the values of the components shown in appendix A with one Current Feedback Operational Amplifier (with resistor R4) having supply voltages as ±4.05 V while another having ±11.23 V, the system exhibits double scroll behavior. Note that unlike reported in [12], the SPICE results presented here show double scroll behavior for L=9 mH.

The several advantages provided by this design are:

Figure 2.11: Current Feedback Operational Amplifier

1. Current through the inductor is available externally.
2. It employs minimal passive components to implement the inductor. (It uses 3 components in comparison to 5 used by Torres *et al* 2000).
3. The design intelligently incorporate the parasitic associated with Current Feedback Operational Amplifier that makes help the design work at very high frequency.
4. It does not require any component matching.

However, the use of highly precise components and voltages makes it unattractive.

2.3.5 Elwakil-Kennedy Current Feedback Operational Amplifier based implementation

Aimed at designing *Chua's Circuit* for high frequency, a novel implementation of Chua's diode was introduced by Elwakil *et al.* This Current Feedback Operational

Figure 2.12: Senani-Gupta Implementation of Chua's circuit

Amplifier based Chua's diode exploits both the voltage and current characteristics of Current Feedback Operational Amplifier. It uses standard available components and requires fewer resistors than reported in [10]. The designed *Chua's Circuit* is as shown in Fig. 2.13.

For the values reported in the appendix A, the circuit of Fig. 2.13 exhibits double scroll behavior. Apart from the possibility of high frequency applications and the only use of commercially available components, availability of a buffered state variable V_{c1} is one of the main advantages of this proposal.

It also provides current I which can be used for designing a current mode random bit generator [99].

Figure 2.13: Elwakil-Kennedy's Current Feedback Operational Amplifier based Chua's circuit

Figure 2.14: Kilic's Current Feedback Operational Amplifier based Chua's circuit

2.3.6 Kilic's *Chua's Circuit* implementation

The unattractiveness of Senani-Gupta implementation of *Chua's Circuit* lies in the use of precise components in designing Chua's diode while that of Elwakil-Kennedy's Current Feedback Operational Amplifier based implementation is the use of a passive inductor. Kilic's *hybrid* implementation [62] uses a Current Feedback Operational Amplifier based inductor from Senani-Gupta's implementation and a Current Feedback Operational Amplifier based Chua's diode from Elwakil-Kennedy's implementation as shown in Fig. 2.14.

This implementation not only makes the design easier to integrate and controllable but can also be implemented using off-the-shelf components. The design was further experimentally verified in [62] at different frequencies.

As pointed out in application section, there exist several possibilities for design-

Figure 2.15: Morgul's Wein's Bridge Oscillator based Chua's circuit

ing/evolving *Chua's Circuit*. The hybrid realization of *Chua's Circuit* [62] can be treated as a subset of such class of evolved circuits. However, since there are several other possibilities, the study of all these circuits for robustness, frequency range and ease of design is out of the scope of the present chapter.

2.3.7 Morgul's Wein's bridge based *Chua's Circuit*

In this chapter the inductorless *Chua's Circuit* was designed by replacing the LC tank circuit of *Chua's Circuit* by a Wein's bridge oscillator [41]. The implementation uses Kennedy's robust implementation of Chua's diode. The complete circuit diagram of *Chua's Circuit* is shown in Fig. 2.15.

The author has in fact studied Wein's bridge based *Chua's Circuit* in two modes:

one, where the Wein's bridge is in oscillating mode [52] and another where it is not in oscillatory mode [50].

For the values presented in appendix A, various chaotic behaviors were observed over a large value of connecting resistor, R. This scheme of replacing the tank oscillator by an Active-RC circuit was later generalized by Elwakil and Kennedy [82].

2.3.8 Gandhi's Dual Output Current Conveyor II based realization

My design proposes a novel implementation of Chua's diode and inductor replacement using a non-commercial device called Dual Output Current Conveyor (DOCCII).
DOCCII is a 6 terminal device much like CCFOA with terminals *x,y,z+,z-,*$V+$ and *V-*, *V+* and *V*-terminals acts as power supplies to the device. The characteristic equation of the device is given by

$$\begin{aligned} &v_x = v_y, \\ &i_y = 0, \\ &i_{z+} = i_x, \\ &i_{z-} = -i_x. \end{aligned} \tag{2.19}$$

where v and i represents the voltage and current through the terminal in subscript *(x,y,z+ or z-)* respectively. This design provides several advantages compared to its earlier counterparts. These advantages include

1. Similar to the Senani's implementation, the current across the inductor is available without modifying the design.

2. Similarly to the Kennedy and Elwakil's Current Feedback Operational Amplifier implementation, the current from Chua's diode is available which can be used to generate true random bits.

3. The voltage across the inductor is available in the form of current, which, as shown, can be used in designing a hyperchaotic system.

4. It also opens up the possibility of designing low area and low power autonomous Cellular Neural/Non-Linear Networks composed of inductorless version of *Chua's Circuit*.

5. This implementation of *Chua's Circuit* provides the advantage over all proposed circuits in terms of no hardware requirement for coupling, availability of several state variables and grounded resistor as control parameter.

The idea was developed during my work at STMicroelectronics and has been granted a US patent [6] while an Indian patent [7] is pending on the same. Topologically it is similar to the one shown in Fig 2.16 wherein MOCCII (Multiple Output Current Conveyor) is replaced by DOCCII. The approach toward VLSI and non-availability of commercial DOCCII makes the design unattractive for implementation using off-the-shelf components.

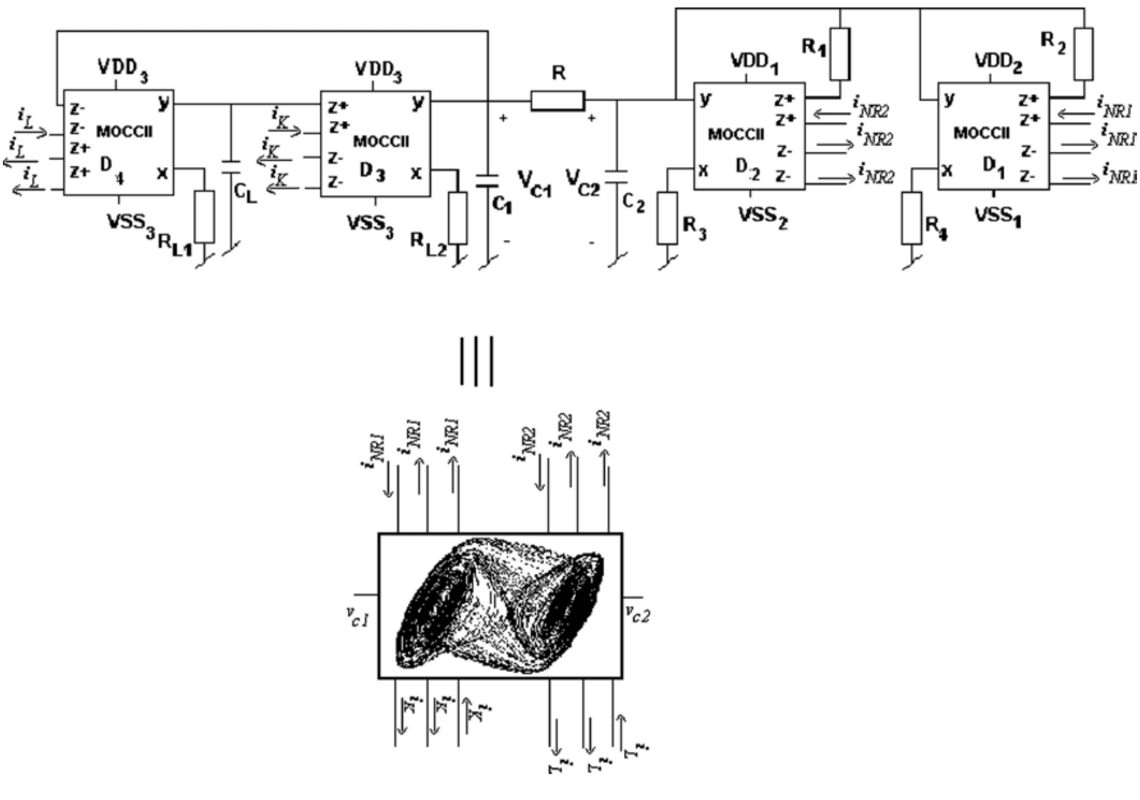

Figure 2.16: MOCCII based Chua's Circuit.

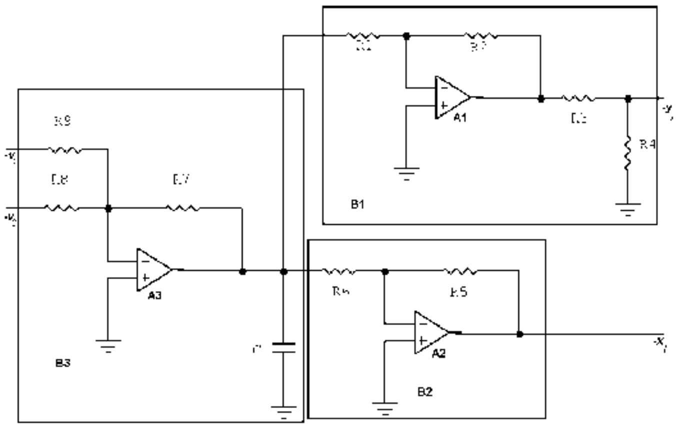

Figure 2.17: State Controlled Cellular Non-linear Network(SC-CNN).

2.3.9 CNN based *Chua's Circuit* implementation

Cellular Neural/Non-linear Networks were first introduced by Chua and Yang [58]. Since then this field has found several applications and is a key to several image processing and non-linear system tasks [87].

Here the original equation of the CNN cell was modified to implement a new type of CNN using an operational amplifier. The equations governing the new CNN cell are

$$\begin{aligned} \dot{x_j} &= -x_j + a_j y_j + G_o + G_s + i_j, \\ y_j &= 0.5\left(|x_j+1| - |x_j-1|\right). \end{aligned} \tag{2.20}$$

Here j is the cell index, x_j is the state variable, y_j is the cell output, a_j is a constant parameter and i_j is the threshold value. G_o and G_s are linear combinations of the output and state variables respectively of the cells used in the CNN model. The implementation of this State Controlled CNN (SC-CNN) cell is shown in Fig. 2.17.

Three fully connected such cells with specific resistor values will constitute a *Chua's Circuit* (Fig. 2.18).

Figure 2.18: Chua's circuit using SC-CNN

An alternative implementation using Four Terminal Floating Nullor is presented in [68]. The implementation is adequately supported by SPICE simulation results. It uses CMOS realization of FTFN as given in [91] for simulations. A point worth noting is that FTFN can also be implemented using negative operational mirrored amplifier OMA- [71, 5, 92, 36] and hence using commercially available operational amplifier and current mirrors it can be implemented in laboratory.

A Current Feedback Operational Amplifier (Current Feedback Operational Amplifier, commercially available as AD844) based SC-CNN has also been implemented recently [68]. This proposed idea of *Chua's Circuit* is adequately supported by experimental results.

Whereas, these designs provide an interesting way of designing *Chua's Circuit* through a state variable approach, the system is unattractive due to high use of active and passive components. These designs are more suitable for studying coupling of several *Chua's Circuit*. Further, the use of programmable resistors in the cells will make the designed CNN more flexible and user friendly to study complex phenomenon in the interaction of several *Chua's Circuits*.

2.3.10 Field Programmable Analog Array (FPAA) implementation

A Field-Programmable Analog Array (FPAA) is an integrated circuit which can be configured to implement various analog functions using a set of configurable analog blocks and a programmable interconnection network, and is programmed with the use of on-chip memories. These devices are available commercially and provide simple and easily programmable re-configurable analog designs. Anadigm provides one such commercially available FPAA called AN221E04.

The easiest way to model *Chua's Circuit* on FPAA is by using the state variable approach. The equations (dimensionless) of *Chua's Oscillator* can be transformed to the following form

$$\begin{aligned} \dot{x_1} &= -x_1 + a_1 y_1 + s_{11} x_1 + s_{12} x_2, \\ \dot{x_2} &= -x_2 + s_{21} x_1 + s_{23} x_3, \\ \dot{x_3} &= -x_3 + s_{32} x_2 + s_{33} x_3, \end{aligned} \quad . \tag{2.21}$$

where

$$a_1 = \alpha(m_1 - m_0), \quad s_{33} = 1 - \gamma, \quad s_{21} = s_{23} = 1, \quad s_{11} = 1 - \alpha \cdot m_1, \quad s_{12} = \alpha \text{ and } s_{23} = -\beta \tag{2.22}$$

These equations can be easily programmed on the FPAA kit provided by Anadigm as shown in [90]. Apart from implementing single *Chua's Circuit* , this kit can also be used to implement interconnected *Chua's Circuits.*

One important aspect of this electronic realization of *Chua's Circuit* is that similarly to [37], this approach can be used for educational purpose to study complex systems. Apart from the ease of design, it also provides the advantage of complete control of all the parameters of *Chua's Circuit* and hence permits flexibility to explore circuit behavior for an entire range of parameters, a flexibility missing in [37].

2.3.11 O' Dohonogue *et al* Four transistor diode implementation

This is the simplest and very fast *Chua's Circuit* implementation. It uses only four transistors (or two inverters) to design Chua's diode and the parasitic associated with Chua's diode was taken as C_1. The circuit diagram of the complete *Chua's Circuit* is shown in Fig. 2.19. This oscillator is designed using off-the shelf components and is simple enough to be used by people from non-electrical background to investigate chaotic behavior in electronic circuits.

Apart from being a simple, robust and fast implementation of *Chua's Circuit*, it also has a cubic like non-linearity for Chua's diode. Thus many of the features, which otherwise are missing in piecewise linear V-I characteristics can be observed in the present design. Both in comparison to previous piecewise linear implementations and the cubic implementation of Chua's diode [31], the present design provides a major reduction in hardware without compromising the performance.

For the values reported in appendix A, double scroll behavior was observed.

2.3.12 Alternate Implementation of Fast and Simple *Chua's Oscillator* with Cubic Non-linearity

Even though the above proposal of *Chua's Circuit* is very simple and fast, it has its inherent shortcomings as use of a passive inductor, the extra hardware requirement to monitor state variables, the extra hardware requirement to couple several *Chua's Circuit*,the non-availability of current across the inductor, etc.

However, replacing the synthetic inductor and the resistor by 3 commercially available devices (Current Feedback Op-Amp; AD844) increases the versatility of the oscillator to a large extent without compromising the performance, simplicity and the cost-effectiveness of the solution provided above.

Figure 2.19: Simplest *Chua's Circuit* Implementation.

Fig. 2.20 shows the implementation of *Chua's Oscillator* using an AD844 based inductor as the replacement for the inductor.

Under ideal conditions the value of inductance is given by $L = CR_1R_2$. The parasitic effects of Current Feedback Operational Amplifier (50 Ω resistance at X terminal and 4.5pF ||3M Ω at Z terminal) can be easily incorporated by an appropriate choice of C, R1 and R2.

For VDD = -VSS =15V, $R_1 = R_2 = 950\ \Omega$, C_1 =534 pF, C_2=49 pF, C=25 pF and R = 0.95k Ω, the system shows a double scroll behavior. The SPICE simulations results are shown in Fig. 2.21.

The advantages of the present proposals are as follows:

1. The current across the inductor is available in form of buffered voltage at W_2 that can further be used in designing complex circuits on board [65, 4]. This voltage can also be used to study the behavior of the current across the inductor. This behavior is normally not studied in circuit realizations of *Chua's Circuit*

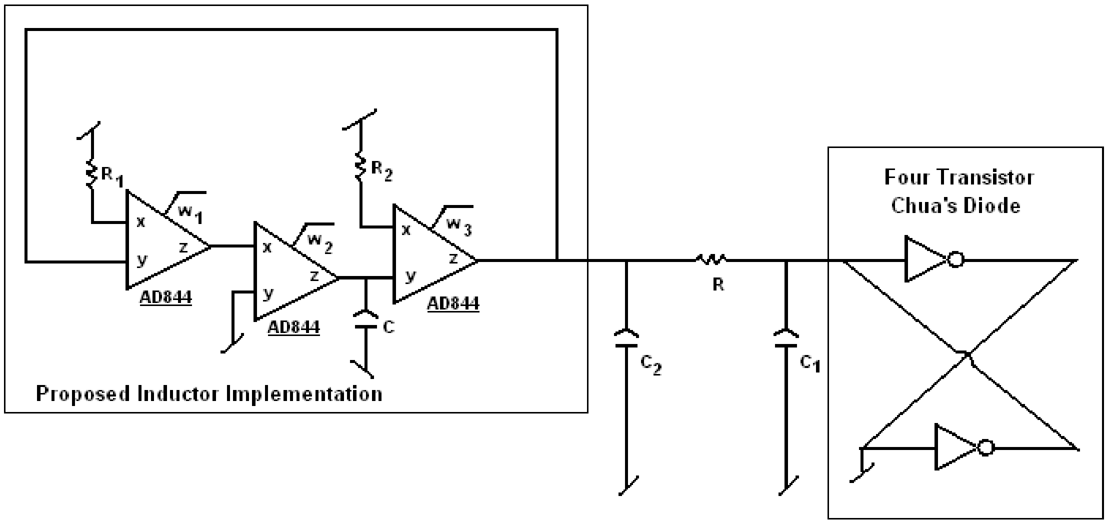

Figure 2.20: Improvement to the simplest *Chua's Circuit* Implementation.

oscillator due to the difficulty of tapping this current. This can be stated as the major advantage of the present idea.

2. No additional voltage buffer is required for the voltage across capacitor C_2. This voltage is available at W_3 (Fig. 2.20).

Comparison with other ideas is as follows

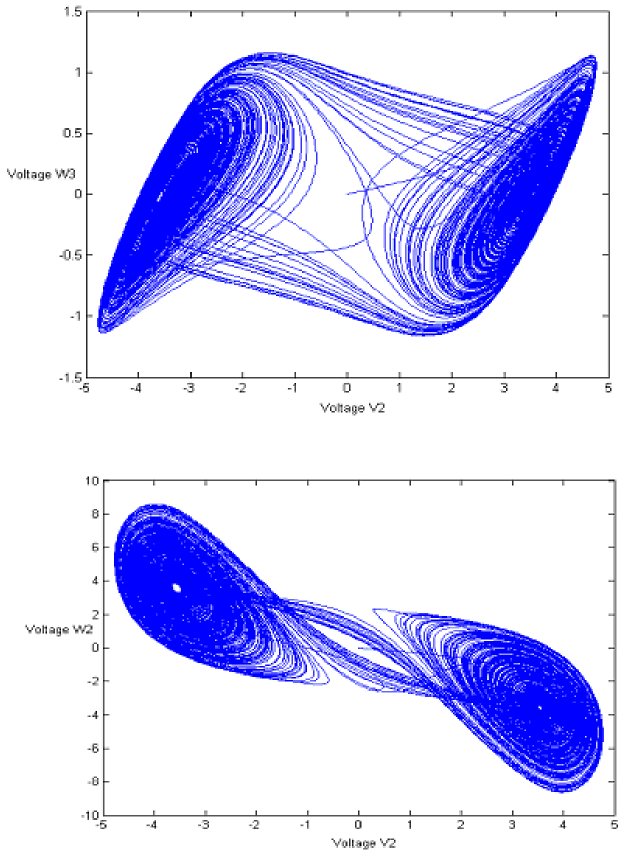

Figure 2.21: SPICE Simulations of my implementation

Reference Number	Advantages of my proposal with respect below mentioned implementations
Kennedy 1992	Cubic non-linearity, inductor less realization.
Torres *et al* 2000	Less active and passive components and cubic nonlinearity.
Elwakil-Kennedy 2000	Cubic non-linearity, inductor less realization.
Senani-Gupta 1998	Cubic non-linearity, grounded passive components.
Morgul O. 1995 (inductorless)	Cubic non-linearity, grounded passive components.
Zhong-Ayrom 1985	Cubic non-linearity, inductor less realization.
Zhong 1994	Reduced hardware, inductor less realization.
Arena *et al* 1995	Reduced hardware.
Morgul O. 1995 (wein's bridge)	Cubic non-linearity.

Note that the main advantage of the inductorless realizations like the current one is that the bifurcation sequence can also be studied by varying the inductance value (and hence β) without varying the resistance R. Herein also the β factor of bifurcation diagram (Fig. 2.22) is inversely proportional to R_1 and R_2.

Thus the present proposal provides several advantages over earlier proposals including [48] without compromising the simplicity and the speed of the design.

2.3.13 Kilic *et al* Current Feedback Operational Amplifier based Inductorless Chua's circuit

The design presented in the chapter refers to a mixed-mode Inductorless *Chua's Circuit* designed by transforming autonomous *Chua's Circuit* and non-autonomous Murli-Lakshmanan-Chua's circuit via switching method. For the purpose of the present chapter, the design of the Current Feedback Operational Amplifier based

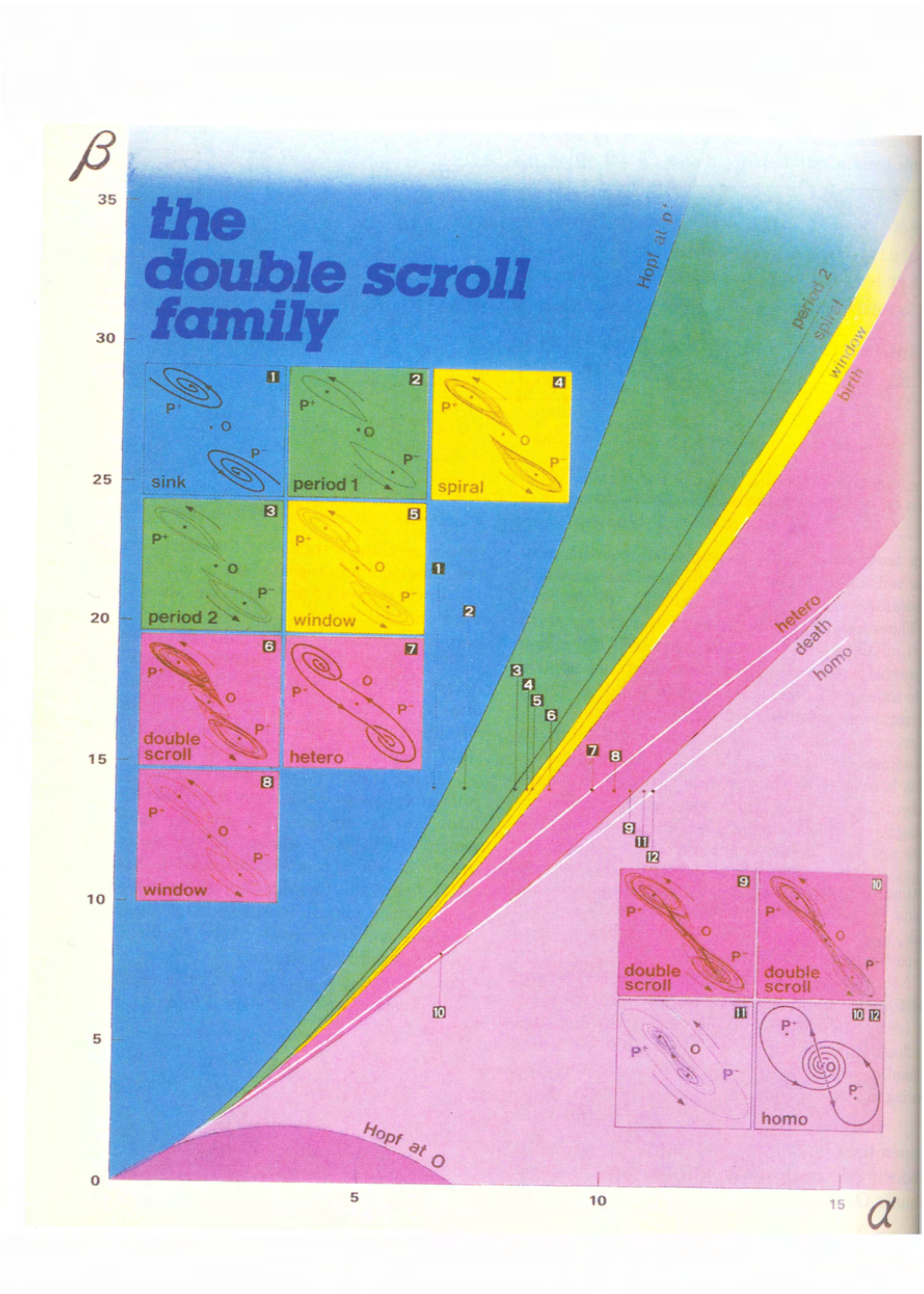

Figure 2.22: Bifurcation Diagram.

Figure 2.23: Chua's circuit from Kilic-Yildrim's mixed mode implementation

Chua's Circuit presented in Kilic's paper will be considered.

In designing *Chua's circuit*, the inductor of an original *Chua's Circuit* was replaced by a Current Feedback Operational Amplifier based design shown in Fig. 2.23. Herein two Current Feedback Operational Amplifiers along with two resistors and one capacitors simulates the inductance with the value given by $L = C_L R_{L1} R_{L2}$. Thus by choosing appropriate values of $C_L, R_{L1} and R_{L2}$, inductance required designing for *Chua's Circuit* could be realized.

For the values give in appendix A, double scroll was observed in this implementation. The SPICE results are shown in Fig. 2.24.

Figure 2.24: Double Scroll

2.3.14 A Four Element Chua's Circuit

Recently a four element *Chua's circuit* has also been proposed by Prof. Chua and his collaborator [106] where in they have designed a simple four element lossless *Chua's circuit* which doesnt requires the bifurcation resistor. It is attributed to the fact that it requires negative passive compoments. Following are the few observations with respect to this design

1. It shows double scroll at R=0 but to observe the routes to chaos it has to vary the value of resistor and hence becomes five terminal device.

2. It requires negative passive components. Since negative passive components realization requires active components the final circuitary tends to be bulky.

3. The advantage of present proposal will lie in realizing negative components as impedence converters. This will make the design tunable with respect to α and β parameters.

Our aim was to explore a robust plug and play design which can be easily realized using off-the-shelf components using positive passive components. Another aim was to expose students to the field of Chaos theory using a very simple plug and play circuit. Thus we are not taking into account this design for comparison. Indepth study of this design requires a separate module and is not the topic of current dissertation.

Table 2.1: Robustness Analysis of *Chua's circuits*

Design	**Tolerance Value (%)**			**Runs**	**Fail**	**One Scroll**	**Success %)**
	R	**C**	**L**				
Kennedy	**5%**	**5%**	**5%**	**50**	**15**	**5**	**60%**
	3%	**3%**	**3%**	**50**	**5**	**1**	**88%**
	1%	**1%**	**3%**	**50**	**0**	**0**	**100%**
Torres et al]	**5%**	**5%**	**-**	**50**	**2**	**6**	**84%**
	3%	**3%**	**-**	**50**	**0**	**2**	**96%**
Elwakil Kennedy	**5%**	**5%**	**5%**	**50**	**11**	**10**	**58%**
	1%	**1%**	**3%**	**50**	**1**	**7**	**84%**
	3%	**3%**	**10%**	**50**	**7**	**10**	**66%**
O'Dohonogue	**3%**	**3%**	**5%**	**50**	**2**	**1**	**94%**
	5%	**5%**	**10%**	**50**	**8**	**3**	**78%**
My design	*3%*	*3%*	*-*	*50*	*7*	*3*	*80%*
	1%	*1%*	*-*	*50*	*0*	*2*	*96%*
Senani et al	**5%**	**5%**	**-**	**50**	**15**	**3**	**64%**
	3%	**3%**	**-**	**50**	**10**	**6**	**68%**
	1%	**1%**	**-**	**50**	**0**	**1**	**98%**
Kilic et al Case 1	**5%**	**5%**	**-**	**50**	**15**	**3**	**90%**
	3%	**3%**	**-**	**50**	**10**	**6**	**98%**
Kilic et al Case 2	**5%**	**5%**	**-**	**50**	**1**	**3**	**92%**
	3%	**3%**	**-**	**50**	**0**	**0**	**100%**
Kilic et al Case 3	**5%**	**5%**	**-**	**50**	**0**	**2**	**98%**
	3%	**3%**	**-**	**50**	**2**	**4**	**88%**
Morgul	**3%**	**3%**	**-**	**50**	**21**	**4**	**50%**
	1%	**1%**	**-**	**50**	**16**	**5**	**58%**
Kilic 2006	**3%**	**3%**	**-**	**50**	**0**	**3**	**94%**

2.3.15 Summary of Different Designs

Following table will compares different topologies

Table 2.2: Comparison of Different Implementations Of Chua's Circuit

Reference Number	Inductorless	Active Components	Passive Components	Current across inductor	Buffered Voltages
Kennedy 1992	No	2	9	No	No
Torres *et al* 2000	Yes	4	13	No	No
Elwakil-Kennedy 2000	No	2	8	No	No
Senani-Gupta 1998	Yes	4	10	Yes	No
Arena *et al* 1995	Yes	9	30	No	Yes
Morgul O. 1995 (wein's bridge)	Yes	3	14	No	No
Gandhi DOCCII	Yes	4	10	Yes	Yes
Kilic 2006	Yes	5	10	Yes	No
O'Dohonogue	No	2	4	No	No
My Implemenation	Yes	5	6	Yes	Yes

2.4 Conclusion

In this chapter a series of electronic implementations of *Chua's circuits* is explored and several interesting observations are made. These observations are summarized as under

1. A comparison of Chua's attractor with Lorenz attractor is done and it was found that in addition to being algebraically simpler, *Chua's Circuit*

provides several advantages compared to Lorenz attractor and hence can be used as the best example for the study and development of systems based on chaos.

2. Several electronic realizations of *Chua's Circuit* were studied for robustness through SPICE simulations and it was found that the most robust implementation for moderate frequency operation is that given by Kilic.

3. An alternative implementation of *Chua's Circuit* with cubic non-linearity is proposed which provides several advantages over previous implementations of the *Chua's circuit.* These advantages have been thoroughly discussed and proposed implementation is adequately supported by SPICE simulation results. An important aspect of this design also lies in its modification to the programmable third order complex cell, which can be used in CNN-Universal Machines giving rise to a new type of Cellular Wave Computer [42]. I will show one such Cellular Wave Computer in the application chapter of dissertation.

4. Chua's circuits can also be easily programmed on commercially available Field Programmable Analog Arrays (e.g. AN221E04 provided by AnadigmŽ) and hence can be used for pedagogical purpose.

Apart from the above mentioned observations and results, a systematic procedure to built *Chua's Circuit* in lab is presented (Appendix A). With the 15 different *Chua's Circuit* implementations were built using the described procedure and the birth and death of double scroll was successfully observed in each of them. Several other aspects like effect of supply voltage variation on scrolls and bifurcation with respect to inductance variations was also observed.

Concluding Statement :

1.1.1 I compared the robustness of different proposed Chua's circuits.
1.1.2 I have analyzed all the proposed *Chua's Circuit* as a coupling between a sine wave oscillator and Chua's diode.
1.1.3 Based on this analysis, I have designed a novel *Chua's Circuit* using AD844 based inductor and simplest Chua's diode. My design

provides advantages as high frequency operation (order of MHz), simple design, availablity of current across inductor and grounded passive components as one of the few advantages over previous designs.

This *Chua's circuit* decomposition methodology can be helpful in developing a software module which can automate the design of newer *Chua's circuit* design topologies. These newly evolved topologies may not only be human competitive in terms of time taken to evolve, performance and robustness but can also be patentable. We will discuss this aspect of chaotic circuit evolution in our next chapter.

Chapter 3

Evolution of Chua's Chaotic Circuits using Genetic Algorithms

3.1 Evolution of Chua's Chaotic Circuits using Genetic Algorithms

3.1.1 Introduction

Electronic Design Automation (EDA) has emerged as a backbone to the Integrated Circuits (IC) industry over the past few decades. The exceptional growth of EDA vendors like Cadence, Synopsys, Mentor Graphics, etc. act as a testimonial to this revolution. With "time to market" taking paramount importance in IC industry, these companies are moving rapidly toward analog circuit automation.

An interesting emerging field in analog circuit design is the field of nonlinear circuit designing. Recent success of Cellular Nonlinear Networks [87, 42] in several image processing tasks, modeling mammalian retina, sensory computation, etc. has fueled an increasing interest in designing nonlinear circuits. One reason for this is that nonlinear circuits yield rich and relatively unexploited phenomenon like bifurcation, fractals and chaos. One of the highly studied nonlinear analog chaotic circuit is Chua's circuit [56].

I have recently demonstrated a fast, reliable and human competitive automation of nonlinear analog circuit. In the current subsection, building human competitive Chua's diode and Chua's circuit was taken as a prototype to demonstrate the use of GA. The reason for choosing this circuit is that since the inception of Chua's circuit only around ten different electronic versions of Chua's circuit has been designed. One reason for this small number of implementation is attributed to the lack of nonlinear resistor design techniques. A software which can design such system takes off the burden from the shoulder of the designer.

I have evolved a whole novel set of nonlinear circuits by implementing Genetic Algorithms (GAs) in SPICE. I have also evolved a new class of Chua's diode and Chua's circuits using discrete components. This is an original case study and is a first successful attempt to evolve a whole class of nonlinear circuits including Chua's circuit using any of the automated methods.

3.1.2 A Brief Introduction to Genetic Algorithms

GAs are adaptive heuristic search algorithm based on the evolutionary ideas of natural selection and genetics. As such they represent an intelligent exploitation of a random search used to solve optimization problems.

GAs simulate the survival of the fittest among individuals over consecutive generation for solving a problem. Each generation consists of a population of character strings that are analogous to the chromosome that we see in our DNA. Each individual represents a point in a search space and a possible solution. The individuals in the population are then made to go through a process of evolution.

GAs are based on an analogy with the genetic structure and behavior of chromosomes within a population of individuals using the following foundations:

1. Individuals in a population compete for resources and mates.

2. Those individuals most successful in each 'competition' will produce more offspring than those individuals that perform poorly.

3. Genes from 'good' individuals propagate throughout the population so that two good parents will sometimes produce offspring that are better than either parent.

4. Thus each successive generation will become more suited to their environment.

3.1.2.1 Implementation Details

Based on Natural Selection

After an initial population is randomly generated, the algorithm evolves the through three operators:

1. selection which equates to survival of the fittest;

2. crossover which represents mating between individuals;

3. mutation which introduces random modifications.

3.1.2.2 The Algorithms

1. randomly initialize population(t)

2. determine fitness of population(t)

3. repeat

   (a) select parents from population(t)

   (b) perform crossover on parents creating population(t+1)

   (c) perform mutation of population(t+1)

   (d) determine fitness of population(t+1)

4. until best individual is good enough

3.1.3 Genetic Algorithms to design nonlinear resistors

The input provided by the user to the software interface is the number and type of active components the user plans to use. The system takes a population of 60 individuals in the first generation and then evolves the new generations from them. The new generation contains genetically fit chromosomes which are obtained by sorting the fitness function and eliminating the weakest members of the generation. The fitness function is defined by the following equation:

$$g(x) = ax + (b - a)\left[|x + B_p| - |x - B_p|\right], \tag{3.1}$$

where a, b are slope constants and B_p is called the break point constant. The equation is same as described in Equation 2.2.
The mutation of chromosomes is random and they also cross over randomly to generate a child. The selection criteria is based on fitness function and the fitness is calculated by the standard least mean square error calculation method.

Thus movement from one generation to another involves the selection, crossover of the selected parents based on various schemes, mutating the evolved child chromosome and testing its fitness value. In order to make the process more natural, sometimes crossover is replaced by cloning with a pre-defined probability.

It takes 5-20 minutes to evolve one Chua's diode (assuming a success) on a single Xeon 3.4GHz HT personal computer. Interestingly, in order to avoid the bottlenecks from the SPICE simulator as much as possible, the source-code of the SPICE simulator was modified to incorporate the GAs module. The bottleneck of the present approach is the fact that only one circuit can be simulated at a time. Since it pertains DC simulation, the man-minutes for the single simulation is almost negligible. Thus without even using a cluster of computers or a better algorithm for parallel computation, the system is way faster than the human intuitive way of designing.

3.1.4 Evolved Analog Circuits and SPICE results

An easily available operational amplifier from Analog Devices with fixed supply voltages was provided to the program and the system was instructed to evolve specified analog nonlinearity (in present case Chua's diode) using two operational amplifiers of the same type. The circuit is called 'evolved' completely if the fitness value is less than the specified error. Further, it was also instructed to the system to stop evolving if the result is not achieved in a specified number of generations. An option to force the circuit to stop due to the excessive 'memory requirement' of the SPICE simulator after certain generations was also provided to save time and redundant results. Note that in order to speed up the evolution and avoid memory constraints, a template circuit was provided initially in the first generation.

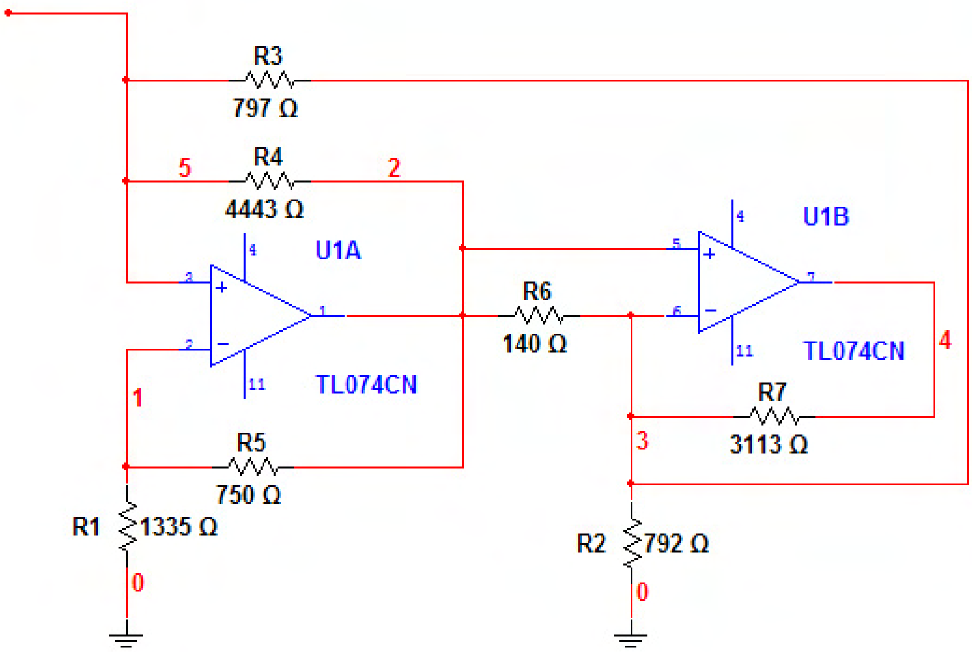

Figure 3.1: One Evolved Nonlinear Resistor using TL074CN operational amplifier

3.1.4.1 *Evolved Analog Nonlinear Resistors (Chua's Diode)*

A novel Chua's diode was evolved when the above template was allowed to run for 2-3 minutes. Fig. 3.1 shows the schematic diagram of the evolved nonlinear analog resistor or Chua's diode. Since the priority to the system was to map the fitness function with as few errors as possible, the component values of resistances were allowed to have floating (maybe commercially non available) values. The values of resistances used are provided in Table 3.1. The supply voltage to the operational amplifier has been assumed to have the constant value of ±12 V.

parameter	software value	real value
C_1	10 nF	10 nF
C_2	100 nF	100 nF
L_1	18 mH	18 mH
R_1	1334.760010 Ω	1334 Ω
R_2	792.000000 Ω	792 Ω
R_3	797.880005 Ω	797 Ω
R_4	4443.279785 Ω	4443 Ω
R_5	750.520020 Ω	750 Ω
R_6	140 Ω	140 Ω
R_7	3112.879883 Ω	3112 Ω

Table 3.1: Software and real parameter values

Fig. 3.2 shows the SPICE simulation results for the evolved Chua's diode with component values presented in Table 3.1. Note that along each I-V characteristic of each amplifier is not exactly but approximately similar to that provided by the original equation. This is the best approximation achieved by the system in specified number of generations and time allocated to the system.

3.1.4.2 *Evolution of Chua's chaotic circuits*

In order to design a Chua's circuit, the approach to break the chaotic system into nonlinear and linear components is followed in the present case. The nonlinearity was specifically chosen to evolve a whole new set of different implementations of

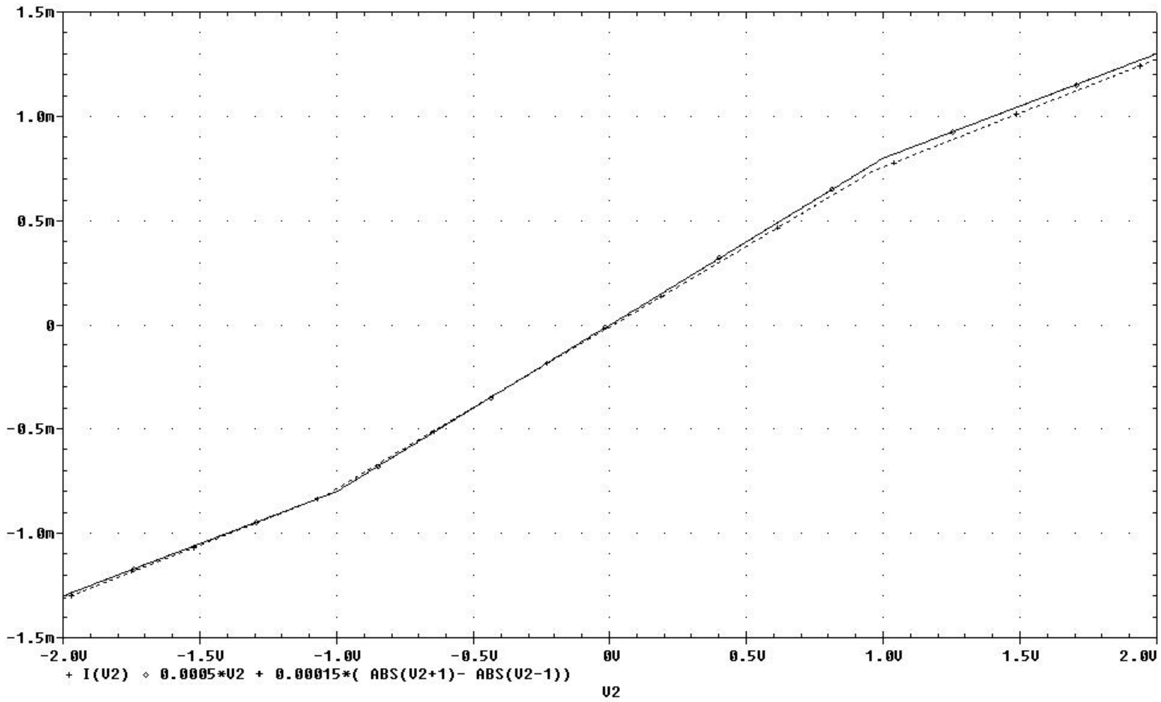

Figure 3.2: The I-V plot (SPICE) for nonlinear analog resistor also called Chua's diode

Chua's circuits using GAs. Thus in this regard, in the circuit implementation of Chua's circuit the original nonlinearity of Chua's circuit was replaced by the evolved Chua's diode and the route to Chaos via period doubling was observed.

The time series of Chua's circuit designed using evolved Chua's diode is as shown in Fig. 3.3.

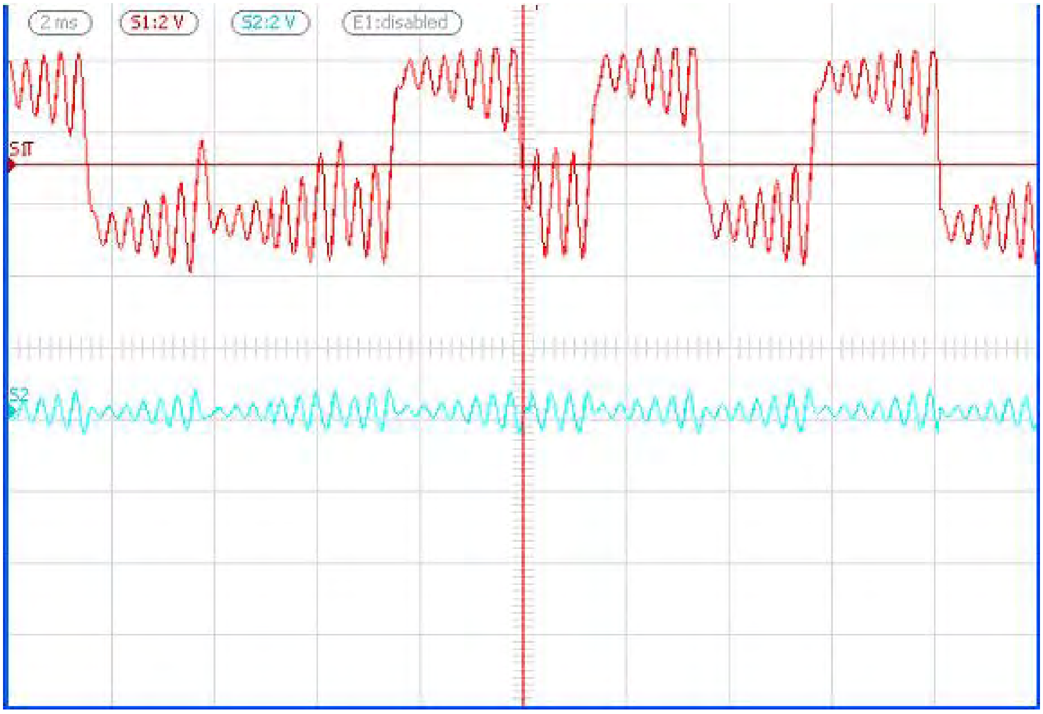

Figure 3.3: Time Series of Evolved Chua's Circuit (SPICE)

Fig. 3.4 provides the simulation results obtained by using Chua's diode of Fig. 3.1. The other component values can be seen in the second column of Table 3.1.

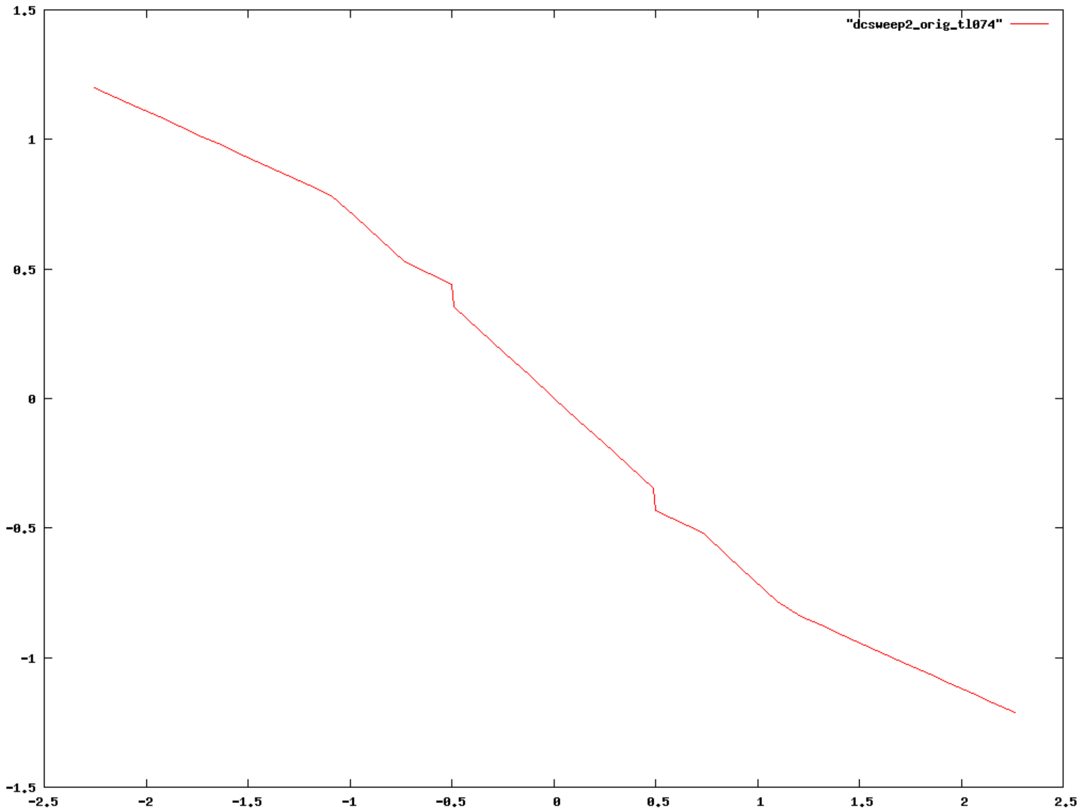

Figure 3.4: The I-V plot (oscilloscope trace) for nonlinear analog resistor also called Chua's diode

3.1.5 Experimental Verification

Since the system is asked to generate characteristics with very high accuracy, these values to 6 decimal places are generated by the system. Once the values are achieved, the decimal places can be truncated and still I get the required nonlinear resistor with almost negligible change with respect to exact values. The breadboarded version of the Chua's circuit with the evolved Chua's diode is as shown in Fig. 3.5.

The entire route of the bifurcation via α parameter variation was observed. I have obtained similar results with all the evolved nonlinear resistors.

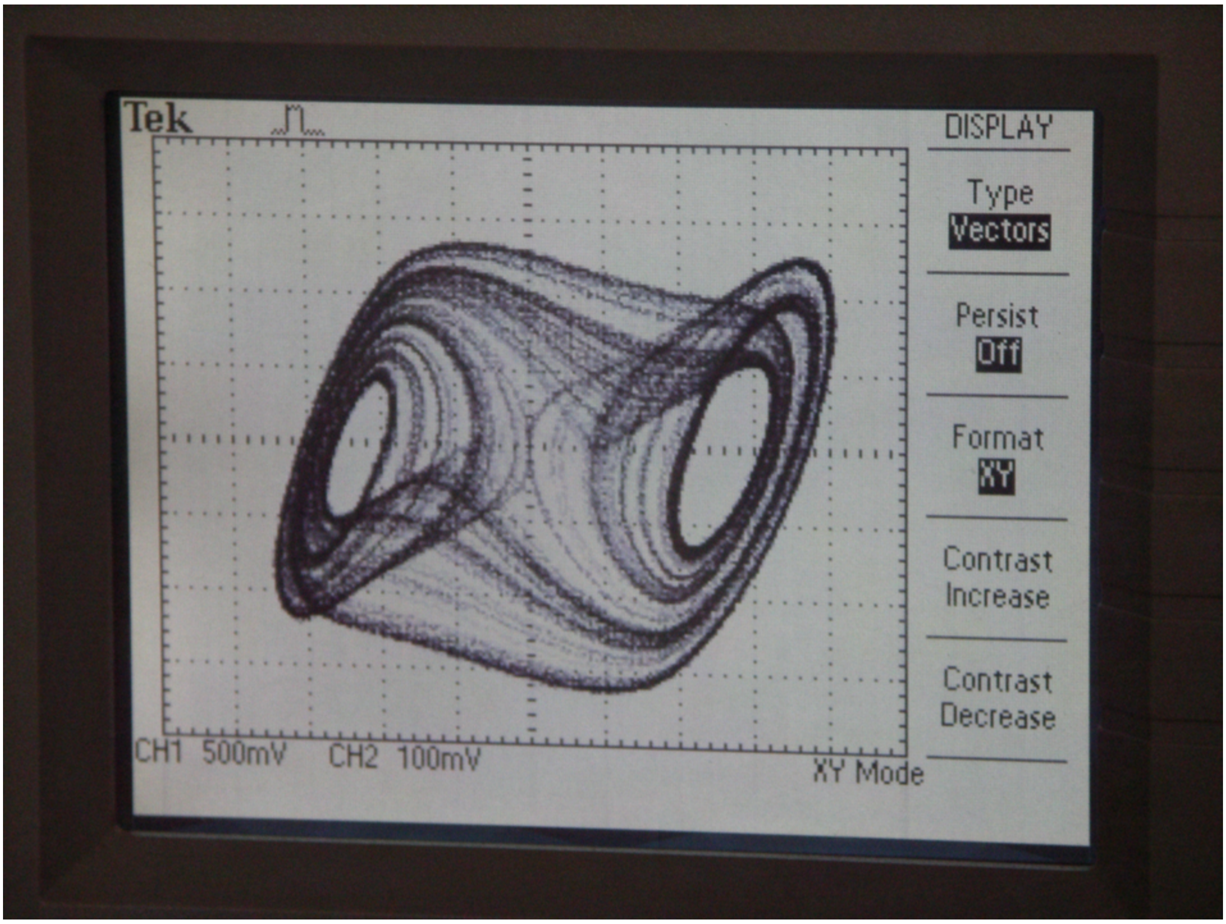

Figure 3.5: The chaotic double scroll of Chua's circuit obtained from oscilloscope

Fig. 3.6 shows the implementation of evolved Chua's circuit in lab and Fig. 3.7 shows the connections between different components.

3.1.6 Discussion

Exploiting GAs to develop Chaotic Circuits is a novel approach toward obtaining its electronic implementation. Note that the GA approach is close to a brute force approach and hence it overcome the limitation of mindset alignment toward the problem to some extent. Even in the present case of evolving Chua's circuits,

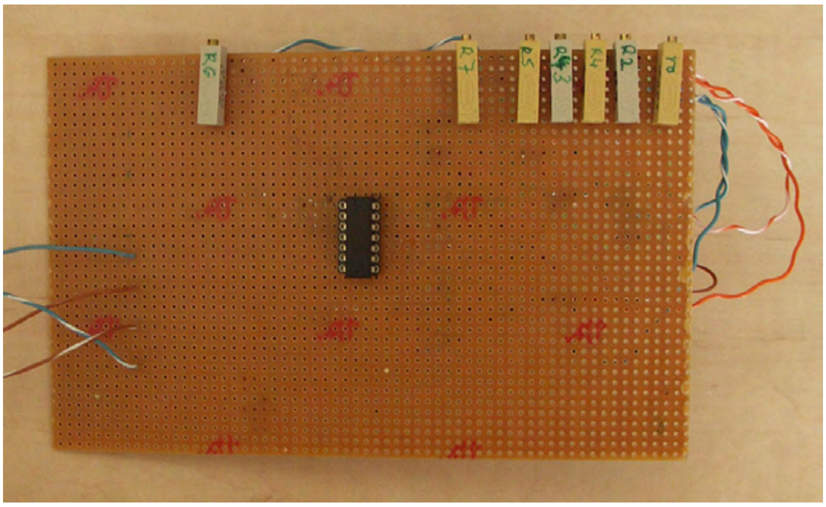

Figure 3.6: The realization of evolved Chua diode (Foreside)

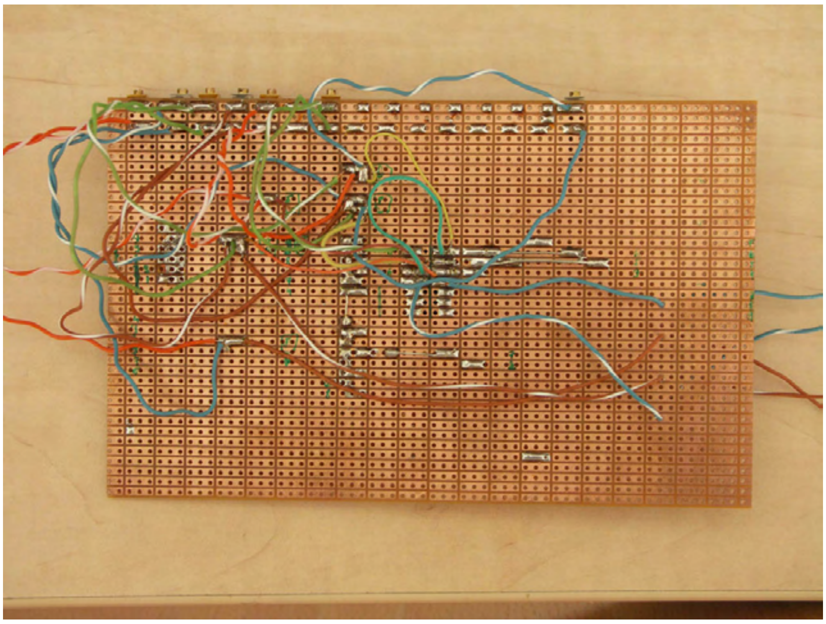

Figure 3.7: The realization of evolved Chua diode (Backside)

previous knowledge of breaking the system in two parts is used. The knowledge of time series of chaotic system is not used and hence this approach is limited to those chaotic circuits whose dynamics is known through its electronic implementation.

This case is not only limited to Chua's Circuit but also can be extended to evolve different nonlinear circuits. One direct application can be the fine tuning the nonlinear transconductors in the SET based Chua type circuit.

A whole new set of nonlinear negative analog resistors also called Chua's diodes were evolved using GA. Their application in designing variants of Chua's circuits is shown. It has been shown that the evolution of nonlinear analog resistors using GAs is much faster than the human intuitive way of thinking. The evolved design of Chua's diode and hence Chua's circuit has been shown to work satisfactorily both on SPICE as well as on breadboarded components, thereby proving the utility of incorporating GAs to SPICE to evolve human competitive complex circuits reliably and faster.

The designed module is a generic one and can be used to implement any nonlinear resistor with specified nonlinearity. Thus any chaotic circuit which can be decomposed to a combination of nonlinear resistor and rest of the circuit can be implemented using present module. In the next two chapters we will discuss about another simple chaotic circuit and will try to implement a generic architecture to develop the same at nanoscale as well as VLSI.

Concluding Thesis Statement :
1.2.1 I concieved the idea of a Genetic Algorithm based SPICE wrapper to design and evolve several new Chaotic circuits.
1.2.2 I have evolved several new Chua's circuits as an illustraion for this wrapper
1.2.3 I have breadboarded some of the newly evolved Chua's circuit in lab and observed their response on oscilloscope

Chapter 4

MOS integrated circuit architecture of MultiScroll-MultiGrid Chaotic System

Thesis II. *I developed a novel integrated circuit architecture for Multigrid Multiscroll chaotic circuits in VLSI.*

4.1 Introduction

There has been a recent growing interest on designing chaotic circuits. Several successful attempts have been made in the past to design double scroll chaotic systems. These attempts not only included implementations of Chua's double scroll circuit but also several new circuits were discovered and implemented.

Recent past has also witnessed the emerging interest of the research community toward analysis and design of multi-scroll multi-grid (MSMG) circuits. Several attempts have also been made to increase the complexity of the system by designing Multi-Scroll chaotic circuits [95, 96, 97, 98, 99, 100, 101, 102, 103, 104, 105, 39, 32, 17, 15]. Some of these circuits design one-dimensional n-Scroll attractors using generalized multi-breakpoint piecewise linear functions in existing circuits

[96, 97, 98, 99, 100, 101, 102, 103, 104, 105], other implementations suggests two-dimensional or three-dimensional n-Scroll-Grid attractors [39]. There have been many attempts to build these multi-scroll circuits using discrete components [96, 97, 101, 17].

Despite all such attempts not much has been written about VLSI implementation of these multiscroll circuits. The present chapter aims at implementing a generalized circuit architecture using MOS transistors to implement multi-scroll chaotic grid attractors. The main motivation behind the current approach is to present a simple architecture for very large-scale integration engineers to implement multi-scroll chaotic grid attractors in integrated circuit form. Note that this chapter presents a SPICE-assisted proof and no chip implementation has been done for the design.

This chapter is organized as follows: Section 4.2 demonstrates the basic circuit element, the transconductor cell, used to design the required nonlinearities for the system. Section 4.3 describes the MOS-integrable circuit, which provides several possibilities for designing one-, two- and three dimensional MSMG attractors using those nonlinearities. The possible applications of the proposed design are discussed in Section 4.4. This chapter concludes with a discussion of several realizations and their possible merits.

4.2 Nonlinear Transconductor

Consider the circuit shown in Fig. 4.1 with aspect ratios as defined in table 4.1. For $V_{dd_1} = -V_{ss_1} = 1.5\ V$, the circuit represents a nonlinear transconductor. This nonlinear transconductor acts as a comparator (referred henceforth as G-comparator) with input compared to $|\mathrm{V_{dd_1}}| - |\mathrm{V_{ss_1}}|$

The transfer characteristics (I-V) plot is shown on the right-hand side of Fig. 4.1. The gate voltages (or the aspect ratio) of the transistors M3 and M6 can control the value of the current I_0. For SPICE simulations, models of MIETEC 0.5-

Table 4.1: Aspect Ratios for Nonlinear Transconductor

Transistor of G-Comparator	**Aspect ratio**
M1	40/15
M2	40/65.5
M3	8.6/15
M4	40/1
M5	40/4.5
M6	8.6/65.5

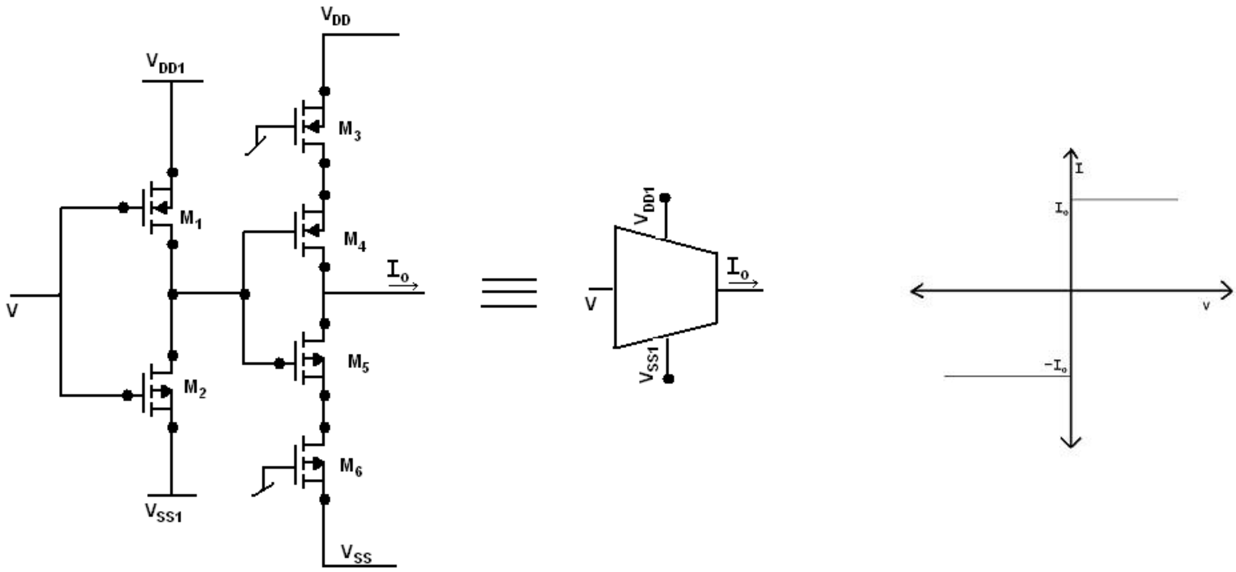

Figure 4.1: The non-linear transconductor

micron technology process were used.

The present proposal modifies the comparator by introducing several breakpoints in the nonlinear function. The multi-step nonlinearity function generated is shown later to design a class of MSMG attractors.

Note that by similar addition of G-comparators with different rail voltages, other similar nonlinear functions with more breakpoints can also be realized. However, as the number of breakpoints increases, higher supply voltage may be required. Considering the fact that higher-dimensional complex circuits and hence nonlinearity with more breakpoint may never be required as they don't add appreciably to increasing the entropy.

4.2.1 Three step nonlinearity

Consider the following non-linear function

$$f(V) = \begin{cases} I_0 & V > V_0 \\ 0 & |\mathrm{V}| < V_0 \\ -I_0 & V < -V_0 \end{cases} \tag{4.1}$$

For $V_{dd_1} = 1.7$ V, V_{ss_1} =-1.49 V; $V_{dd_2} = 1.51$ V, V_{ss_2} =-1.7 V, the circuits of Fig. 4.2 shows a response depicted by above equation with $V_0 = 0.1$V and $I_o =$ 12 uA. Note that varying the rail voltages can change the breakpoints.

4.2.2 Five step nonlinearity

Consider the following non-linear function

$$f(V) = \begin{cases} 2I_0 & V > V_1 \\ I_0 & V_1 > V > V_0 \\ 0 & |\mathrm{V}| < V_0 \\ -I_0 & -V_0 < V < -V_1 \\ -2I_0 & V < -V_1 \end{cases} \tag{4.2}$$

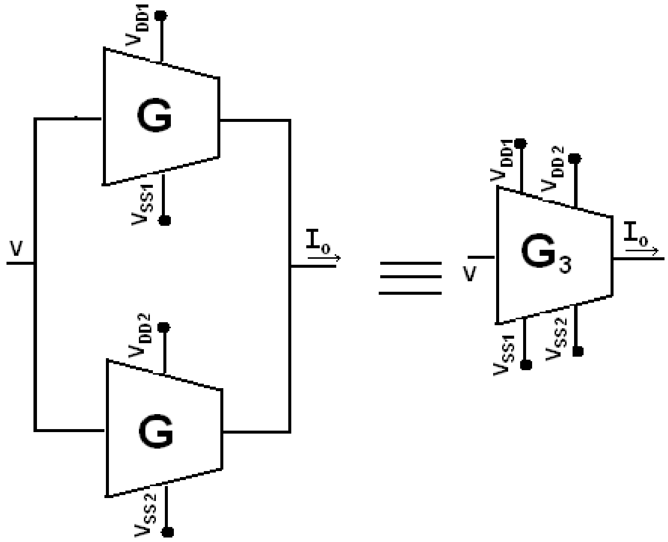

Figure 4.2: Nonlinear transconductor with three breakpoints

Adding two similar trans-conductor with different breakpoints can easily generate the non-linear function of the given equation.

Thus for V_{dd_1} = 1.7 V, V_{ss_1} =-1.49 V; V_{dd_2} = 1.51 V, V_{ss_2} =-1.7 V; V_{dd_3} = 2.4 V, V_{ss_3} =-1.76 V; V_{dd_4} = 1.85 V, V_{ss_4} = -2.4 V.

where V_{dd_1},V_{ss_1},V_{dd_2} *and* V_{ss_2} represents the rail voltages of the first transconductor and V_{dd_3},V_{ss_3},V_{dd_4} *and* V_{ss_4} represents the rail voltage of second transconductor, the Equation 4.2 with $V_0 = 0.1$ V, $V_1 = 0.3$ V and I_o=12 uA can be realized.

Note that by similar addition of G-comparators other non-linear functions with more breakpoints can also be realized. The present case has been illustrated as an example to show that higher breakpoint designs are also possible. However, as the number of breakpoints increases, it will no longer remain a low-voltage implementation. But considering the fact discussed later in the chapter higher dimensional complex circuits and hence nonlinearity with more breakpoint may never be required.

4.3 MultiScroll Attaractor

4.3.1 One Dimensional MultiScroll Attractor

Consider the following equations given by Yalcin et al. [21]

$$\begin{aligned} \frac{dX}{dt} &= Y, \\ \frac{dY}{dt} &= Z, \\ \frac{dZ}{dt} &= -a(X + Y + Z - f(X)), \end{aligned} \tag{4.3}$$

where the non-linear function is defined by

$$f(\theta) = \sum_{i=1}^{M_x} g_{0.5-i}(\theta) + \sum_{i=1}^{N_x} g_{i-0.5}(\theta). \tag{4.4}$$

Here M_x and N_x are the numbers of staircases required in positive and negative direction of voltage axis of the transconductor respectively and
With

$$g_\delta(\beta) = \begin{cases} 1, \beta \geq \delta > 0 \\ 0, \beta < \delta > 0 \\ 0, \beta \geq \delta < 0 \\ 1, \beta < \delta < 0 \end{cases} \tag{4.5}$$

Equilibrium points: The equilibrium of the present equation can be found by following set of equations

$$\begin{aligned} X &= f(X), \\ Y &= 0, \\ Z &= 0. \end{aligned} \tag{4.6}$$

The proposed system exhibits chaos with 'a' as the bifurcation parameter [21].

4.3.1.1 One Dimensional Three Scroll Attractor

For $M_X = 1, N_X = 1$ the system exhibits a 3-Scroll attractor. The MOS implementation of the current design is as shown in Fig. 4.3.

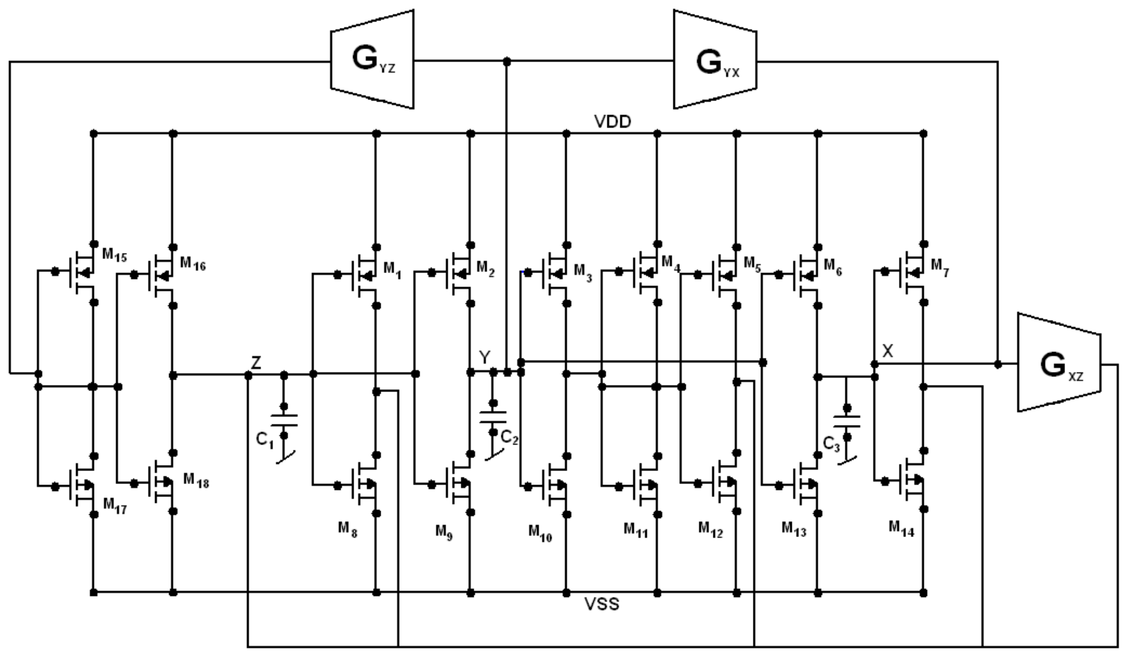

Figure 4.3: Generalized MOS-integrable circuitry for multi-scroll multi-grid chaotic attractor

Here in the G_{XZ} is replaced by G_3. SPICE simulation of the design using 0.5 micron SPICE model was done and the simulation results are shown in Fig. 4.4 and Fig. 4.5. Note that all PMOS and NMOS except that of G-Comparator have the aspect ratio of 20u/15u and 20u/65.5u respectively.

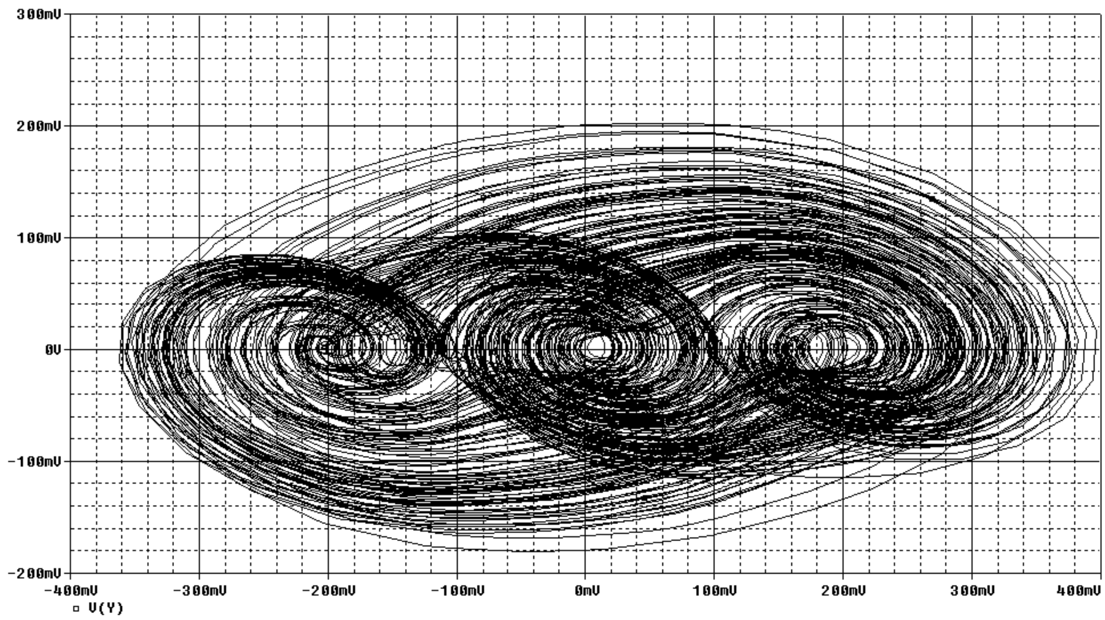

Figure 4.4: SPICE simulation results: one-dimensional 3-scroll chaotic circuit

4.3.1.2 One Dimensional Five Scroll Attractor

For $M_X = 2, N_X = 2$ the system exhibits a 5-scroll attractor. The schematic for low-voltage 5-Scroll circuit is as shown in Fig. 4.3 with G_{XZ} is replaced by G_5. SPICE simulation results of the design are shown in Fig. 4.5.

4.3.1.3 One Dimensional Seven Scroll Attractor

Similarly for $M_X = 3, N_X = 3$ the system exhibits a 7-Scroll attractor. The seven Scrolls are obtained by replacing G_{XZ} is replaced by G_7 in Fig. 4.3 and the corresponding simulations results are shown in Fig. 4.6.

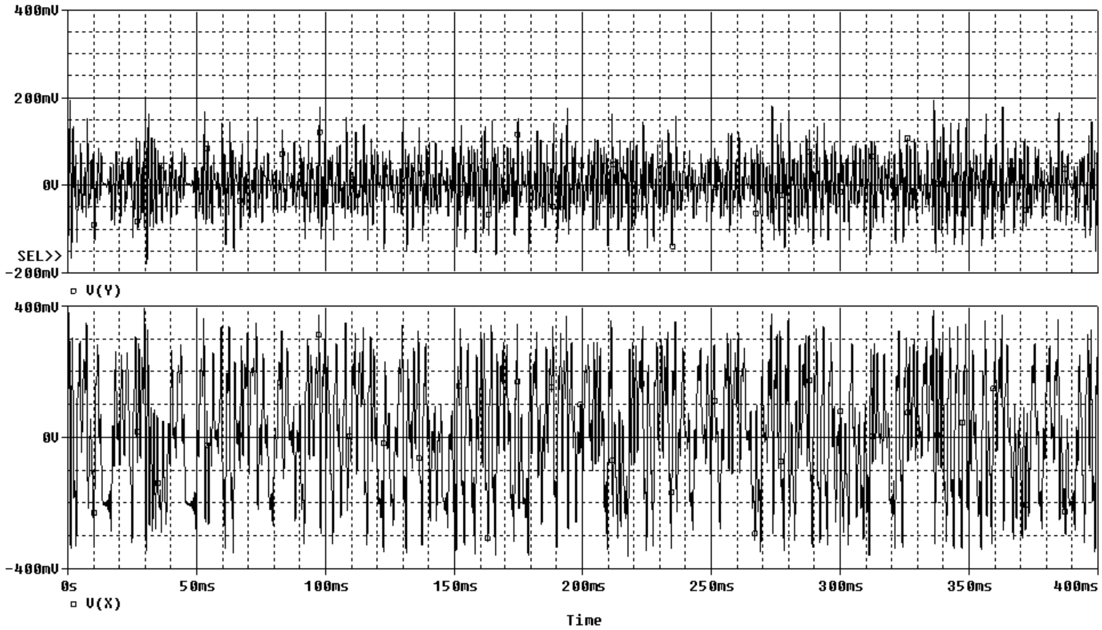

Figure 4.5: SPICE simulation results: one-dimensional 3-scroll circuit (time series of V_x and V_y)

Several other MSMG attractors can be designed by adding more breakpoints to the non-linear function. These breakpoints can be added in similar fashion.

4.3.2 Two-dimensional Multi-Scroll Circuits

Consider the following equations generated by modification to previous equation

$$\begin{aligned} \frac{dX}{dt} &= Y - f(Y), \\ \frac{dY}{dt} &= Z, \\ \frac{dZ}{dt} &= -a(X + Y + Z - f(X)), \end{aligned} \tag{4.7}$$

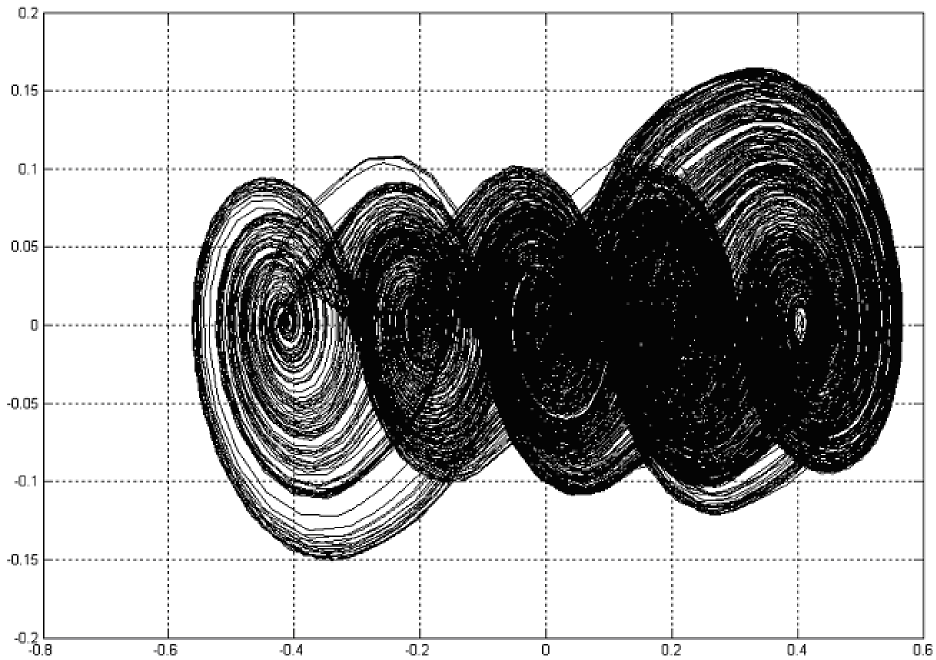

Figure 4.6: SPICE simulation results: 1-dimensional 5-scroll circuit (V_x *vs* V_y)

where the non-linear function remaining the same as given in above equations

Equilibrium points: The equilibrium of the current equation can be found by following set of equations

$$\begin{aligned} &X = f(X) - f(Y), \\ &Y = f(Y), \\ &Z = 0 \end{aligned} \tag{4.8}$$

Different cases using different combination of M_X, M_Y, N_X, N_Y were studied and several different MOS implementations were derived using the same. Thus, a whole class of low-voltage two dimensional Scroll attractors was designed by adding/subtracting different G-Comparator. The designed circuit is shown in Fig. 4.3 and the corresponding studied cases are depicted in Table 4.2. One such simulation result is as shown in Fig. 4.7

Table 4.2: Cases for 2D MultiScroll Attractor

Case	MX	NX	MY	NY	GXZ	GYX
1	1	1	1	1	G_3	G_3
2	1	1	2	2	G_3	G_5
3	1	1	3	3	G_3	G_7
4	2	2	1	1	G_5	G_3
5	2	2	2	2	G_5	G_5
6	3	3	1	1	G_7	G_3

4.3.3 Three-dimensional Multi-Scroll Circuits

Consider the following set of equations

$$\begin{aligned} \frac{dX}{dt} &= Y - f(Y), \\ \frac{dY}{dt} &= Z - f(Z), \\ \frac{dZ}{dt} &= -a(X + Y + Z - f(X)), \end{aligned} \tag{4.9}$$

where the non-linear function definitions remaining the same as earlier.

Equilibrium points: The equilibrium of the current equation can be found by the following set of equations

$$\begin{array}{l} X = f(X) - f(Y) - f(Z) \\ Y = f(Y) \\ Z = f(Z) \end{array} . \tag{4.10}$$

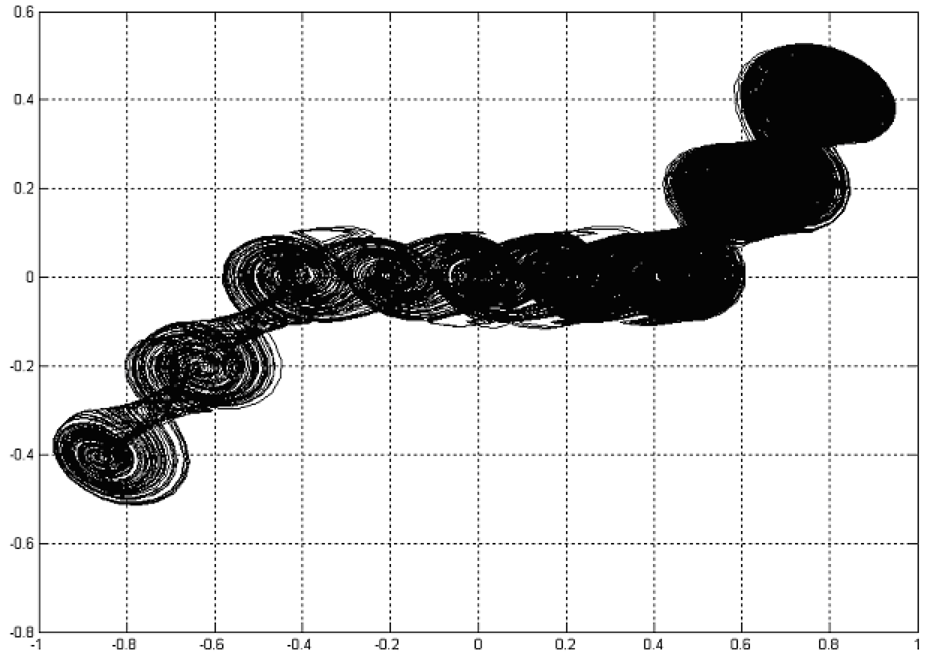

Figure 4.7: SPICE simulation results for two-dimensional multi-scrolls circuit ($V_x vs V_y$). In the present case G_{XZ} and G_{YX} of Fig. 4.3 are both replaced by $G_5$and the third transconductor is removed.

Several combinations of $M_X, M_Y, M_Z, N_X, N_Y, N_Z$ were studied by designing the MOS implementation of the circuit. The different circuits realized are mentioned in Table 4.3. Refer to Fig. 4.3 for the MOS implementation of the design.

Note that as the complexity of the system increases, the system's response becomes sensitive to the offset current, breakpoints and the value of I_0. This is the reason why several scrolls, which are observed on software, are non-existent in Table 4.2 and Table 4.3.

Table 4.3: Cases for 3D MultiScroll Attractor

Case	MX	NX	MY	NY	MZ	NZ	GXZ	GYX	GYX
1	1	1	1	1	1	1	G_3	G_3	G_3
2	1	1	2	2	1	1	G_3	G_5	G_3
3	1	1	3	3	1	1	G_3	G_7	G_3
4	2	2	1	1	1	1	G_5	G_3	G_3
5	2	2	2	2	1	1	G_5	G_5	G_3
6	2	2	3	3	1	1	G_5	G_7	G_3
7	2	2	3	3	2	2	G_5	G_7	G_5
8	3	3	1	1	1	1	G_7	G_3	G_3
9	3	3	2	2	1	1	G_7	G_5	G_3
10	3	3	3	3	2	2	G_7	G_7	G_5

4.3.4 Other cases

Several individual cases of references [21] were also replicated using the present design of non-linear functions. Some of these cases are as under.

$$\begin{aligned}
\frac{dX}{dt} &= Y - g(Y) \\
\frac{dY}{dt} &= Z \\
\frac{dZ}{dt} &= -a(X + Y + Z - 2f(X))
\end{aligned} \tag{4.11}$$

4.3.4.1 Two dimensional Multi Scroll Circuit

With $f(\theta) = \mathrm{sgn}(\theta)$ and $g(\theta) = \mathrm{sgn}(\theta)$, the system represents a 2 dimensional Scroll system. This system can be implemented by replacing G_{YX} of Fig. 4.3 with the simple G-comparator and G_{XZ} by two parallel connection of G-comparator. The corresponding simulation results are as shown in Fig. 4.8.

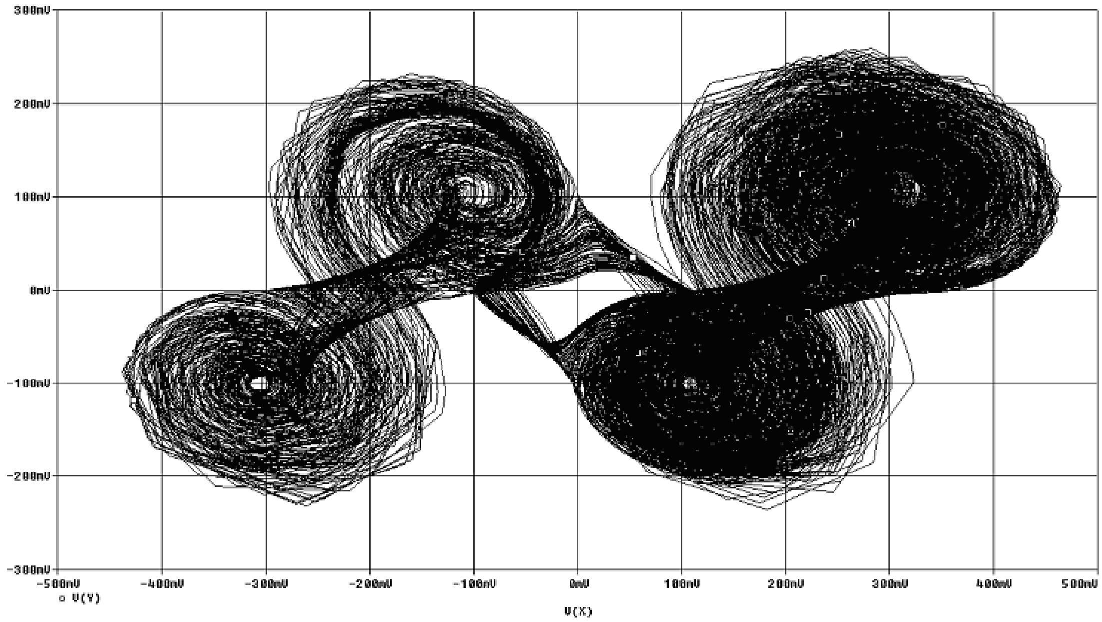

Figure 4.8: SPICE simulation results for above multi-scrolls circuit

By suitable choice of $g(\theta) and f(\theta)$ the number of scrolls can be increased in the present system.

4.4 Discussion

The SPICE simulation-based results for a possible MOS-integrable circuitry for MSMG oscillators are presented in current chapter. The simulations were performed with MIETEC 0.5 micron technology parameters, assuming that the availability of a specified voltages, external to the present circuit, has eased off a part of design complexity. A separate section providing suitable bias voltages can be designed to meet the need. However that is not the aim of the current brief. It has been shown that using different implementations of G-comparators, multidimensional MSMG systems can be implemented. As chaotic systems are highly sensitive to initial conditions and become even more sensitive as the number of scrolls are increased, a robust MOS design needs to take into account process variations, the frequency of operation, temperature, etc. An experiment would be revealing, but that is not the subject of this chapter. This chapter was aimed at implementing a MOS-integrable circuitry for multi-step nonlinearity and using the same to design a MOS-integrable chaotic grid attractor.

Switching from one chaotic system to another among the above-presented cases can be achieved by implementing appropriate switches around the comparator that can also lead to new insights and applications [42]. Also it has been shown very recently [99] that the system's entropy increases with the number of scrolls for some values and after which there is no appreciable change. This implies that for applications such as random number generators 'very high'-dimensional chaotic systems may never be required, as they do not provide any appreciable benefit. One interesting application of chip implementation of these designs can be the study of qualitative behavior of several coupled and different MSMG oscillators in real-time environment. Even though the frequency of operation of the presented design is 0.8 kHz (we have taken external capacitors to be around 10 nF), the qualitative behavior of either such coupled systems or hyperchaotic systems can be studied. The period doubling route to chaos can be observed by varying the grounded capacitors.

The core application that chaotic attractors provide is the implementation of random number generator. As it has been recently shown, the entropy of the system increases with the increasing number of scrolls therefore MOS implementation of the above design can generate a better random number [99].

The current designs of circuits can also be converted to a hyperchaotic circuit by the scheme described in [65]. Thus herein the transition from chaotic to hyperchaotic region can be seen as a transition of systems from synchronization to de-synchronization. A similar approach has been used in [4] to generate hyperchaos using coupled Chua's circuit. One of the applications of the designed hyperchaotic circuits will be the design of true random bit generator (TRBG) or a spatio-temporal TRBG [98]. In addition, ease of programmability of breakpoints may lead to several new insights and applications.

The next chapter will explore similar opportunities at nanoscale.
Concluding Statement :
2.1 I designed a G-comparator used as a nonlinear block for Multigrid Multiscroll chaotic circuit.
2.2.1 I developed a new integrated circuit architecture for MultiGrid MultiScroll circuit.
2.2.2 As a proof of concept I have simulated the design in 0.5 micron technology via SPICE

Chapter 5

Chua Type SET based circuit

Thesis III. *I designed a nano size Chua type Chaotic circuit using Single Electron Transistors and verified it with SPICE simulations.*

5.1 Introduction

Single Electron Transistors (SETs) have demonstrated their presence in many applications on analog and digital circuits, memories and standardization. However, no attempt in the direction of chaotic circuit design using SETs has been reported. Also, to the best of the authors' knowledge the design of double scroll chaotic systems in nanotechnology is also lacks in the literature.

In the present chapter a Chua type double scroll circuit based on one of the equations described in [16] is presented. This double scroll is implemented using SET, and the dynamics is explored by SPICE simulation. Note that this paper is not concerned with specific technological realizations of SETs but acts as 'existence proof' to show that chaotic behavior is possible in SET circuits. It is based on a published device model of SET and no experiments were performed. This paper is an original case study to show that chaotic behavior is possible in small set of interconnected SETs.

5.2 Single Electron Transistors

The simplest device in which the effect of Coulomb blockade can be observed is the so-called SET. It consists of two tunnel junctions sharing one common electrode with a low self-capacitance, known as the island. The electrical potential of the island can be tuned by a third electrode (the gate), capacitively coupled to the island.

In the blocking state no accessible energy levels are within tunneling range of the electron (red) on the source contact. All energy levels on the island electrode with lower energies are occupied.

When a positive voltage is applied to the gate electrode the energy levels of the island electrode are lowered. The electron can tunnel onto the island, occupying a previously vacant energy level. From there it can tunnel onto the drain electrode where it scatters and reaches the drain electrode level.

The energy levels of the island electrode are evenly spaced with a separation of ΔE. ΔE is the energy needed to each subsequent electron to the island, which acts as a self-capacitance C. The lower C the bigger ΔE gets. It is crucial for ΔE to be larger than the energy of thermal fluctuations $k_B T$, otherwise an electron from the source electrode can always be thermally excited onto an unoccupied level of the island electrode, and no blocking can be observed.

5.3 SET Based Inverter

The inverter consists of two identical SETs in series that share same common input gate as shown in Fig. 5.1. Every SET is a four terminal device connected to all the four terminals by capacitance. It has one drain, one source and two gate terminals. In most of the cases one gate terminal is always connected to ground.

Figure 5.1: Single Electron Transistor Based Inverter

The SPICE simulations for the input-output characteristics of the SET based inverter are shown in Fig. 5.2. These simulations use the SPICE models based on orthodox theory using the values provided in the next section.

5.4 Brief Introduction To Orthodox Theory

In the orthodox theory a way of describing SET devices is given. In this theory several assumptions are made. The important assumptions related to the SPICE model are given below:

1. Tunneling occurs instantaneously. This means the time needed for the tunnel event equals zero.

Figure 5.2: Inverter Characteristics

2. Tunneling is only possible when the electrostatic energy of the junction will be lowered due to the event. Thus $E_{before} - E_{after} = \Delta E > 0$.

3. The charge transfered through the junction due to tunnel-event, is discrete, by multiples of e, where e equals the electron charge.

4. The tunnel rate is given by the following expression: $\Gamma = \frac{\Delta E}{R_T e^2 \left(1 - e^{\frac{\Delta E}{k_B T}}\right)}$

   Where R_T equals the tunnel-resistance and k_B equals the constant of Boltzmann.

5. The junctions must operate in a high-ohmic environment, this is given by: $R_T \gg R_Q = \frac{\hbar}{e^2} = 26k\Omega$

5.5 SET Based Chaotic Circuit

The simple equation modeling the Chua type double scroll dynamics is described by the following equation.

$$\dddot{X} = a\left(\ddot{X} + \dot{X} + X - f(X)\right). \tag{5.1}$$

Here *'a'* acts as a bifurcation parameter and X represents the state variable.

Further it has been shown in previous chapter as well that different nonlinear functions give rise to different chaotic attractors [2].

Consider the circuit shown in Fig. 5.3. The triangular symbols represent the SET based inverter circuits shown in Fig. 5.1. The ratio of the capacitances C_1 and C_2 provides the bifurcation parameter for controlling the system behavior.

Figure 5.3: SET based Chua Type Chaotic Circuit

Note that normally the capacitance of wires is approximately 100 aF/um thereby implying that in an actual design the wire can act as a capacitor and no special capacitors need to be designed.
The nonlinear block used in Fig. 5.3 has the following nonlinearity

$$f(X) = \operatorname{sgn}(X) = \left\{ \begin{array}{cc} 1 & X \geq 0 \\ -1 & X < 0 \end{array} \right\} \tag{5.2}$$

For the current design an ideal nonlinear bock is assumed. The idea presented in [2] can be explored to generate this type of nonlinearity.

5.6 SPICE Simulation Results

For simulating the design, SPICE models based on orthodox theory were used.

5.6.1 *SET based Inverter*

The following parameters were used for simulating the SET based inverter shown in Fig. 5.1.

The resistance of the source junction equals to the resistance of the drain junction.Three different simulations at different temperatures (i.e. 4.2 K, 27 K and 77 K) were performed and the results are as shown in Fig. 5.2. The background charge was assumed to be 0.15e. The simulations were performed with a supply voltage of +/- 20 mV.

To avoid any floating node warning by the simulator, a high load resistance (1000 TOhm) at output node is applied.

5.6.2 *SET based Double Scroll Circuit*

Inverter parameters used for SETs to design double scroll attractors were the same as presented in the above section with the exception of background charge which is assumed here to be negligible. The other parameters are $V_b = 17$ mV, $V_{g1} = V_{g2} = 0$, $C_2 = 0$, $C_1 = 3$ aF and $C_{drain} = C_{source} = 1$ aF while the non-linear block satisfies the following condition.

$$I_{out} = \left\{ \begin{array}{ccc} 2 & nA & V_{in} \geq 0 \\ -2 & nA & V_{in} < 0 \end{array} \right\} \tag{5.3}$$

In order to start the oscillator the supply voltage at V_b was ramped from 0 to 17 mV in one ns keeping the voltage of negative supply constant at -17 mV.
Also to avoid any floating node warning, a high resistance (1000 TOhm) parallel to C_3 and the ground is applied. SPICE simulation results of chaotic time series at three different nodes are given in Fig. 5.4.

Figure 5.4: Timeseries

Fast Fourier Transforms (FFTs) on signal at node A shows that although the circuit is operating at the wide range of frequencies, it is mostly concentrated around 315 MHz, which is the fastest for any double scroll reported so far. The FFT simulation results are shown in Fig. 5.5.

Figure 5.5: Fast Fourier Transform (FFT) of voltages at different nodes

Fig. 5.6 and Fig. 5.7 show the phase plot of the voltage at node A (V_A) versus voltage at node B (V_B) and the voltage at node A (V_A) versus the voltage at node C (V_C), respectively.

The chaotic double scroll attractor is observed. The curve outside the scroll corresponds to the time series obtained during the supply voltage ramping (i.e. the first ns). By notation, the voltage at node A is V_A

Figure 5.6: Phase plot of A versus B

5.7 Discussion

The present design offers a very high frequency operation at very low voltage and power consumption. Note that this paper is not concerned with specific technological realizations of SETs but acts as 'existence proof' to show that chaotic behavior is possible in SET circuits.

A new application of SETs in chaotic circuit designing is presented and its dynamics is explored through SPICE simulations.

Exploiting functionalities in layout is emerging as a new approach in designing chips in order to sustain Moore's law. Thus in terms of fabrication, the parasitic capacitance of wires (100aF/um) can be used as a functional capacitor for the design, thereby avoiding the use of designing the capacitance. The parasitics associated with SETs is taken accounted for while modeling the SET in SPICE. Other parasitics which may arise are in itself is an open point in literature and

Figure 5.7: Phase plot of A versus B

methods used to avoid them can be implemented here as well.

Since an ideal nonlinear block is assumed for the current reporting, I cannot comment anything about the total power consumption of the design. Nevertheless, looking at the past designs at nanoscale, a significant reduction is expected in power consumption.

There are several issues that still exist, like the effect of background charge, low temperature operation, noise-free signal amplification, etc. that may make the current design impractical. However, these issues are already confronting SET community and are true for any SET based designs. The results are as valid and as faithful as SPICE models of SETs. These models are available at `http://lamp.tu-graz.ac.at/ hadley/set/spice/index.html` for downloading. As long as it captures the probabilistic nature of electron's tunneling accurately enough, the conclusions of the paper are correct. An experiment would be revealing, but that is not the subject of this paper.

Chapter 6

Applications

6.1 Hands-on-Experience with Chaos Theory for High School Students

6.1.1 Introduction

Chaos is a new physical and mathematical phenomenon rediscovered by E. Lorenz in 1963. The first physical and simple implementation had been invented by L. O. Chua in 1984. This electronic circuit, called *Chua's circuit* provides easy implementation.

In the current chapter I will explain how to build Chua's chaotic circuit using *Chua's circuit* kit with inexpensive components. For readers without access to an oscilloscope, this section proposes the use of a laptop/Personal Computer to capture the voltage waveforms generated from the circuit and plot the waveforms on a computer screen using a virtual oscilloscope software provided by the authors.

6.1.2 Chua's circuit and its components

Chua's Circuit is the simplest electronic circuit exhibiting chaos, and many well-known bifurcation phenomena. It has been verified from numerous laboratory experiments, computer simulations, and rigorous mathematical analysis.

The circuit diagram of the Chua Circuit is shown in Fig. 2.2. It contains 5 circuit elements. As discussed in the previous section, it must contain at least three energy-storing elements. *Chua's circuit* contains two passive capacitors (denoted by symbol C) C_1, C_2 and inductor (denoted by symbol L) L_1 as three different passive energy storing elements. They are called passive elements because they do not need a power supply (e.g., battery). These components are available off the shelf and can be seen in Fig. 6.1.

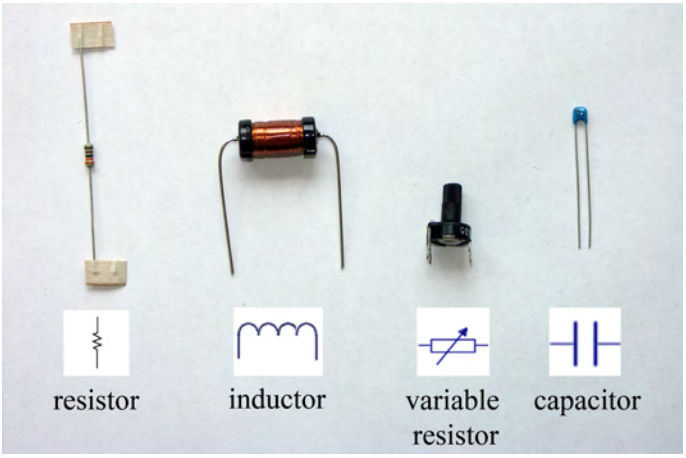

Figure 6.1: Passive components used in Chua's circuit kit

Chua's circuit has the passive resistor (denoted by symbol R) as the simple energy-dissipating device. A standard passive resistor looks like the one shown in Fig. 6.1. In order to observe different ways by which chaos can be obtained, a resistor whose value can be varied by the user is required. This type of resistor is called variable resistor or potentiometer. A most commonly used variable resistor is shown in Fig. 6.1.

The third requirement is a locally active nonlinear device. *Chua's circuit* uses Chua's diode (one special type of negative resistor) as a nonlinear circuit. This is not available off-the-shelf and has to be built using the battery, some commercially available integrated chips and some passive resistors. In Fig. 2.2, it is represented by the symbol N_R.

Fig. 6.2 shows the current-voltage behavior of a simple passive resistor. In case of Chua's diode this behavior (also called characteristics) is modified to the one as shown in Fig. 2.1. Looking at the curve, one can easily understand the reason of naming it as "nonlinear" and "negative" resistor. In Fig. 2.1, G_a and G_b define the slope of two segments separated by the breakpoint B_p.

Figure 6.2: Transfer characteristics (V-I) of a normal resistor

One circuit implementation of such a diode is give in Fig. 6.3. It contains some integrated chips, voltage batteries and resistors connected in a specific fashion. In order to avoid confusion I am providing a pre-connected Chua's diode in the kit.

Once all the three sections (5 components) are connected, the voltage across the capacitors C_1 and C_2 and the current across the inductor L will show oscillatory behavior. The shape and the quality of the oscillations is dependent on the value of the resistor R.

6.1.3 The Chua's Circuit Kit

A kit for building *Chua's Circuit* in 15 minutes was developed. This section will introduce the method of putting the components into the kit and observing Chaos

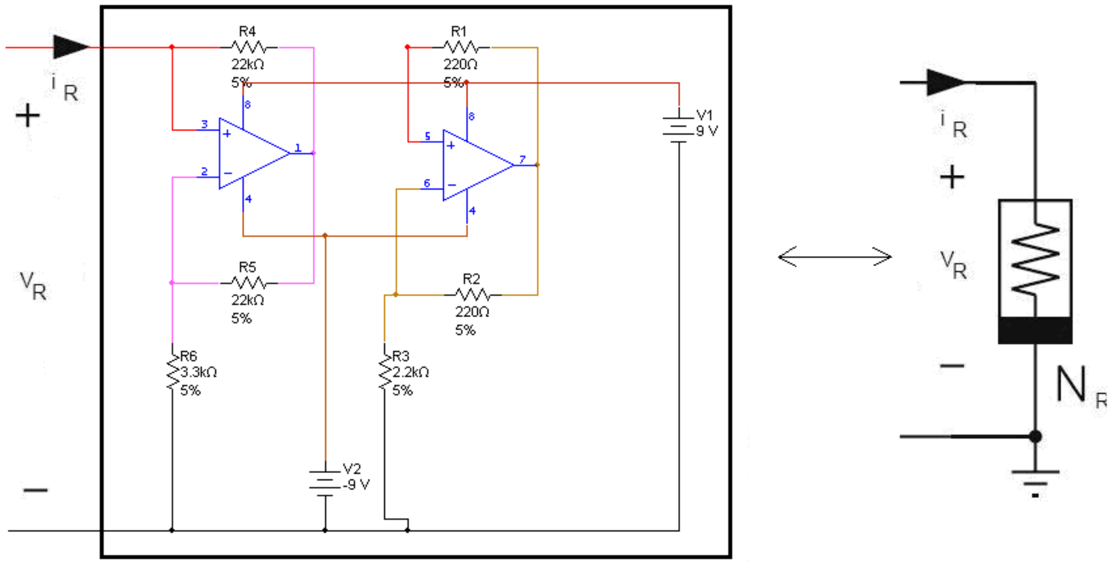

Figure 6.3: Chua's diode implemented using two op amps, resistors and two batteries

in less than another 15 minutes on a laptop or PC.

Fig. 6.4 shows the snapshot of the kit.

The component values are as follows: $c_1 = 100\ nF$, $c_2 = 10\ nF$, $l = 18\ mH$, $r_1 = 3.3\ k\Omega$, $r_2 = 220\ \Omega$, $r_3 = 22\ k\Omega$, $r_4 = 2.2\ k\Omega$.
It can easily be seen that *Chua's Circuit kit* is a *Chua's Circuit* implemented on a Printed Circuit Board (PCB). There are some resistors connected to it. The value of resistances is written on the PCB. Users can insert appropriate resistances at prescribed locations.

In order to build *Chua's Circuit* on the kit, simply insert the components at their corresponding locations.

Connect the batteries to appropriate jacks.

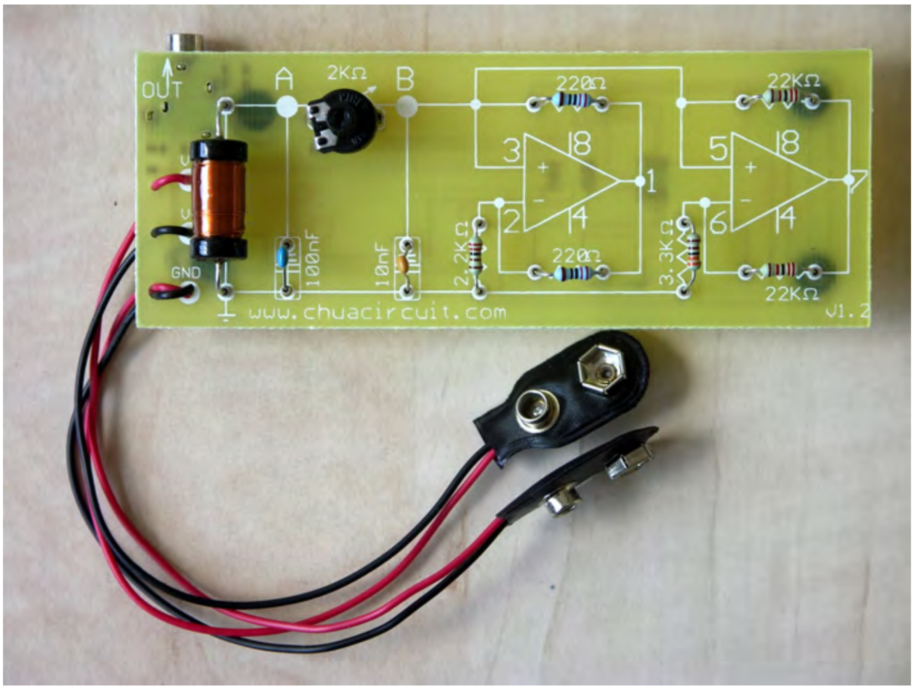

Figure 6.4: Chua's Circuit Kit

Connect the microphone plug to the laptop or PC.

6.1.4 Measurement on PC using a software oscilloscope: A Poor Man's Oscilloscope

1. Plug the microphone plug in the Line-in input of your soundcard. You can usually find the Line-in input on the rear connector of your desktop.

2. Enable the Line-in input in Windows[1]: Left-click on Start → Control Panel. Fig. 6.5 will pop up. Left-click Sounds, Speech and Audio Devices.

[1]Note: the instructions below assume that you are using a Windows operating system.

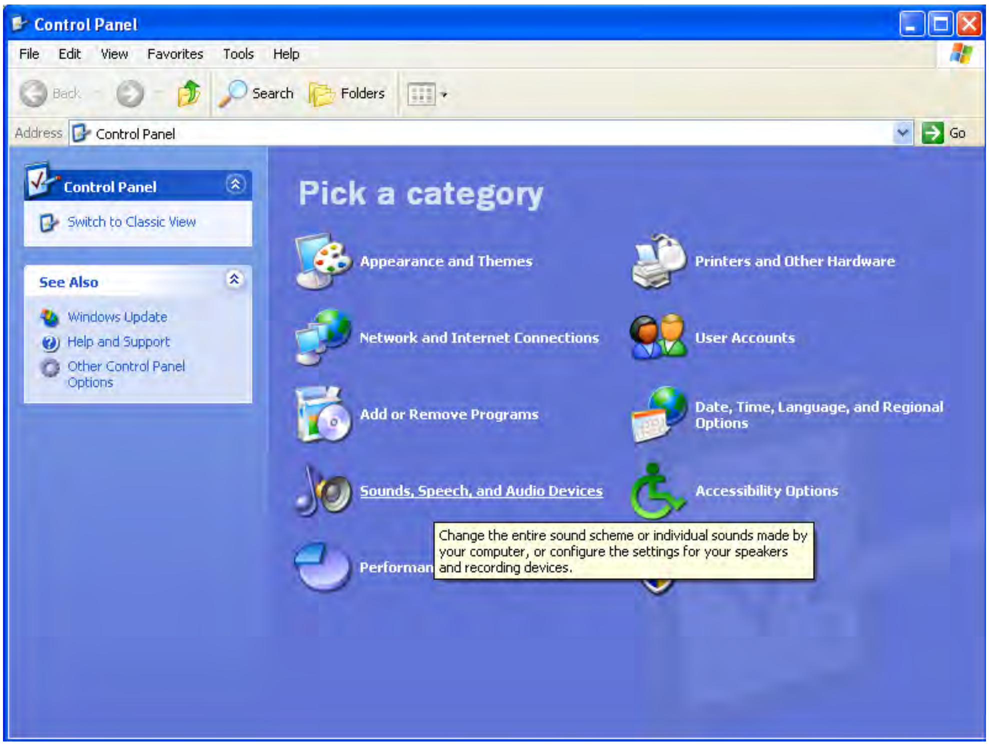

Figure 6.5: Control Panel as seen in the Category View

3. Left-click on Sounds and Audio Devices. Fig. 6.6 will pop up.

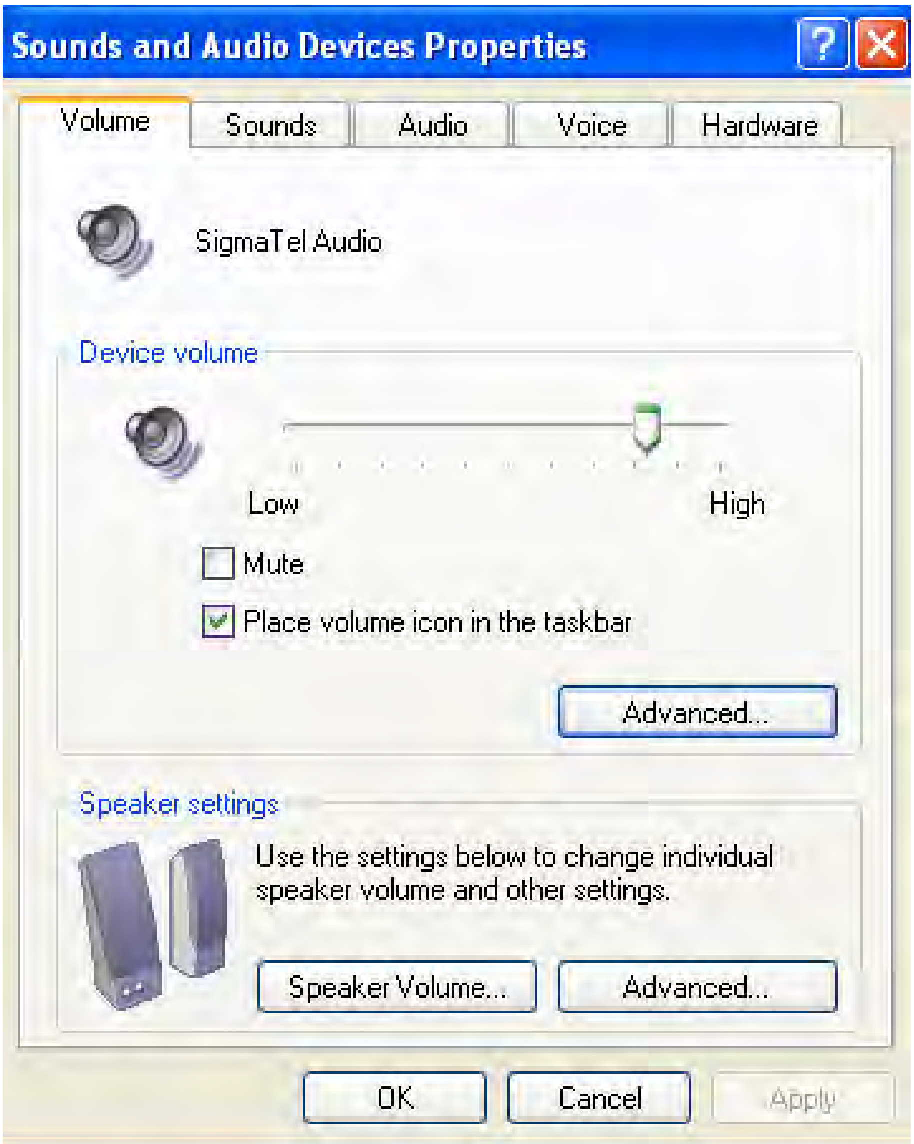

Figure 6.6: Open Sounds and Audio Devices Properties panel and left-click on Advanced... button.

4. Left-click "'Advanced ..."' Fig. 6.7 will pop up.

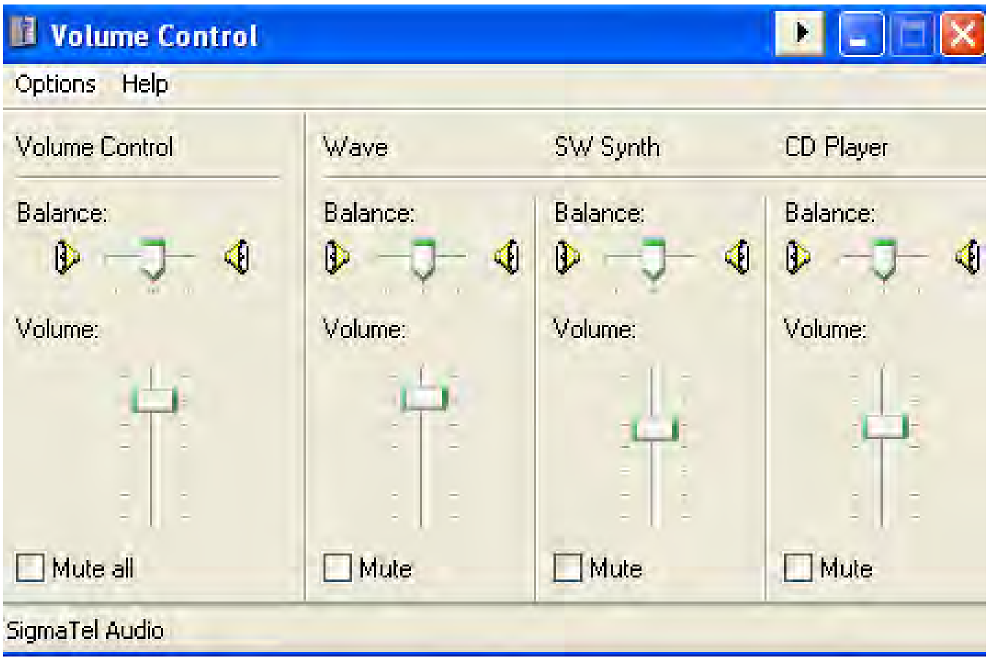

Figure 6.7: Volume control dialog box. Open options menu, chose Properties item

5. In the new window Left-click Options → Properties and select "Recording". Refer to Fig. 6.8.

6. Left-click **OK**. In the next figure(Fig. 6.9), make sure that the "Select" box under Line In is checked. Left-click to select box. Left-click and drag the slider to set the slider to minimum.

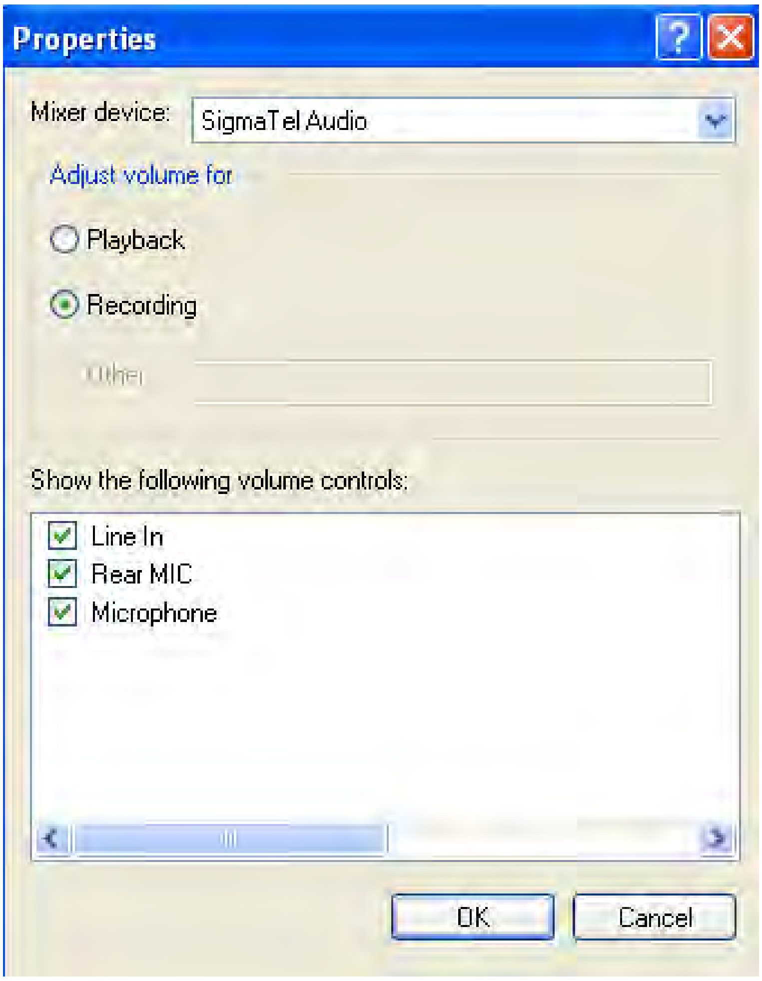

Figure 6.8: Properties dialog box, select Recording box.

Download and install the PC software-oscilloscope available at www.chuacircuit.com. The PC oscilloscope software is designed in Labview (National Instruments) software environment and available for educational purposes.

Launch the PC software-oscilloscope.

Start varying the variable resistor (potentiometer). At around its mid value it will enter the state of Chaos.
The snapshot of the software results in the mode when the system enters Chaos

Figure 6.9: Line In input selected and the slider bar is all the way down

shown in Fig. 6.10.

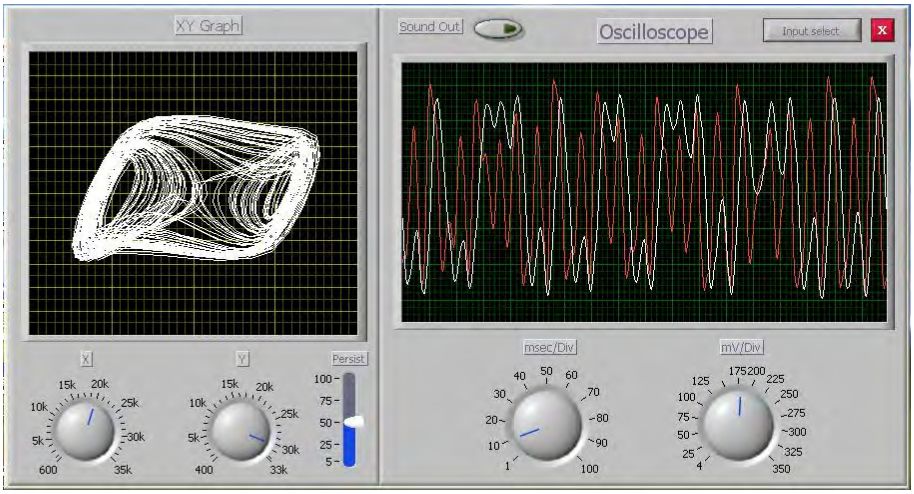

Figure 6.10: Trajectory of the two output signals (V_{c1}, V_{c2}) and signals in time [ms] as observed on PC-Oscilloscope: chaos

6.1.5 Discussion on *Chua's Circuit*

Once the kit is working, let us try to understand the phenomenon of Chaos through *Chua's Circuit*. On the extreme left of the kit one inductor is parallel to the capacitor. This acts as a driving force for the circuit as an oscillator. An ideal combination of parallel L-C, if taken standalone, is called tank circuit and gives rise to simple harmonic motion or sine waves.

The nonlinear resistor i.e. Chua's diode is a very simple negative resistor yet it is the one responsible for such rich dynamics of the circuit. This dynamics has fascinated scientists and researchers all over the world.

The variable resistor (potentiometer) is used for tuning the circuit and hence Chaos dynamics. As the potentiometer is varied from it's maximum value (right) to minimum value (left) *Chua's Circuit* passes through a period doubling route. This is illustrated as a series of images as shown in Appendix B.

6.1.6 Further Exploration: Fun while you learn

Enthusiasts can observe different behaviors in *Chua's Circuit* by varying different components. For example, in order to observe the effect of the slope of the non-linear resistor, they can buy different set of resistances and replace the ones on board by them. Similarly, different capacitors can be purchased from the nearby electronic component store (Radioshack, for example) and the user can replace the one's provided on the kit by them.

Chaotic music is another interesting field for research. Users can also listen to the musical beats produced by *Chua's Circuit* through the speaker of the laptop.

The current section was aimed at enhancing the curiosity of a student toward chaotic systems through the plug-n-play *Chua's Circuit* kit. Once that curiosity is generated, students can apply their knowledge of chaos theory in their field of interest. Further information can be found at `www.chuacircuit.com` and a wikipedia `www.chuacircuit.com/wiki`.
In the next section we will discuss one research application of *Chua's Circuit* kit that I have explored at Jedlik Laboratory.

6.2 Hardware Implementation of A 3-Dimensional Autonomous Cellular Nonlinear Network With Chaotic Cells

Synchronization of oscillatory and chaotic networks have sprung as a completely new field of nonlinear dynamics. Whereas several studies have been performed, a single platform to test several similar or different autonomous networks connected is missing from literature. The present brief provides the information about the test bed that was created by me in the lab to address such need. As a test bed, it was also demonstrated to observe different interesting phenomena among several interconnected Chua's chaotic circuits.

Note that the aim of the paper was to develop a hardware test bed which can have easy to plug oscillators. It was aimed at studying synchronization phenomena in coupled systems and was in no way aimed at exploring any new results, though some interesting phenomena were observed. These and many similar observations are subject for a separate study.

Besides the fact that the hardware implementation of the design provides an easy-to-use topology, it is the inherent design of the *Chua's circuit* kit that helps to have different parameters for different chaotic cells. This further enhances the flexibility to study cases having cells with different parameters.

6.2.1 Hardware Architecture

The designed architecture is aimed for experimental purposes, so we made an effort to ensure maximal flexibility in the design of the topologies and the joining of the elements. Topologies are not strictly bound, in a given $n \times n \times n$ 3D matrix, the elements can be coupled to each other by the rule of four neighborhood (i.e. North, South, East and West). The hardware architecture contains 3 electronic sections that can be separately well defined:

- Interconnecting Interface
- Programmable Logic
- Coupling Grid

A programmable logic along with a coupling grid constitute a single layer of autonomous CNN. Each coupling grid can manage the coupling of *4x4* cells and also the coupling through the next layer allowed to a cell to have maximum six neighbors connection. By connecting more layer together *4x4xn* architecture can be realized. The architecture allows the possibility to disconnect the coupling between cells, thereby providing the flexibility to explore several architectures of interconnected chaotic *Chua's circuits*. The design can be treated as a five neighborhood anisotropic CNN with autonomous cells. The currently designed system supports a $4 \times 4 \times n$ size 3D matrix. We have used variable resistors in our experiments as the coupling between the neighboring cells. Note that since it is a generalized architecture, the hardware is prepared to plug in easily any capacitive or inductive or they combinations or any two-port passive components.

6.2.1.1 *Interconnecting Interface and Programmable Logic*

The *Chua's circuit* kit originally was designed to connect to a personal computer and runs on two 9V batteries. Therefore an interconnecting interface was designed which helps to achieving common power supply to all connected *Chua's circuits* and at the same time to transferring all four outputs of the *Chua's circuit* to the programmable logic board through a single bus.

An interface circuit to choose one output from the four of the *Chua's circuit kit*. These four outputs are ungrounded nodes of capacitors V_A and V_B and M_A and M_B where M_A and M_B are the nodes of the output of voltage buffers whose input is connected to V_A and V_B respectively. This chosen node will then be connected to another *Chua's circuit* through a coupling resistor. A dedicated programmable logic is developed for selecting different signals from different *Chua's circuits* to be coupled to each other. This is done to achieve maximum flexibility in exploring different possible architectures of interconnecting *Chua's circuits*.
The general architecture for connecting several such layers having a similar programmable logic is as shown in Fig. 6.11.
Each programmable logic board can handle 16 independent *Chua's circuits* (4x4). The main part of the board is PIC type micro controller this can be connected to a personal computer through RS232 port. On the computer we can determine which outputs we want to use of the connected *Chua's circuits* and it can be loaded into the micro controller memory. The PIC updates the states of the shift registers. Each shift register controls two analog multiplexers. For each *Chua's*

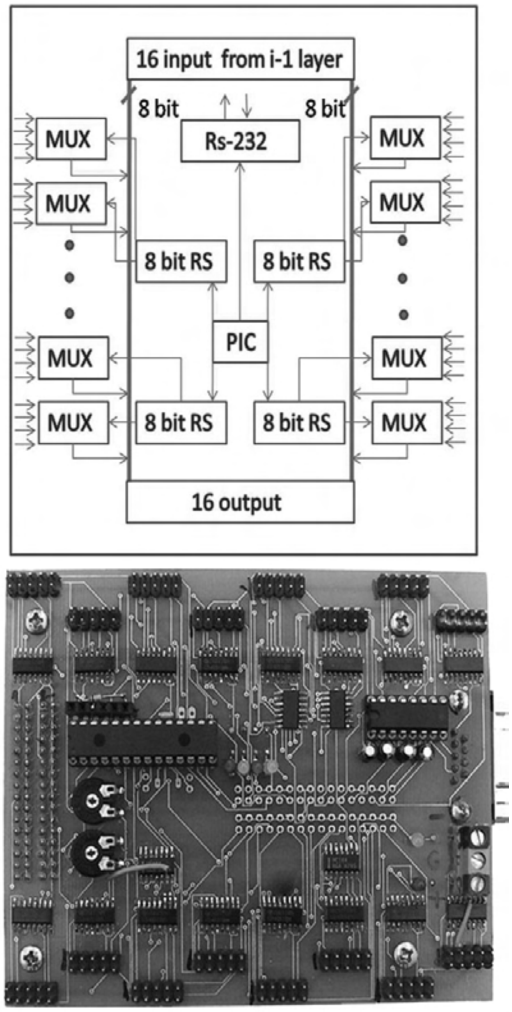

Figure 6.11: On the top, the general architecture for Programmable Logic can be seen. Herein each MUX receives 4 different signals (A, B, MA and MB) from respective *Chua's circuit* design and selects one out of them to be put on the general bus as one of the signals to be interconnected. The output (in present case of 4×4 it is 16 channel) is then transferred to a coupling grid which performs different possible desired couplings between different cells. Lower snapshot shows the programmable logic board.

circuit there is a dedicated analog multiplexer which connects the desired channel to the programmable logic board output ports.

6.2.1.2 *Coupling Grid*

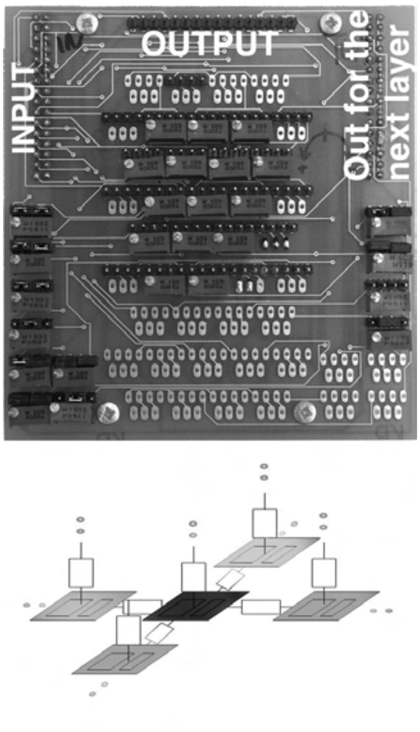

Figure 6.12: On the top, is snapshot of the coupling grid. The input and output parts are marked. In the middle of the panel, we can connect different passive two-port coupling components. A programmable logic along with a coupling grid constitutes a single layer of autonomous CNN. On the bottom the possible coupling directions can be seen according to a cell. Each coupling element can be any two port passive two-port component.

The output from the programmable logic board is then fed to the coupling grid that has the possibility to manually add different passive two-port coupling components to the design. This provides an interesting opportunity for testing several cases with different coupling components between different cells of 3D-CNN.

These components can be different not only in their component values but also their type, thereby making it suitable for studying different test cases. Fig. 6.12 shows one such coupling grid with few interconnected variable resistors.

The output port is at the top of the coupling grid. It connects one of the output of each *Chua's circuits* that has been chosen by the programmable logic board. In our experiments I used only the A terminals of connected *Chua's circuits*.

6.2.2 Experimental results

A number of experiments with different architectural topologies were performed and several interesting phenomena were observed. As the first experiment I only connected two *Chua's circuit* together with one coupling resistor. Both of them were in double scroll. By modifying the coupling resistor from 10 $k\Omega$ to 0 Ω the system moved from de-synchronization to synchronization. The two stage can be observed in Fig. 6.13.

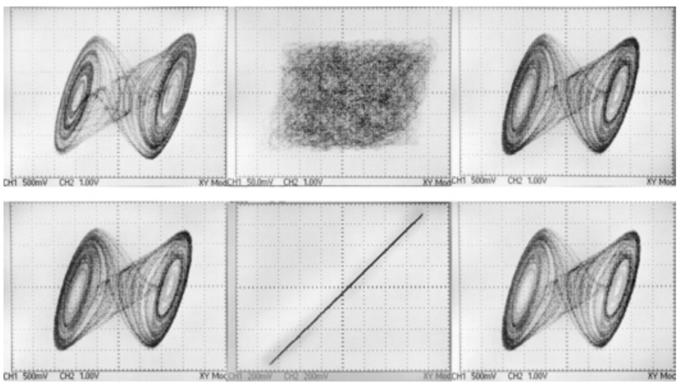

Figure 6.13: Two connected *Chua's circuit* can be seen here. On the top the coupling value is $10k\Omega$, meaning not synchronized, on the bottom at 0 Ω and the system is synchronized. On the figure, left and right oscilloscope trace shows the two circuits state (A vs. B channel). In the middle, the correlation between two of them can be observed.

An interesting observation was made. As I decreased the coupling value and the system moved from de-synchronization to synchronization it was found that there is a specific coupling value where the two oscillators synchronize and they are in phase lag with each other. During this time neither of the chaotic circuits showed chaotic behavior. The oscilloscope tracing of such phenomenon is shown on Fig. 6.14. At a lower coupling value, they de-synchronized again and they did not shows this phenomenon until at 0 Ω where they showed linear correlation.

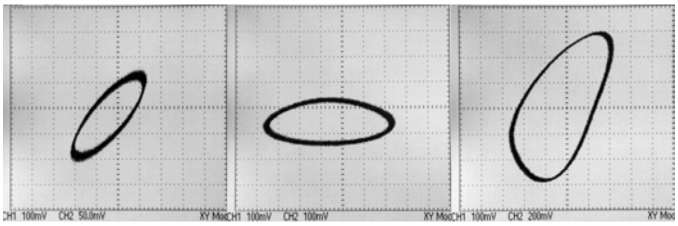

Figure 6.14: Two connected *Chua's circuits* can be seen here. The left and right oscilloscopes show the states of the *Chua's circuits*, in the middle, the coupling behavior can be observed. There is a value of coupling coefficient where the two *Chua's circuits* are in phase lag with each other. During this time neither of the chaotic circuits remains chaotic.

6.2.2.1 Common point connection

This experiment was further extended by using more *Chua's circuits*. Due to the connection flexibility of the designed hardware architecture, I made a connection type where every new *Chua's circuit* connected to a common point through it's coupling weight. The system contains as many coupling values as connected circuits. The connection topology can be seen on Fig. 6.15 / A.

Each circuit was in double scroll showing chaotic oscillations and were connected by the A terminal. I decreased all of the coupling values together from 10 $k\Omega$ to 0 Ω. During the tests while increasing the number of connected *Chua's circuits* up to 9 in every case I can observed the same phenomena. The coupling values for the test cases are shown in Table 6.1.

Taking the mean of the values it could be pointed out that the phenomena can be observed for the resistance value of around 2.7 $k\Omega$ to 1.5 $k\Omega$ so it is in a range of

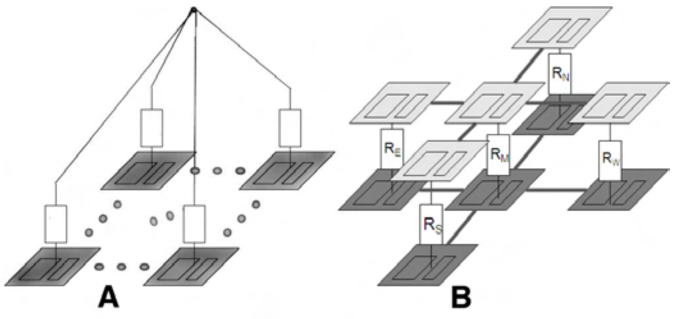

Figure 6.15: On this figure, Connection topologies used during the experiment. On the left, each *Chua's circuit* is connected to a virtual point through it's coupling weight. On the right, ten circuits are connected in a plus form creating 3D architecture. On each layer, the coupling resistors were 0 Ω and only the coupling values between layers were set.

Table 6.1: Different number of *Chua's circuits* are connected together. Each circuit was in double scroll showing chaotic oscillation. They were connected by the A terminals to a virtual point each through it's coupling weight. The range of the coupling values can be seen here where I observed the similar phenomena.

Chua Circuits are connected								
Num. of Chua Circuits	2	3	4	5	6	7	8	9
Start value (k Ω)	3	2.6	2.5	2.7	3.2	3.3	2.7	2.7
End value (k Ω)	2.5	1.2	1.5	1.6	1.6	1.6	1.5	1.7

around 1 $k\Omega$. One of the reasons for the different values could be due to the difference of each *Chua's circuit*. While one circuit is at the edge of the double scroll for a specific bifurcation resistance value, the other is more stable. In the first case, the circuits are more likely synchronize to other cells then in the second case.

As a result, I can conclude that the system in every case around 3 $k\Omega$ down to 2 $k\Omega$ showed similar phenomenon. In this test case, I have modified all the coupling values together. As the next steps, I modified them separately to observe how each coupling value effects the others.

By connecting two circuits together and applying the coupling at 3 $k\Omega$ the similar phenomena appeared and then I added one more *Chua's circuit* to the system with a 10 $k\Omega$ weighting. The whole system moved back to chaotic oscillation.

By decreasing the coupling of the third (just connected) circuit at around 2.6 $k\Omega$ the system showed the similar phenomena. Meaning that the third oscillator only at a specific coupling value synchronized to the other oscillators.

For the same 3 circuits connected I set the first and second weights to 3.8-3.8 $k\Omega$ and the last at 0.9 $k\Omega$. The mean weighting is around $3k\Omega$ and the system showed a similar behavior. It proves that the whole system coupling weighting has stronger impact and not just the independents cells weights.

To confirm this theory, I tested it on different numbers of connected *Chua's circuits* and I can conclude that:
The phenomena in this current topology proves that the independent cell coupling weight are not important as the determining factor is the mean of the used coupling values.

This phenomena can be observed in the mean coupling values of $3k\Omega$ and $2k\Omega$ in range. The correct values could depend on the bifurcation potmeter value used.

6.2.2.2 3D connection

Due to the limited number of *Chua's circuits* available, the number of possibilities of connecting them in 3D were restricted. We connected them in a cross formation. Each layer contained five-five circuits so the middle cells had 5 while the side cells had 2 neighboring connections. The connection topology can be seen on Fig. 6.15/ B.

All of the *Chua's circuits* were in double scroll showing chaotic oscillation.
On each layer, I set the coupling resistance to 0 Ω so on a layer level they were synchronized. I only modified the coupling between layers moving from 10 $k\Omega$ to 0 Ω. In this case I could also observe the similar phenomena that I found in the previous experiments. It started at 7.2 $k\Omega$ and at 4.2 $k\Omega$ and the system turned back to chaotic oscillation. The oscilloscope trace of the middle cells and the correlation phase portrait was very similar as illustrated on Fig. 6.14.

Appendix A

Practical Tips For Chua's Circuit

A.1 Five simple steps for building Chua's Circuit

In this section, I will discuss how *Chua's circuit* can be built using off-the-shelf components. This section is intended to offer practical tips along with the step-by-step guide to non-specialists to build *Chua's circuit* and observe chaos in the laboratory.

A.1.1 Practical Tips for building Chua's circuit and observing Chaos

A.1.1.1 Step 1. Choosing the component values

The choice of component values is important and is a compromise between the available components and the intended frequency of operation. It is also dependent on the frequency limits of the measuring devices.

1. Choose the frequency of operation.

2. Set the value of capacitor C_1. Take into account the parasitic capacitance of Chua's diode. Thus C_1 $=C_{1_{used}} + C_{parasitic}$, where $C_{1_{used}}$ is the external capacitance applied and $C_{parasitic}$ is the parasitic capacitance of Chua's diode used.

3. Set the value of capacitor C_2 using the relation $C_2 = \alpha C_1$. Take into account the parasitics associated with the measuring device and probes.

4. Select the value of the inductor by solving equations given in earlier sections. Also note that $R^2 = \frac{\beta L}{C_2}$

Note that setting α in the range of 10-12 and β in the range of 18-20 will display a wide variety of bifurcation phenomenon. Interested readers are referred to [55] for α-β diagram.

In order to built several electronic *Chua's circuits* using off-the-shelf components and to have a comparative analysis, $C_1 = 10$ *nF,* $C_2 = 100$ *nF,* $L = 18$ *mH* is chosen. Note that these values are the same as presented in [10]

The accuracy of the components is an important factor toward the successful working of the designed *Chua's circuit.* As evident from the α-β diagram, higher is the accuracy of components; more is the success of operating *Chua's circuit* in the intended range.

One of the bottlenecks in designing *Chua's circuit* is the choice of the value of inductance as most of the values might not be available off-the-shelf. In that case, two or more inductors with large quality factor, Q (50-100), can be connected in series to achieve the desired value of inductance. High Q is important as it minimize the internal (read: parasitic) resistance of the inductor. Note that inductors are normally large in size compared to other components used (Fig. A.1). However, size and weight of the inductor used will have no effect on the operation of *Chua's circuit.*

A.1.1.2 Step 2. Testing the active components used

Once the component values have been chosen, the next step is to test the available active components.

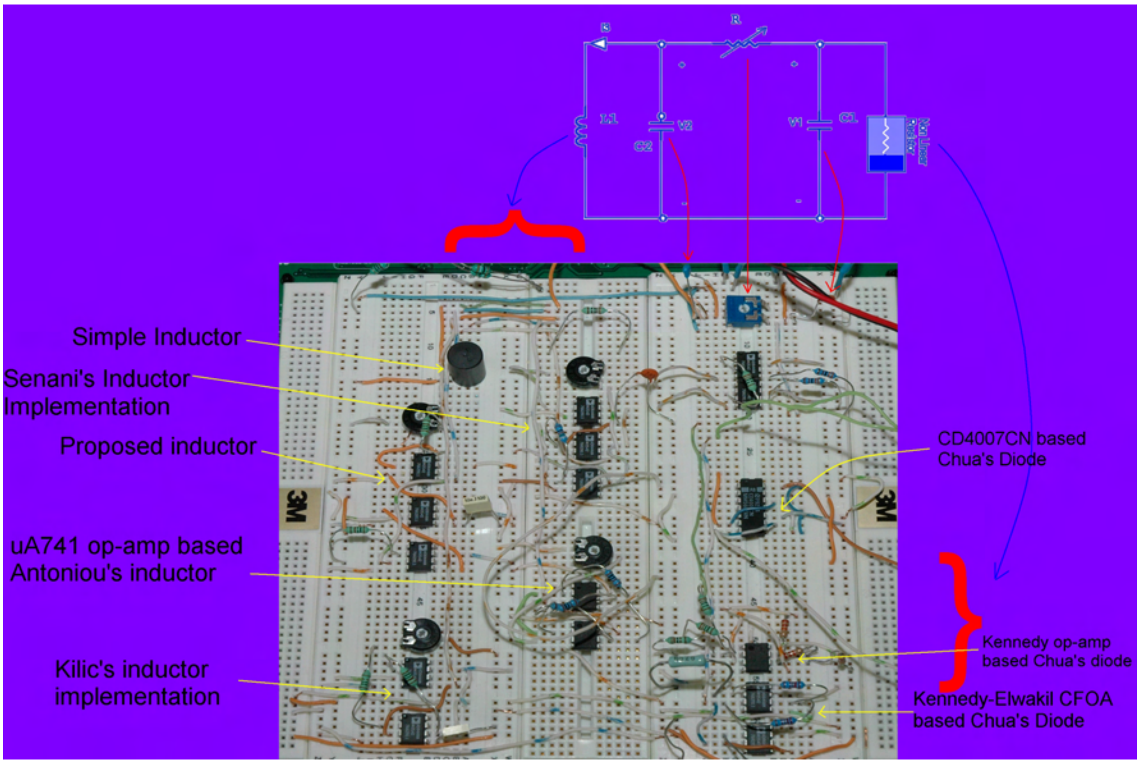

Figure A.1: Fifteen Chua's circuits built on breadboard

Figure A.2: Testing images.

(a) Testing operational amplifier

(b) Testing CFOA-case1

(c) Testing CFOA-case2

Since most of the *Chua's circuits* built so-far have used either operational amplifier or AD844 based CFOA, I will build a simple voltage inverter circuit to test the functioning of the chip.

Testing op-amp

1. Connect the supply pins appropriately. Refer to the datasheet for the pins of amplifier used.

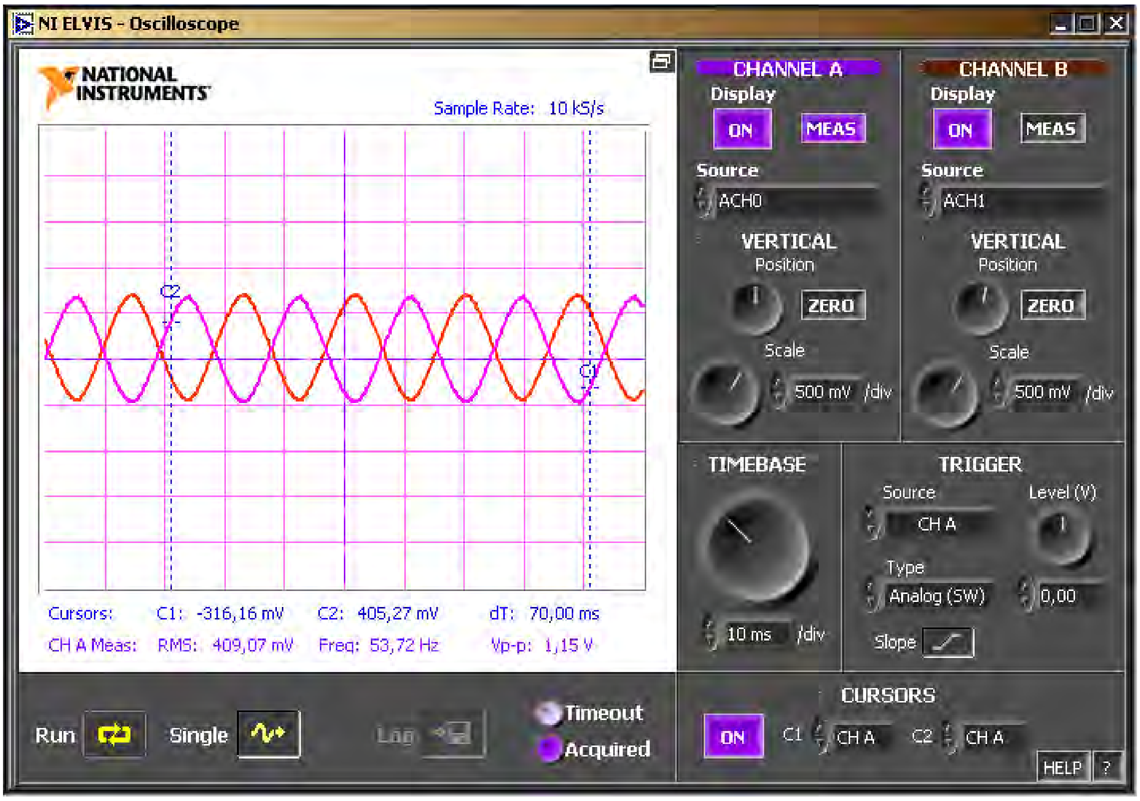

Figure A.3: Laboratory results-voltage inverter.

2. Connect the circuit as shown in Fig. A.2a for the operational amplifier and Fig. A.2b and Fig. A.2c for AD844. Take care of the polarities of the op-amp.

3. Supply a sinusoidal wave at the input and monitor the output for each case.

The captured data on oscilloscope is as shown in Fig. A.3. Herein channel A represents the input signal while channel B represents the output signal.

Some of the commercially available op-amps are uA741, TL082, AD712 etc. can be obtained for a cost less than \$0.50 per item from any nearby electronic component shop. The current cost of AD844 obtained from analog devices is less than \$3 per item. Alternatively, samples can be ordered from manufacturers like Analog

Devices (www.analog.com), STMicroelectronics Pvt. Ltd. (www.st.com), Texas Instruments (www.ti.com) etc. or can also be obtained from www.digi-key.com. Other components can also be easily obtained from www.digi-key.com.

Note that some ICs, like TL082, have more than one operational amplifier with common supply voltages. The following test should be applied to both the operational amplifier inside the chip.

A.1.1.3 Step 3. Building the Chua's Diode

An interesting in-depth analysis of piecewise linear Chua's diode designing using standard available components is given in [Kennedy 1992]. The same implementation will be used here to demonstrate building of Chua's diode.

***Step 3(a)*: Measuring V-I characteristics of a resistor**

The following three ways can be applied to measuring the V-I characteristic of a given resistor.

1. Most of the oscilloscopes are equipped with ports to measure V-I characteristics of a device. Use those ports to plot Chua's diode's characteristics on oscilloscope.

2. Connect the circuit as shown in Fig. A.4 and follow the below-mentioned steps

   (a) For different values of V1, measure the value of V2. Here V1 and V2 are the voltages as shown in Fig. A.4.

   (b) Calculate I = (V1-V2)/100.

   (c) Plot V1 - I curve.

3. Connect the circuit as shown in Fig. A.5

   (a) Apply a triangular wave at V1

   (b) Plot V1-V2. This curve is same as V-I curve for the unknown resistor.

Figure A.4: Test circuit for measuring V-I characteristic of unknown device (Case II).

Figure A.5: Test circuit for measuring V-I characteristic of unknown device (Case III)

Chua's Diode

The piecewise linear Chua's diode can be divided into two parallel combinations of negative resistors with different slopes and breakpoints.

1. Connect the circuit as shown in Fig. A.6 taking care of the polarities and the supply voltage of the op-amp.
2. Adjust the slope of the V-I characteristics of this negative resistor by varying R3 and breakpoint by varying supply voltage. The required V-I is as shown in Fig. A.7. Herein R1 = 220 Ohm, R2 = 220 Ohm and R3 = 2.2 Kohm is used.
3. Build another similar circuit with R1 = 22 Kohm , R2 = 22 Kohm, and R3 = 3.3 Kohm. The required V-I is as shown in Fig. A.8.
4. Connect the two circuits parallelly as shown in Fig. A.9. This Chua's diode has a characteristic as shown in Fig. A.10.

A.1.1.4 Step 4.Building the Oscillator

Parallel combination of the inductor (L) and the capacitor (C_2) makes a sine-wave oscillator. In case of the inductorless realizations, either the inductor (L) or the complete L-C oscillator is replaced by an active R-C circuit.

1. Connect C_2 in parallel with either an inductor (L). Any other implementations of inductor from the literature [Toumazou 1991] can also be used. Alternatively, design a sine wave oscillator with same frequency of operation as calculated in step 1.
2. Monitor the output channel as the power is switched on.
3. A sustained sinusoidal wave implies successful working of the oscillator. A decaying sinusoidal wave reflects the presence of an energy-dissipating device (parasitic resistance) in the oscillator. In case of *Chua's circuit*, sustained oscillations are required whereas for designing Chua's oscillator, decaying oscillations are needed.

Figure A.6: Negative resistor: Schematic.

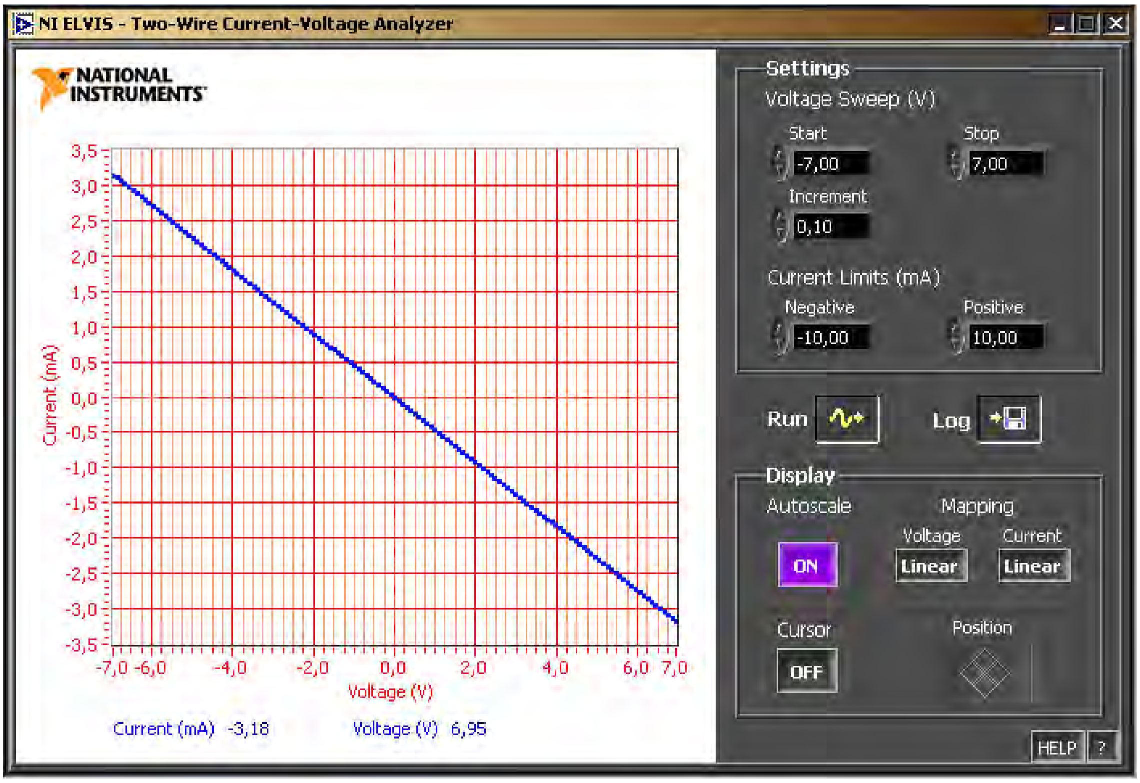

Figure A.7: Negative resistor: Results - I.

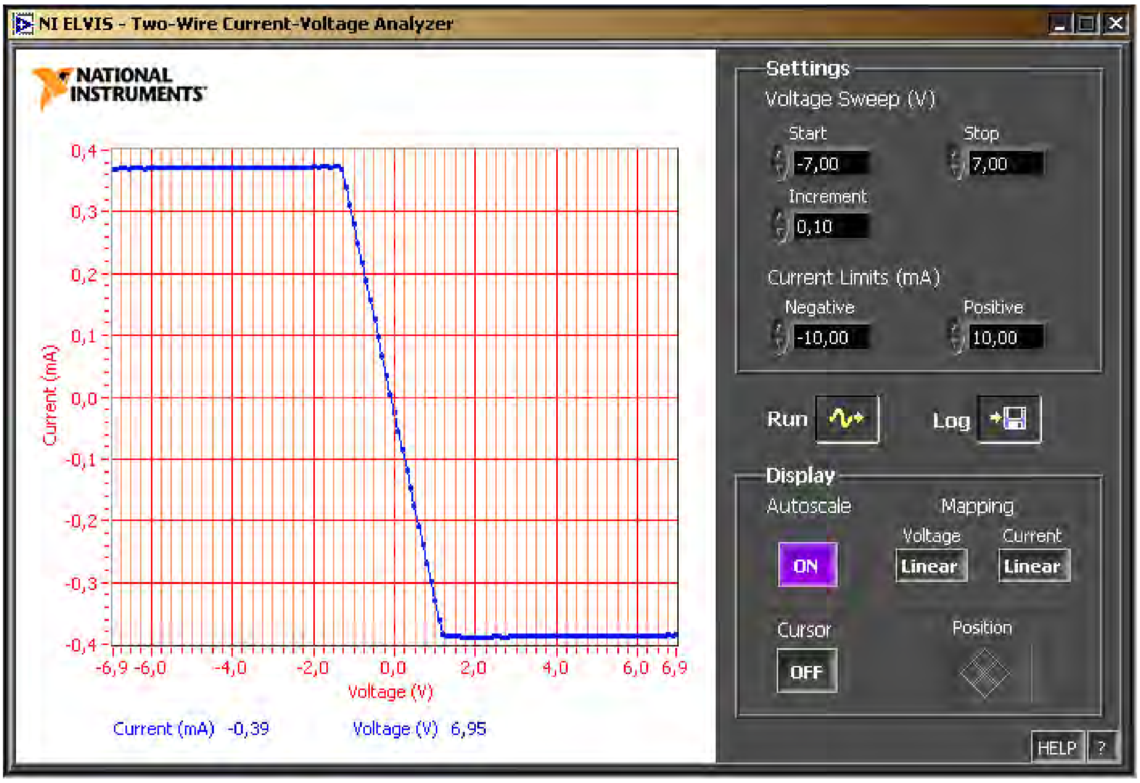

Figure A.8: Negative resistor: Results - II.

Figure A.9: Chua's diode.

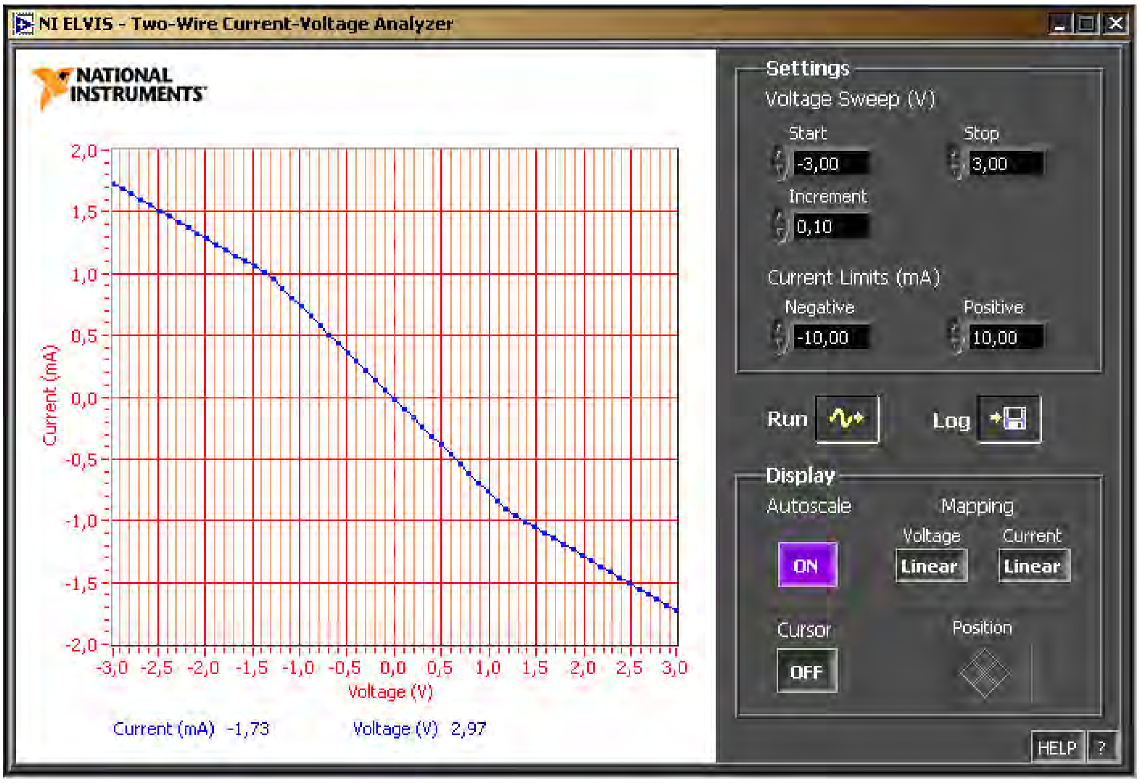

Figure A.10: Chua's diode: Results.

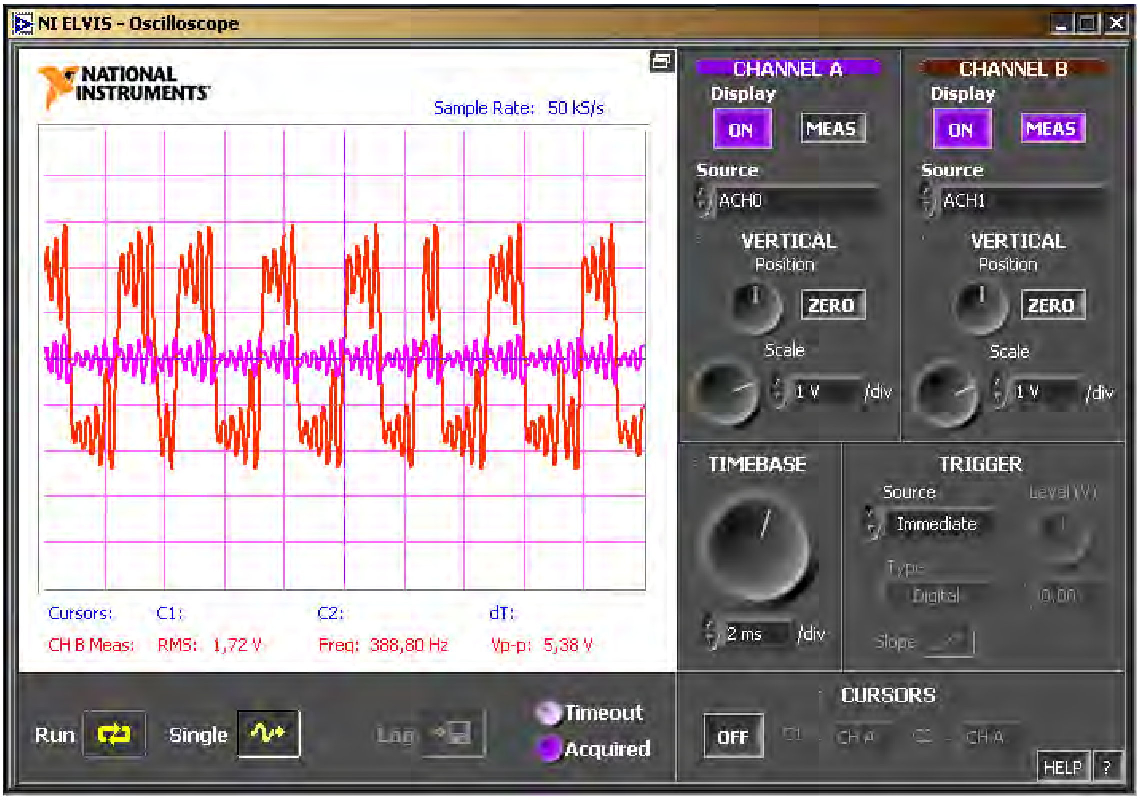

Figure A.11: Chua's circuit: Results (Voltages across capacitors versus time).

A.1.1.5 Step 5. The Final Step

1. Connect C_1 in parallel with Chua's diode.

2. Connect a potentiometer (variable resistor) between the oscillator and Chua's diode.

3. Connect all the ground terminals together.

4. Vary the resistor to observe voltage variations across capacitors C_1 and C_2. Fig. A.11 shows one such observation. These voltages can be plotted against each other to observe different phenomenon in *Chua's circuit*.

5. In case the chosen frequency lies in the audible range, a headphone can be connected between the buffered voltage across C_1 or C_2 to listen to the music generated by *Chua's circuit*.

6. In case of inductorless versions, bifurcation behavior with respect to inductance variation can also be observed.

A.1.1.6 Discussion

Fifteen different implementations of *Chua's circuit* using three different Chua's diode implementations and five different inductance implementations were built and found to work successfully.

The three Chua's diode implementations include:

i) Kennedy's op-amp based implementation,
ii) Kennedy-Elwakil CFOA based implementation,
iii) O' Donoghue *et al* CD4007 based Chua's diode.

The five different implementations of inductors include:

i) Simple inductor,
ii) Antonio's RC inductance realization. $L = \frac{C_{L1} R_{L1} R_{L3} R_{L4}}{R_{L2}}$,
iii) Senani's CFOA base implementation. $L = C_L R_{L1} R_{L2}$,
iv) Kilic's recent CFOA [Kilic 2006] based implementation. $L = C_L R_{L1} R_{L2}$,
v) CFOA based implementation. $L = C_L R_{L1} R_{L2}$.

In order to have a comparative analysis, all circuits were built with C_1 = 10 nF, C_2 = 100 nF, L=18 mH.

Fig. A.1 shows the breadboard design for the implementation of all the cases. The route to chaos is demonstrated in appendix B.
Many other results were recorded and can be observed at www.chuacircuit.com

Components used for *Chua's circuit*

Amplifiers:
AD712

AD844
TL082
LMC6482AIN

Resistances (in Ω):

220 (1% tol.)
2.2k (1% tol.)
22k (1% tol.)
3.3k (1% tol.)
1k (1% tol.)
950 (1% tol.)

Capacitances (in nF):
100n (1% tol.)
10n (1% tol.)

Inductances:
181LY-183 TOKO 10RB 18 mH (5% tol.)

Inverter Pair
CD4007CN

and few variable resistors with maximum values of 1 KΩ and 2 KΩ.

Appendix B

Birth and Death of Double Scroll

The following figure shows the period doubling route to chaos in Chua's circuit and is observed when the interconnecting resistor is varied. This behaviour was observed in almost all the Chua's circuit that were designed. The videos of oscilloscope traces of the same can be found on the website `www.chuacircuit.com`. The route is to be observed row-wise with route starting from left of the first row, evolving all the way in the first row and then moves to the second row and so on and so forth. The curve plots the two state variables (voltage across two capacitors) across two axis.

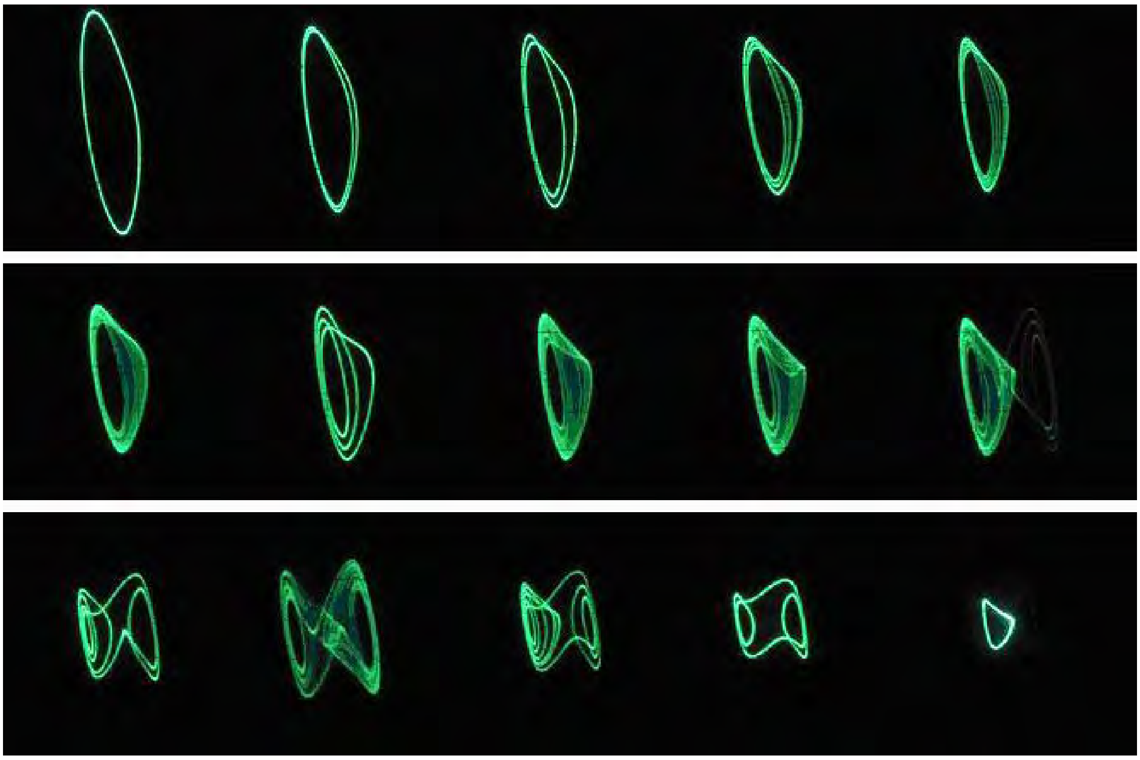

Figure B.1: Birth and Death of Double Scroll: Route to and from Chaos

Appendix C

Some Commonly Used Terms

C.1 Glossary

Current section briefly describes some of the terms related to the dissertation. For indepth treatment the reader is advised to refer to relevant journals, wikipedia or Internet.

Attractor:
An attractor is a set to which a dynamical system evolves after a long enough time. That is, points that get close enough to the attractor remain close even if slightly disturbed. Geometrically, an attractor can be a point, a curve, a manifold, or even a complicated set with a fractal structure known as a strange attractor.

Bifurcations
Most commonly applied to the mathematical study of dynamical systems, a bifurcation occurs when a small smooth change made to the parameter values (the bifurcation parameters) of a system causes a sudden 'qualitative' or topological change in its long-term dynamical behaviour.

Butterfly Effect:
The butterfly effect is a phrase that describes sensitive dependence on initial conditions in chaos theory. Small variations of the initial condition of a dynamical system may produce large variations in the long term behavior of the system.

Chaos Theory and Chaos:

Chaos theory describes the behavior of certain dynamical systems that may exhibit dynamics that are highly sensitive to initial conditions. As a result of this sensitivity, which manifests itself as an exponential growth of perturbations in the initial conditions, the behavior of chaotic systems appears to be random. This happens even though these systems are deterministic, meaning that their future dynamics are fully defined by their initial conditions, with no random elements involved. This behavior is known as deterministic chaos, or simply chaos.

Chromosomes:

In genetic algorithms, a chromosome (also sometimes called a genome) is a set of parameters which define a proposed solution to the problem that the genetic algorithm is trying to solve. The chromosome is often represented as a simple string, although a wide variety of other data structures are also used.

Device modeling:

Semiconductor device modeling creates models for the behavior of the electrical devices based on fundamental physics, such as the doping profiles of the devices. It may also include the creation of compact models (such as SPICE transistor models), which try to capture the electrical behavior of such devices.

Dynamical Systems:

Dynamical Systems are the systems systems whose state evolves with time.

Double Scroll:

Double scroll is one of the attractors in phase space which qualitatively has two lobes just like butterfly's wings. It is most comonly known state of chaos and is observed in Chua's circuit and Lorentz system.

Fitness Function:

A fitness function is a particular type of objective function that quantifies the optimality of a solution (that is, a chromosome) in a genetic algorithm so that

that particular chromosome may be ranked against all the other chromosomes.

Genetic Algorithms (GAs):
Genetic Algorithms (GAs) are adaptive heuristic search algorithm based on the evolutionary ideas of natural selection and genetics. They represent an intelligent exploitation of a random search used to solve optimization problems.

Genetic Programming):
Genetic programming (GP) is an evolutionary algorithm based methodology inspired by biological evolution to find computer programs that perform a user-defined task. It is a specialization of genetic algorithms where each individual is a computer program.

Limit Cycle:
In dynamical systems, a limit-cycle on a plane or a two-dimensional manifold is a closed trajectory in phase space having the property that at least one other trajectory spirals into it either as time approaches infinity or as time approaches minus-infinity.

Logistic Map:
The logistic map is a polynomial mapping of degree 2, often cited as an archetypal example of how complex, chaotic behaviour can arise from very simple non-linear dynamical equations.

MultiScroll MultiGrid Attractor:
MSMG attractor is refered to a class of attractors from the dynamical system having several number of scrolls and equilibrium points lying in all the three axis.

1-D MultiScroll Attractor:
This the class of MSMG where the equilibrium points lies exactly on one of the axis.

2-D MultiScroll Attractor:

This the class of MSMG where the equilibrium points lies between two of the axes.

3-D MultiScroll Attractor:
This the class of MSMG where the equilibrium points lies on all the three axes.

Period Doubling:
Period doubling is one of the route to chaos where the phase space of the system doubles with different variations in bifurcation parameter. When the period is infinite, the system is said to have reached the state of chaos.

Phase Space:
In mathematics and physics, a phase space, is a space in which all possible states of a system are represented, with each possible state of the system corresponding to one unique point in the phase space.

Route to Chaos:
Route to chaos specifies a set of stages through which a system undergoes before entering chaos.

SPICE:
Simulation Program with Integrated Circuit Emphasis or SPICE is a general purpose analog electronic circuit simulator. It is a powerful program that is used in IC and board-level design to check the integrity of circuit designs and to predict circuit behavior.

Single Electron Transistors:
The simplest device in which the effect of Coulomb blockade can be observed is the so-called single electron transistor. It consists of two tunnel junctions sharing one common electrode with a low self-capacitance, known as the island. The electrical potential of the island can be tuned by a third electrode (the gate), capacitively coupled to the island.

Strange Attractor:

While most of the motion types mentioned above give rise to very simple attractors, such as points and circle-like curves called limit cycles, chaotic motion gives rise to what are known as strange attractors, attractors that can have great detail and complexity.

C.2 Abbreviations

The following section lists some of the abbreviations used commonly in the program.

CC
Chua's Circuit
CCII
Second Generation Current Conveyor
DOCCII
Dual Output Second Generation Current Conveyor
CFOA
Current Feedback Operational Amplifier
CMOS
Complimentary Metal Oxide Semiconductor
FPAA
Field Programmable Analog Array
GA
Genetic Algorithm
GP
Genetic Programming
MOCCII
Multiple Output Second Generation Current Conveyor
MOS
Complimentary Metal Oxide Semiconductor
MSMG
MultiScroll MultiGrid

C. SOME COMMONLY USED TERMS

Op-Amp
Operational Amplifier
SET
Single Electron Transistors
TRBG
True Random Bit Generator
VLSI
Very Large Scale Integration

References

Publications

The author's publications concerning the dissertation

[1] G. Gandhi, T. Roska, and A. Csurgay, "Single Electron Transistor Based Chua Type Chaotic Circuit: A SPICE Assisted Proof," *European Conference of Circuit Theory and Design*, 2007.

[2] G. Gandhi and T. Roska, "MOS-integrable 03-20-230ircuitry for Multi-Scroll Chaotic Grid realization:A SPICE assisted proof," *accepted at International Journal of Circuit Theory and Application*, to be published in 2008.

[3] A. Tar, G. Gandhi, and G. Cserey, "3D Modular CNN Architecture using Chua's Circuits," *accepted at International Journal Of Circuit Theory and Applications*, to be published in 2008.

[4] G. Gandhi, "An Improved Chua's Circuit and Its Use in Hyperchaotic Circuit," *Analog Integrated Circuits and Signal Processing*, vol. 46, no. 2, pp. 173–178, 2006.

[5] G. Gandhi, "Comment on "Novel Lossless Floating Immittance Simulator Employing Only Two FTFNs"," *Analog Integrated Circuits and Signal Processing*, vol. 32, no. 2, pp. 191–191, 2002.

[6] G. Gandhi and T. Roska, "Electronic Realization of Chua's Circuit: A Designer's Perspective," *submitted at International Journal of Bifurcation and Chaos*, 2008.

[7] G. Gandhi, G. Cserey, Z. John, and T. Roska, "Anyone can build Chua's circuit," *submitted at International Journal of Bifurcation and Chaos*, 2008.

The patents by author

[8] G. Gandhi, "Chua's circuit and it's use in a hyperchaotic circuit," *US Patents*, No. 7,119,640, 2006.

[9] G. Gandhi, "Chua's circuit and it's use in a hyperchaotic circuit," *Indian Patents*, Application Number IN 200400000985327, 2006.

[10] G. Gandhi, "Comparator circuit, transconductor circuit and MultiScroll Chaotic circuit," *Hungarian Patents*, Application Number P 06 00582, 2006.

Publications related to dissertation

[11] L. O. Chua, "The Genesis of – Chua's circuit," *AEU. Archiv für Elektronik und Übertragungstechnik*, vol. 46, no. 4, pp. 250–257, 1992

[12] M. Kennedy, "Robust OP Amp realization of Chua's circuit.," *Frequenz.*, vol. 46, no. 3, pp. 66–80, 1992

[13] T. Matsumoto, "A chaotic attractor from Chua's circuit," *IEEE Transactions on Circuits and Systems*, vol. 31, no. 12, pp. 1055–1058, 1984

[14] R. Senani and S. Gupta, "Implementation of Chua's chaotic circuit using current feedback op-amps," *Electronics Letters*, vol. 34, no. 9, pp. 829–830, 1998

[15] R. Kilic, M. Alci, and H. Kuntman, "Improved realization of mixed-mode chaotic circuit," *International Journal of Bifurcation and Chaos*, vol. 12, no. 6, pp. 1429–1435, 2002

[16] A. Radwan, A. Soliman, and A. El-Sedeek, "An Inductorless CMOS realization of Chua's circuit," *Chaos, Solitons and Fractals*, vol. 18, no. 1, pp. 149–158, 2003

[17] M. Yalcin, J. Suykens, J. Vandewalle, and S. Ozoguz, "Families of scroll grid attractors," *International Journal of Bifurcation and Chaos*, vol. 12, no. 1, pp. 23–41, 2002

[18] J. Sprott, "Simple chaotic systems and circuits," *American Journal of Physics*, vol. 68, p. 758, 2000

[19] A. Radwan, A. Soliman, and A. El-Sedeek, "MOS realization of the double-scroll-like chaotic equation," *IEEE Transactions on Circuits and Systems I: Fundamental Theory and Applications, [see also IEEE Transactions onCircuits and Systems I: Regular Papers,]*, vol. 50, no. 2, pp. 285–288, 2003

[20] D. Chorafas, *Chaos Theory in the Financial Markets: Applying Fractals, Fuzzy Logic, Genetic Algorithms, Swarm Simulation & the Monte Carlo Method to Manage Market Chaos & Volatility* McGraw-Hill, 1994

[21] J. Lü and G. Chen, "Generating multiscroll chaotic attractors: Theories, methods and applications," *International Journal of Bifurcation and Chaos*, vol. 16, no. 4, pp. 775–858, 2006

[22] E. Lorenz, "Deterministic Nonperiodic Flow," *Journal of the Atmospheric Sciences*, vol. 20, no. 2, pp. 130–141, 1963

[23] M. Yalcin, J. Suykens, J. Vandewalle, and S. Ozoguz, "Families of scroll grid attractors," *International Journal of Bifurcation and Chaos*, vol. 12, no. 1, pp. 23–41, 2002

[24] H. Ahmed and K. Nakazato, "Single-electron devices," *Microelectronic Engineering*, vol. 32, no. 1-4, pp. 297–315, 1996

[25] A. Csurgay, W. Porod, and S. Goodnick, "The circuit paradigm in nanoelectronics-field-coupled and hybrid nanoelectronic circuits [Plenary lecture]," *Proceedings of the 2005 European Conference on Circuit Theory and Design*, vol. 2, 2005

[26] I. Nanotubes, I. Models, and S. Devices, "Scanning the Issue," *Proceedings of the IEEE*, vol. 91, no. 11, 2003

[27] A. Schmid and Y. Leblebici, "Robust circuit and system design methodologies for nanometer-scale devices and single-electron transistors," *IEEE Transactions on Very Large Scale Integration (VLSI) Systems*, vol. 12, no. 11, pp. 1156–1166, 2004

[28] S. Mahapatra, V. Vaish, C. Wasshuber, K. Banerjee, and A. Ionescu, "Analytical modeling of single electron transistor for hybrid CMOS-SET analog IC design," *IEEE Transactions on Electron Devices* , vol. 51, no. 11, pp. 1772–1782, 2004

[29] K. Uchida, K. Matsuzawa, J. Koga, R. Ohba, S. Takagi, and A. Toriumi, "Analytical single-electron transistor (SET) model for design and analysis of realistic SET circuits," *Japan Journal of Applied Physics*, vol. 39, no. 4B Part 1, pp. 2321–2324, 2000

[30] A. Ionescu, M. Declercq, S. Mahapatra, K. Banerjee, and J. Gautier, "Few electron devices: Towards hybrid CMOS-SET integrated circuits," *Proceedings of the 39th conference on Design automation*, pp. 88–93, 2002

[31] K. Likharev, "Single-electron devices and their applications," *Proceedings of the IEEE*, vol. 87, no. 4, pp. 606–632, 1999

[32] G. Zhong and F. Ayrom, "Periodicity and Chaos in Chua's Circuit," *IEEE Transactions on Circuits and Systems*, vol. 32, no. 5, pp. 501–503, 1985

[33] G. Zhong, "Implementation of Chua's circuit with a cubic nonlinearity," *IEEE Transactions on Circuits and Systems I: Fundamental Theory and Applications, [see also IEEE Transactions on Circuits and Systems I: Regular Papers]*, vol. 41, no. 12, pp. 934–941, 1994.

[34] M. Yalcin, J. Suykens, and J. Vandewalle, "Experimental confirmation of 3- and 5-scroll attractors from ageneralized Chua's circuit," *IEEE Transactions on Circuits and Systems I: Fundamental Theory and Applications*, vol. 47, no. 3, pp. 425–429, 2000.

[35] G. Zhong and K. Tang, "Circuitry implementation and synchronization of Chen's attractor," *International Journal of Bifurcation and Chaos*, vol. 12, pp. 1423–1427, 2002.

[36] J. Lu and G. Chen, "A new chaotic attractor coined," *International Journal of Bifurcation and Chaos*, vol. 12, no. 3, pp. 659–661, 2002.

[37] C. Wu and L. Pivka, "From Chua's circuit to Chua's oscillator: A picture book of attractors," *Nonlinear Dynamics of Electronic Systems, Proc. Workshop, eds. Davies, AC & Schwarz, W.(World Scientific, Singapore)*, 1994.

[38] C. Toumazou, F. Lidgey, and D. Haigh, "Analog IC Design: The Current-Mode Approach," *Peter Peregrinus Ltd*, 1990.

[39] L. AB Torres and L. Aguirre, "PCCHUA - A Laboratory Setup for Real-Time Control and Synchronization of Chaotic Oscillations," *International Journal of Bifurcation and Chaos*, vol. 15, no. 8, pp. 2349–2360, 2005.

[40] K. Tang and K. Man, "An alternative Chua's circuit implementation," *Industrial Electronics, 1998. Proceedings. ISIE'98. IEEE International Symposium on*, vol. 2, 1998.

[41] J. C. Sprott, "A new class of chaotic circuit," *Physics Letters A*, vol. 266, no. 1, pp. 19–23, 2000.

[42] R. Senani and S. Gupta, "Implementation of Chua's chaotic circuit using current feedback op-amps," *Electronics Letters*, vol. 34, no. 9, pp. 829–830, 1998.

[43] A. Sedra and K. Smith, *Microelectronic circuits.* Holt, Rinehart & Winston Austin, TX, USA, 1987.

[44] T. Roska, "Computational and computer complexity of analogic cellular wave computers," *Cellular Neural Networks and Their Applications, 2002.(CNNA 2002). Proceedings of the 2002 7th IEEE International Workshop on*, pp. 323–338, 2002.

[45] A. Rodriguez-Vazquez and M. Delgado-Restituto, "CMOS design of chaotic oscillators using state variables: amonolithic Chua's circuit," *IEEE Transactions on Circuits and Systems II: Analog and Digital Signal Processing,[see also IEEE Transactions on Circuits and Systems II: Express Briefs]*, vol. 40, no. 10, pp. 596–613, 1993.

[46] M. Rashid and M. Rashid, *Introduction to PSpice using OrCAD for circuits and electronics*. Upper Saddle River, NJ: Pearson/Prentice Hall, 2004.

[47] A. Radwan, A. Soliman, and A. El-Sedeek, "An inductorless CMOS realization of Chua's circuit," *Chaos, Solitons and Fractals*, vol. 18, no. 1, pp. 149–158, 2003.

[48] L. Pivka, "Loretz Equation and Chua's Equation," *International Journal of Bifurcation and Chaos [in Applied Sciences and Engineering]*, vol. 6, no. 12B, pp. 2443–2489, 1996.

[49] S. Ozoguz, A. Elwakil, and M. Kennedy, "Experimental Verification of The Butterfly Attractor in a Modified Lorentz System," *International Journal of Bifurcation and Chaos*, vol. 12, no. 7, pp. 1627–1632, 2002.

[50] K. O'Donoghue, P. Forbes, and M. Kennedy, "A Fast And Simple Implementation of Chua's Oscillator With Cubic-Like Nonliearity," *International Journal of Bifurcation and Chaos*, vol. 15, pp. 2959–2972, 2005.

[51] K. Murali and M. Lakshmanan, "Observation of many bifurcation sequences in a driven piecewise-linear circuit," *Physics Letters A*, vol. 151, no. 8, pp. 412–419, 1990.

[52] Ö. Morgül and R. An, "Realization of Chua's Circuit Family," *IEEE Transaction on Circuits and System-I*, vol. 47, no. 9, pp. 1424–1430, 2000.

[53] O. Morgul, "Wien bridge based RC chaos generator," *Electronics Letters*, vol. 31, no. 24, pp. 2058–2059, 1995.

[54] O. Morgul, "Inductorless realisation of Chua oscillator," *Electronics Letters*, vol. 31, no. 17, pp. 1403–1404, 1995.

[55] K. Mischaikow and M. Mrozek, "Chaos in the Lorenz equations: A computer assisted proof. Part II: Details," *Mathematics of Computation*, vol. 67, no. 223, pp. 1023–1046, 1998.

[56] K. Mischaikow and M. Mrozek, "Chaos in the Lorenz equations: a computer-assisted proof," *Arxiv preprint math.DS/9501230*, 1995.

[57] T. Matsumoto, L. Chua, and M. Komuro, "Birth and death of the double scroll," *Physica D*, vol. 24, no. 1-3, pp. 97–124, 1987.

[58] R. Madan, "Special Issue on Chua's Circuit: A Paradigm for Chaos," *Journal of Circuits, Systems and Computers*, 1990.

[59] W. Liu and G. Chen, "A new chaotic system and its generation," *International Journal of Bifurcation and Chaos*, vol. 13, pp. 261–267, 2003.

[60] L. Chua and L. Yang, "Cellular Neural Networks: Theory and Applications," *IEEE Transactions on Circuits and Systems*, vol. 35, no. 10, pp. 1257–1290, 1988.

[61] P. Kumar and R. Senani, "Bibliography on Nullors and Their Applications in Circuit Analysis, Synthesis and Design," *Analog Integrated Circuits and Signal Processing*, vol. 33, no. 1, pp. 65–76, 2002.

[62] L. Kocarev and T. Roska, "Dynamics of the Lorenz equation and Chua's equation: A tutorial. Chua's circuit: A paradigm for Chaos," 1993.

[63] R. Kilic, "Experimental Study of CFOA-Based Inductorless Chua's Circuit," *International Journal of Bifurcation and Chaos*, vol. 14, pp. 1369–1374, 2004.

[64] R. Kilic, "On Current Feedback Operational Amplifier-Based Realization of Chua's Circuit," *Circuits, Systems, and Signal Processing*, vol. 22, no. 5, pp. 475–491, 2003.

[65] A. Khibnik and D. Roose, "On periodic orbits and homoclinic bifurcations in Chua's circuit with a smooth nonlinearity," *International Journal of Bifurcation and Chaos*, vol. 3, no. 2, pp. 363–384, 1993.

[66] M. Kennedy, "Three steps to chaos - Part II: A Chua's circuit primer," *IEEE Transaction Circuits and Systems*, vol. 40, pp. 657–674, 1993.

[67] T. Kapitaniak and L. Zhong, "Experimental hyperchaos in coupled Chua's circuits," *IEEE Transactions on Circuits and Systems I: Fundamental Theory and Applications [see also IEEE Transactions onCircuits and Systems I: Regular Papers]*, vol. 41, no. 7, pp. 499–503, 1994.

[68] A. Huang, L. Pivka, C. Wu, and M. Franz, "Chua's equation with cubic nonlinearity," *Int. J. Bifurcation and Chaos*, vol. 6, no. 8, pp. 2175–2222, 1996.

[69] P. Gray and R. Meyer, *Analysis and Design of Analog Integrated Circuits.* John Wiley & Sons, Inc. New York, NY, USA, 1990.

[70] E. Gunay, M. Alçi, and F. Yildirim, "An Experimental Study on Chaotic Dynamics of CFOA-Based SC-CNN Circuit," *International Journal of Bifurcation and Chaos*, vol. 15, no. 8, pp. 2551–2558, 2005.

[71] E. Günay, E. Uzunhisarcıklı, R. Kılıç, and M. Alçı, "A Realization of SC-CNN-Based Circuit using FTFN," *Turkish Journal of Electrical Engineering and Computer Sciences, TÜBİTAK*, vol. 13, no. 1, pp. 39–50, 2005.

[72] A. Stoica, D. Keymeulen, R. Zebulum, A. Thakoor, T. Daud, G. Klimeck, Y. Jin, R. Tawel, and V. Duong, "Evolution of Analog Circuits on Field Programmable Transistor Arrays," *Proceedings of the Second NASA DoD Workshop on Evolvable Hardware*, pp. 99–108, 2000.

[73] U. Çam, O. Çiçekoğlu, and H. Kuntman, "Novel Lossless Floating Immittance Simulator Employing Only Two FTFNs," *Analog Integrated Circuits and Signal Processing*, vol. 29, no. 3, pp. 233–235, 2001.

[74] Z. Galias and P. Zgliczynski, "Computer assisted proof of chaos in the Lorenz system," *Physica D*, vol. 115, pp. 165–188, 1998.

[75] T. Fujiwara, Y. Horio, and K. Aihara, "An integrated multi-scroll circuit with floating-gate MOSFETs," *International Symposium on Circuits and Systems, 2003. ISCAS'03. Proceedings of the 2003*, vol. 3, 2003.

[76] A. Elwakil and M. Kennedy, “Improved implementation of Chua’s chaotic oscillator using current feedback op amp,” *IEEE Transactions on Circuits and Systems I: Fundamental Theory and Applications* , vol. 47, no. 1, pp. 76–79, 2000.

[77] R. Kiliç and F. Yildirim, “A survey of Wien bridge-based chaotic oscillators: Design and experimental issues,” *Chaos, Solitons and Fractals*, 2008.

[78] R. KiliÇ, “A Harmony of Linear and Non Linear Oscillations: Win Bridge - based mixed-mode Chaotic Circuit,” *Journal of Circuits, Systems, and Computers*, vol. 13, no. 1, pp. 137–149, 2004.

[79] X. Yang and Q. Li, “Chaos generator via Wien-bridge oscillator,” *Electronics Letters*, vol. 38, no. 13, pp. 623–625, 2002.

[80] A. Elwakil and M. Kennedy, “Three-phase oscillator modified for chaos,” *Microelectronics Journal*, vol. 30, no. 9, pp. 863–867, 1999.

[81] A. Elwakil and M. Kennedy, “Inductorless hyperchaos generator,” *Microelectronics Journal*, vol. 30, no. 8, pp. 739–743, 1999.

[82] A. Elwakil, K. Salama, and M. Kennedy, “An equation for generating chaos and its monolithic implementation,” *International Journal of Bifurcation and Chaos*, vol. 12, no. 12, pp. 2885–2896, 2002.

[83] A. Elwakil, S. Ozoguz, and M. Kennedy, “Creation of a complex butterfly attractor using a novel Lorenz-Typesystem,” *IEEE Transactions on Circuits and Systems I: Fundamental Theory and Applications*, vol. 49, no. 4, pp. 527–530, 2002.

[84] A. Elwakil and M. Kennedy, “Novel chaotic oscillator configuration using a diode-inductor composite,” *International Journal of Electronics*, vol. 87, no. 4, pp. 397–406, 2000.

[85] A. Eltawil and A. Elwakil, “Low-Voltage Chaotic Oscillator With an Approximate Cubic Nonlinearity,” *AEU - International Journal Of Electronics and Communication*, vol. 3, pp. 158-60, 1999.

[86] J. Cruz and L. Chua, “An IC chip of Chua’s circuit,” *IEEE Transactions on Circuits and Systems II: Analog and Digital Signal Processing* , vol. 40, no. 10, pp. 614–625, 1993.

[87] L. Chua, M. Komuro, and T. Matsumoto, “The double scroll family,” *IEEE Transactions on Circuits and Systems*, vol. 33, no. 11, pp. 1072–1118, 1986.

[88] L. Chua, C. Wu, and A. Huang, “A universal circuit for studying and generating chaos. I. Routes tochaos,” *IEEE Transactions on Circuits and Systems I: Fundamental Theory and Applications [see also IEEE Transactions on Circuits and Systems I: Regular Papers]*, vol. 40, no. 10, pp. 732–744, 1993.

[89] L. Chua and T. Roska, *Cellular Neural Networks and Visual Computing: Foundation and Applications.* Cambridge University Press, 2002.

[90] L. Chua, C. Desoer, and E. Kuh, *Linear and nonlinear circuits.* McGraw-Hill New York, 1987.

[91] G. Chen and T. Ueta, “Yet another chaotic attractor,” *International Journal of Bifurcation and Chaos*, vol. 9, no. 7, pp. 1465–1466, 1999.

[92] R. Caponetto, A. Di Mauro, L. Fortuna, and M. Frasca, “Field Programmable Analog Array to Implement a Programmable Chua’s Circuit,” *International Journal of Bifurcation and Chaos*, vol. 15, no. 5, pp. 1829–1836, 2005.

[93] U. Cam and H. Kuntman, “A new CMOS realization of a four terminal floating nullor (FTFN),” *International Journal of Electronics*, vol. 87, no. 7, pp. 809–817, 2000.

[94] U. Çam, O. Cicekoglu, and H. Kuntman, “Reply to Comment on ”Novel Lossless Floating Immittance Simulator Employing Only Two FTFNs”,” *Analog Integrated Circuits and Signal Processing*, vol. 32, no. 2, pp. 193–193, 2002.

[95] L. Bruton, *RC active circuits: theory and design.* Englewood Cliffs, NJ: Prentice-Hall, 1980.

[96] A. Antoniou, "Novel RC-active-network synthesis using generalized-immittance converters," *Circuits and Systems, IEEE Transactions on [legacy, pre-1988]*, vol. 17, no. 2, pp. 212–217, 1970.

[97] D. Hillier, S. Gunel, J. Suykens, and J. Vandewalle, "Partial Synchronization in Oscillator Arrays with Asymmetric Coupling," *International Journal of Bifurcation and Chaos in Applied Science and Engineering*, vol. 17, no. 11, p. 4177, 2007.

[98] B. Shi, "An eight layer cellular neural network for spatio-temporal image ÿltering," *International Journal of Circuit Theory and Application*, vol. 34, pp. 141–164, 2006.

[99] J. Cosp and J. Madrenas, "Scene segmentation using neuromorphic oscillatory networks," *IEEE Transactions on Neural Networks*, vol. 14, no. 5, pp. 1278–1296, 2003.

[100] M. Ercsey-Ravasz, T. Roska, and Z. Neda, "Perspectives for Monte Carlo simulations on the CNN Universal Machine," *Arxiv preprint physics/0603121*, 2006.

[101] M. Yalcin, J. Suykens, and J. Vandewalle, "True random bit generation from a double-scroll attractor," *IEEE Transactions on Circuits and Systems I: Regular Papers, [see also IEEE Transactions on Circuits and Systems I: Fundamental Theory and Applications]*, vol. 51, no. 7, pp. 1395–1404, 2004.

[102] S. Ozoguz, "Simple log-domain chaotic oscillator," *Electronics Letters*, vol. 37, no. 23, pp. 1378–1379, 2001.

[103] K. Tang, K. Man, and G. Chen, "Digitized n-scroll attractor model for secure communications," *IEEE International Symposium on Circuits and Systems* , vol. 3, 2001.

[104] S. Ozoguz and N. Sengor, "On the realization of NPN-only log-domain chaotic oscillators," *IEEE Transactions onCircuits and Systems I: Fundamental Theory and Applications [see also , IEEE Transactions on Circuits and Systems I: Regular Papers]*, vol. 50, no. 2, pp. 291–294, 2003.

[105] F. Han, X. Yu, Y. Wang, Y. Feng, and G. Chen, "n-scroll chaotic oscillators by second-order systems and double-hysteresis blocks," *Electronics Letters*, vol. 39, no. 23, pp. 1636–8, 2003.

[106] J. Suykens and A. Huang, "A family of n-scroll attractors from a generalized Chua's circuit," *Archiv fur Elektronik und Ubertragungstechnik*, vol. 51, no. 3, pp. 131–138, 1997.

[107] J. Suykens and J. Vandevalle, "Generation of n-double scrolls(n= 1, 2, 3, 4,...)," *IEEE transactions on circuits and systems. 1, Fundamental theory and applications*, vol. 40, no. 11, pp. 861–867, 1993.

[108] R. Barboza and L. Chua, "The Four Element Chua's Circuit," *International Journal Of Bifurcation and Chaos*, vol. 18, no. 4, pp. 843-955, 2008.